

AD _____

CONTRACT NUMBER: DAMD17-94-C-4043

TITLE: Development and Testing of Treatments for Battlefield
Phosgene Poisoning

PRINCIPAL INVESTIGATOR: Gail H. Gurtner, M.D.

CONTRACTING ORGANIZATION: New York Medical College
Valhalla, New York 10595

REPORT DATE: March 1996

TYPE OF REPORT: Final

PREPARED FOR: Commander
U.S. Army Medical Research and Materiel Command
Fort Detrick, Frederick, Maryland 21702-5012

DISTRIBUTION STATEMENT: Approved for public release;
distribution unlimited

The views, opinions and/or findings contained in this report are those of the author(s) and should not be construed as an official Department of the Army position, policy or decision unless so designated by other documentation.

DTIC QUALITY INSPECTED 3

19961002 067

REPORT DOCUMENTATION PAGE

Form Approved
OMB No. 0704-0188

Public reporting burden for this collection of information is estimated to average 1 hour per response, including the time for reviewing instructions, searching existing data sources, gathering and maintaining the data needed, and completing and reviewing the collection of information. Send comments regarding this burden estimate or any other aspect of this collection of information, including suggestions for reducing this burden, to Washington Headquarters Services, Directorate for Information Operations and Reports, 1215 Jefferson Davis Highway, Suite 1204, Arlington, VA 22202-4302, and to the Office of Management and Budget, Paperwork Reduction Project (0704-0188), Washington, DC 20503.

1. AGENCY USE ONLY (Leave blank)		2. REPORT DATE March 1996	3. REPORT TYPE AND DATES COVERED Final (1 Aug 94 - 31 Jan 96)	
4. TITLE AND SUBTITLE Development and Testing of Treatments for Battlefield Phosgene Poisoning			5. FUNDING NUMBERS DAMD17-94-C-4043	
6. AUTHOR(S) Gail H. Gurtner, M.D.				
7. PERFORMING ORGANIZATION NAME(S) AND ADDRESS(ES) New York Medical College Valhalla, New York 10595			8. PERFORMING ORGANIZATION REPORT NUMBER	
9. SPONSORING / MONITORING AGENCY NAME(S) AND ADDRESS(ES) Commander U.S. Army Medical Research and Materiel Command, Fort Detrick, Frederick, MD 21702-5012			10. SPONSORING / MONITORING AGENCY REPORT NUMBER	
11. SUPPLEMENTARY NOTES				
12a. DISTRIBUTION / AVAILABILITY STATEMENT Approved for public release; distribution unlimited			12b. DISTRIBUTION CODE	
13. ABSTRACT (Maximum 200 words) This project's aim was to characterize changes in microvascular endothelial cells (HMVEC) and type II alveolar epithelial cells (AEpC) after exposure to phosgene <i>in vitro</i> for evaluation of prophylaxis and therapy. We measured release of eicosanoids from lung HMVEC: 6-keto-PGF1 α and thromboxane B2 both increase ~2 h after exposure to 900 ppm-min phosgene. Smaller but statistically significant increases in leukotrienes C4, D4, and E4 are also seen after 2 h. Over the same time course, phosgene-exposed HMVEC which were not killed by exposure accumulate intracytosolic calcium (measured with fluo-3), and generate reactive oxygen metabolites (detected with CDCFH). After a phosgene dose of 300 ppm-min, changes in HMVEC membranes result in loss of cytosolic esterase activity (detected with calcein-AM), along with increased binding of intercalating dyes to DNA. Additional signs of cell injury are decreased lysosomal uptake of acridine orange, and loss of mitochondrial membrane potential (measured by rhodamine 123 uptake and JC-1 aggregation). These changes all occur rapidly after exposure and remain stable for several hours. Type II AEpC are more resistant to phosgene: measures of cytotoxic injury are minimally altered by phosgene levels up to 900 ppm-min and mitochondrial membrane potential is maintained even at this dose. Intracellular calcium levels stay low even after addition of ionophores to A549 AEpC. Permeability of both type II AEpC and HMVEC monolayers increases after exposure to 900 ppm-min phosgene, measured by decreased electrical resistance and increased mannitol permeation. Pretreatment with ~10 ⁻² M N-acetyl cysteine and ~10 ⁻⁴ M pyrrolidine dithiocarbamate protects against some cytotoxic changes, suggesting that intracellular reactive oxygen species may contribute to phosgene induced injury.				
14. SUBJECT TERMS phosgene, alveolar epithelial cells, leukotrienes, rhodamine 123, fluo-3, ethidium, lysosomes, calcium, antioxidants, dichlorofluorescein, mannitol, endothelial cells, prostaglandins, calcein, acridine orange, JC-1, mitochondria, reactive oxygen species, N-acetyl cysteine, pyrrolidine dithiocarbamate			15. NUMBER OF PAGES 155	
16. PRICE CODE				
17. SECURITY CLASSIFICATION OF REPORT Unclassified	18. SECURITY CLASSIFICATION OF THIS PAGE Unclassified	19. SECURITY CLASSIFICATION OF ABSTRACT Unclassified	20. LIMITATION OF ABSTRACT Unlimited	

FOREWORD

Opinions, interpretations, conclusions and recommendations are those of the author and are not necessarily endorsed by the US Army.

NA Where copyrighted material is quoted, permission has been obtained to use such material.

NA Where material from documents designated for limited distribution is quoted, permission has been obtained to use the material.

APD Citations of commercial organizations and trade names in this report do not constitute an official Department of Army endorsement or approval of the products or services of these organizations.

APD In conducting research using animals, the investigator(s) adhered to the "Guide for the Care and Use of Laboratory Animals," prepared by the Committee on Care and Use of Laboratory Animals of the Institute of Laboratory Resources, National Research Council (NIH Publication No. 86-23, Revised 1985).

APD For the protection of human subjects, the investigator(s) adhered to policies of applicable Federal Law 45 CFR 46.

NA In conducting research utilizing recombinant DNA technology, the investigator(s) adhered to current guidelines promulgated by the National Institutes of Health.

NA In the conduct of research utilizing recombinant DNA, the investigator(s) adhered to the NIH Guidelines for Research Involving Recombinant DNA Molecules.

NA In the conduct of research involving hazardous organisms, the investigator(s) adhered to the CDC-NIH Guide for Biosafety in Microbiological and Biomedical Laboratories.

Stephen M. ... 9/16/96
PI - Signature Date

Table of Contents

Foreword	1
Table of Contents	2
Abbreviations	3
Introduction and Background	4
Objectives to be Met	6
Results	6
Effects of Anti-Neutrophil Antibodies on Phosgene-Induced Lung Injury in the Rat	6
Methods for Culture of Microvascular Endothelial Cells	7
Methods for Culture of Type II Alveolar Epithelial Cells	8
Method for Exposure to Phosgene	9
Junctional Integrity of Pulmonary Microvascular Endothelial Cells	9
Junctional Integrity of Type II Alveolar Epithelial Cells after Exposure to Phosgene	10
Detection of Cytotoxic Injury to Nuclear and Plasma Membranes of Microvascular Endothelial Cells Using Fluorescent Probes	12
Detection of Phosgene-Induced Cytotoxic Injury to A549 Epithelial Cells	15
Effects of Phosgene Exposure on Mitochondrial Membrane Potential of Human Microvascular Endothelial Cells	16
Effects of Phosgene Exposure on Mitochondrial Membrane Potential of the A549 Human Pulmonary Epithelial Cell Line	17
Intracellular Calcium Levels in Microvascular Endothelial Cells	18
Intracellular Calcium Levels in the A549 Human Type II Alveolar Epithelial Cell Line	21
Effects of Phosgene on Acidification of Lysosomes by Proton Pumps	21
Effects of Phosgene on Release of Arachidonic Acid Metabolites	23
Effects of Phosgene on Cytokine Release	25
Methods to Detect Generation of Reactive Oxygen Metabolites	25
Protection by Antioxidants - N-acetyl Cysteine	26
Effects of Antioxidants on Phosgene-Mediated Responses - Pyrrolidine Dithiocarbamate	27
Conclusions	31
Future Directions	32
References	33
Table I	37
Figures	38-153

Abbreviations

AEpcC - type II alveolar epithelial cells
-AM - acetoxymethyl ester
AO - acridine orange
BAL - bronchoalveolar lavage
BCEF - bis(carboxyethyl)fluorescein
BPEC - bovine lung endothelial cells
CDCF - carboxydichlorofluorescein
CDCFH - carboxydichlorodihydrofluorescein
DA - diacetate
DCF - dichlorofluorescein
DCFH - dichlorodihydrofluorescein
ECGM - endothelial cell growth medium
ELISA - enzyme linked immunosorbant assay
HBSS - Hank's balanced salt solution
HMVEC - human lung microvascular endothelial cells
IL - interleukin
JC-1 - 5,5',6,6'-tetrachloro-1,1',3,3'-tetraethylbenzimidazolylcarbocyanine iodide
LT - leukotriene
MFI - mean fluorescence intensity
NAC - N-acetylcysteine
PDTC - pyrrolidine dithiocarbamate
PG - prostaglandin
PI - propidium iodide
PMA - phorbol myristate acetate
R123 - rhodamine 123
ROS - reactive oxygen species
Tx - thromboxane

I. Introduction and Background

Phosgene is a toxic gas which can cause fatal pulmonary edema. Lung injuries to U.S. forces exposed to phosgene and other toxic gases used during World War I affected over 70,000 troops [1], while currently, the annual use of one million tons of phosgene by the U.S. chemical industry continues to present a high risk of lung injury to workers [2]. The mechanisms of lung injury caused by phosgene exposure are still not well understood. In a number of animal models, phosgene inhalation triggers infiltration of the lungs with neutrophils, suggesting that one component of the pulmonary injury may be mediated by products of these inflammatory cells. Currie et al. [3] concluded that protein leakage into the alveolar space in the phosgene exposed rat was most closely correlated with the level of neutrophil infiltration, and later Ghio et al. [4] showed that cyclophosphamide, colchicine, and an inhibitor of leukotriene B4 synthesis reduced both neutrophil infiltration and lung injury, but no causal relationship was established. More recently, Ghio and Hatch have described an apparently protective role of infiltrating neutrophils in the lungs of phosgene-exposed rats, in which increased neutrophilic infiltration after a first phosgene exposure was correlated with decreased protein leakage after a second phosgene exposure [16]. The mechanism for such an apparently paradoxical protection was not elucidated. Previously, Hatch et al. [5] had indicated that sensitivity of different animal models to phosgene exposure varied, with mice, rats, and hamsters showing greater sensitivity than rabbits or guinea pigs, but no mechanistic basis for these differences was proposed. The late Project Director's laboratory has shown in a number of studies that phosgene and other oxidant gases trigger lung injury in rabbits which can be ameliorated by free radical scavengers and antioxidants, or by agents which interfere with conversion of arachidonic acid into bioactive eicosanoid products of the cyclooxygenase and lipoxygenase pathways [6-8,39]. Interpretations of these results in animal models were complicated by marked differences in the sensitivity of the species to phosgene-induced injury (primarily protein leakage into the alveolar space and edema) which could not be simply correlated with the levels of arachidonic acid metabolites or with the contribution of neutrophilic infiltration [9]. Rabbits develop pulmonary edema at cumulative phosgene doses of 1500 ppm·min with a relatively low level of neutrophilic involvement, whereas dogs develop a somewhat delayed inflammatory response to cumulative phosgene doses of 4500 ppm·min, with extensive infiltration of neutrophils into the alveolar space. Ambiguities also remain over the mode of action of agents which relieve phosgene-induced injury in different animals. While cAMP, free radical scavengers and antioxidants have been shown to inhibit generation of eicosanoids induced by phosgene exposure, more recent evidence indicates that some of these agents may have additional roles in regulation of intracellular functions. Intracellular antioxidants, for example, may affect the extent of activation of the transcriptional factors NF- κ B and AP-1 and may thereby modulate a wide range of inflammatory responses at the level of mRNA synthesis [10].

Because of the idiosyncratic responses of different species and different cell types to phosgene, as well as the evolving evidence that therapeutic interventions might involve intracellular events which are difficult to study in whole animal models, we proposed to develop a series of *in vitro* human cell based assays for evaluating the potential of prophylactic or therapeutic agents to reduce injury from phosgene exposure *in vivo*. The use of a range of *in vitro* alternatives to animal testing has gained increasing favor among researchers for a number of reasons. There is a growing commitment to reduce the numbers of animals required for scientifically meaningful results and to modify procedures in order to minimize pain and discomfort. This mission has led to efforts of several agencies at the Federal level to promote research on "animal alternatives" [11]. Within the spectrum of *in vitro* methods, models have been developed employing isolated perfused organs, tissue slices and explants, and both primary cultures of normal cells as well as continuous cultures of immortalized cell lines [12]. Cell based studies have certain attractive advantages beyond reducing

the use of animals in research: an exceptionally wide range of normal and transformed human cell types and lines are now available for study; screening studies can be carried out with increased efficiency and reduced cost; reproducibility may be enhanced with greater control over such variables as duration of exposure, concentration of toxicant, and composition of surrounding medium; and probes which are responsive to mechanism-based actions of toxicants on cell functions may be employed. Disadvantages of cell-based models should also be recognized, including the loss of *in vivo* organ morphology, the danger of progressive depletion of nutrients and accumulation of end products in the cultures, and a limited range of measures of physiological function which are organ- rather than tissue- or cell-specific. In the future, cell-based systems for *in vitro* studies are likely to be increasingly directed towards "organotypic" models containing multiple cell types in arrangements which mimic at least some features of the *in vivo* setting.

In the case of the lung, with its diversity of cell types as well as its distinctive gross and microscopic morphological features, *in vitro* studies of toxicant injury at the cellular level are still mostly focused on individual cell types and are designed to address certain specific objectives appropriate to those cell populations [13], rather than attempting to replace animal or isolated perfused organ experiments [14]. Leakage of fluid and protein into the interstitium of the lung would presumably reflect injury to the endothelium of the pulmonary capillary bed, while further leakage into the alveolar space would reflect injury to the epithelial lining as well. Infiltration of the interstitium and the alveolar space with neutrophils would also be consistent with compromise to the cells constituting the endothelial and (in the case of alveolar space infiltration) epithelial barriers as well. Therefore we focussed on studying properties of lung microvascular endothelial and epithelial cells.

Human endothelial cells isolated from the pulmonary artery as well as from the capillary bed are commercially available, permitting a reliable supply of pure subpopulations of both macro- and microvascular endothelial cells. Especially important for our studies has been the "adaptation" of the microvascular endothelial cells to a medium in which the traditionally high levels of serum can be largely replaced by growth factors, hormones, and trace elements. In order to facilitate reproducibility, we have employed both "adapted" endothelial cells and medium from Clonetics Corp. (San Diego, CA). Pure populations of epithelial and smooth muscle cells from the tracheobronchial tree and small airways are also available from Clonetics, but alveolar epithelial cells are not amenable to passaging, and expanded populations cannot be prepared for commercial distribution. Of the epithelial cell types obtainable from the alveolar epithelium, only type II cells and Clara cells have been cultured in reasonably pure populations [13]. We have employed primary cultures of rat type II alveolar epithelial cells for some of our *in vitro* measurements, but in an effort to focus on human cell types as much as possible, we have also employed a stable tumor-derived human cell line, A549, which possesses both ultrastructural and biochemical features distinctive to the human type II pneumocyte [30].

This contract was directed to development of methods to evaluate injury to the endothelium and alveolar epithelium of the lung from phosgene exposure with the objective of developing prophylactic and therapeutic interventions for ameliorating such injury. In the first phase of this project, we concentrated on defining a series of assays of specific endothelial and type II alveolar epithelial cell functions which are associated with cytotoxic injury or with possible activation of intracellular signal transduction pathways resulting in mobilization of calcium ions, synthesis of cytokines, generation of reactive oxygen species, and release of arachidonic acid metabolites. In the second phase of the project, we had planned to employ these assays to evaluate the effectiveness of proposed prophylactic or therapeutic interventions for management of phosgene poisoning, but due to a shift in the priorities of the USAMRMC towards other toxicants, our progress in this second

phase was confined to initial evaluation of the potential uses of two antioxidants, N-acetyl cysteine and pyrrolidine dithiocarbamate, in management of phosgene exposure.

II. Objectives to be Met

This report covers progress on the areas of research defined as "Task 1" and "Task 2" in the Statement of Work. These objectives were:

1. To investigate the role of neutrophils in phosgene-induced lung injury in a rat model by using an anti-neutrophil antibody.
2. To determine the effects of phosgene on bovine and human pulmonary microvascular endothelial cells and on rat and human type II alveolar epithelial cells. The functional properties of the cells to be measured included indicators of cytotoxic injury, generation of reactive oxygen metabolites, release of arachidonic acid mediators, activity of lysosomal proton pumps, maintenance of a mitochondrial membrane electrochemical potential gradient, and alterations in intracellular calcium levels. In addition, it was proposed that the effects of phosgene on junctional integrity of endothelial and epithelial monolayers should be evaluated.
3. To evaluate candidate compounds for their effects as treatments for phosgene toxicosis, using the functional properties described in Objective 2 as criteria of therapeutic efficacy.

III. Results

A. Effects of Anti-Neutrophil Antibodies on Phosgene-Induced Lung Injury in the Rat

In these studies completed during the first three months of the project, we employed a polyclonal antiserum generated in rabbits against rat neutrophils to deplete live rats of their circulating neutrophils by administration 8 h prior to phosgene exposure. This procedure had been previously employed to assess the contribution of neutrophil-mediated injury to the epithelial damage in the lung induced by ozone exposure [15 110]. Those studies demonstrated that the antiserum effectively depleted both circulating neutrophils and appearance of neutrophils in bronchoalveolar lavage fluid but did not affect histologic evidence of epithelial cell necrosis or increase in protein content of bronchoalveolar lavage fluid. It was concluded from the previous studies that neutrophils do not play a major role in ozone-induced protein leak into the alveolar lining fluid or in epithelial cell injury.

Sprague-Dawley male rats of 250-300 g in weight were employed for these experiments. An initial group of six rats was exposed to a stream of 300 ppm phosgene in an acrylic box (cf. section D for details of the phosgene exposure chamber) for a period of 1 minute, followed by 10 minutes of "washing" with a stream of air. All rats survived this exposure to phosgene for 3 days. To evaluate the prophylactic effect of neutrophil depletion on phosgene-induced lung injury, a total of 24 rats was divided into four groups of 6 animals each. On Day 1, two groups were injected intraperitoneally with 0.5 ml of normal rabbit serum (Accurate Chemical #AIS403) while the other two groups received 0.5 ml of an affinity purified preparation of rabbit anti-rat neutrophil antiserum (Accurate #AIAD51140) to render them neutropenic. After an interval of 8 hours, one group of normal serum-treated controls and one group of anti-neutrophil antiserum treated animals were exposed to 300 ppm phosgene in the chamber for 1 minute, followed by a 10 minute air "wash," while the remaining two groups of animals were sham exposed to air only in the chamber for 11 minutes. After an additional interval of 24 hours, the animals were all sacrificed by intraperitoneal injection of pentobarbital. Samples of blood were obtained from the tail vein for differential determinations, and from the jugular vein for total cell counts. The lungs of each animal were lavaged with 20 ml of saline, of which 15-18 ml were routinely recovered by aspiration. The right lung from each animal was frozen at -70°C for future histopathologic examination, while the left lung was weighed, dried, and then reweighed for determination of the ratio of "wet to dry" weight. The

bronchoalveolar lavage samples were centrifuged to determine differential cell counts, and the supernatants were analyzed for total protein by the copper-bicinchoninic acid method (Pierce Chemical).

In our studies, we found that the anti-neutrophil antibody effectively depleted the percentage of circulating neutrophils in the differential counts of both phosgene-exposed and air-exposed animals from ~19% to ~5% (Figure 1), confirming the effectiveness of the procedure for rendering the animals neutropenic. Not surprisingly, this pre-treatment also dramatically reduced the infiltration of the lungs of phosgene-exposed rats with neutrophils (Figure 2). A very low percentage of neutrophils (~1%) was detected in the bronchoalveolar lavage fluid obtained from air-exposed rats, regardless of whether they had been rendered neutropenic. The percentage of neutrophils in phosgene exposed rats pre-treated with normal serum was very high ($72.67 \pm 1.27\%$), but was markedly reduced in the neutropenic rats ($7.79 \pm 0.93\%$). This marked reduction in neutrophilic infiltration was associated with a corresponding reduction in the leakage of protein into the alveolar space (Figure 3). The total BAL protein was low in both groups of air-exposed animals (< 0.5 mg/ml in both groups), whereas the level reached 3.19 ± 0.81 mg/ml in phosgene exposed rats pre-treated with normal serum. This level reached 0.73 ± 0.16 mg/ml in the phosgene exposed neutropenic rats, a value which was greater than those of the air exposed controls at a level of only marginal statistical significance. Interestingly, the accumulation of fluid in the lung, as contrasted with protein, was not markedly affected by phosgene exposure or by rendering the rats neutropenic. As seen in Figure 4, the wet to dry ratio of lung weights was slightly elevated in the lungs from phosgene exposed rats treated with normal serum, but not in the lungs from phosgene exposed neutropenic rats. However, the total fluid gain in rats exposed to phosgene without induction of neutropenia was so modestly elevated over that in the air exposed controls that no conclusions could be drawn from measurements of this parameter.

We conclude that pre-treatment of rats with anti-neutrophil antibody reduced the total alveolar lining fluid protein content 24 h after exposure to phosgene at a dose of 300 ppm·min. It would appear that, in contrast to ozone, phosgene does trigger a pattern of lung injury which includes a neutrophil-mediated inflammatory response. Modulation of this neutrophil-mediated component of lung injury should be considered in the development of prophylactic or therapeutic strategies to deal with cases of phosgene exposure.

The recent results of Ghio and Hatch [16] previously referred to suggest that the role of neutrophilic infiltration into the rat lung after phosgene exposure may be more complex than the results with anti-neutrophil antibodies might imply. In view of the previously observed diversity of species-specific responses to phosgene, it may be premature to extrapolate the significance of these results to mechanisms of phosgene-induced injury to humans.

B. Methods for Culture of Microvascular Endothelial Cells

In these studies we evaluated different methods for culture of microvascular endothelial cells. We found that human lung microvascular endothelial cells obtained from Clonetics can be cultured effectively on Falcon tissue culture plastic flasks and multiwell microplates to confluence, using Clonetics Microvascular Endothelial Cell Growth Medium (ECGM) with 5% serum. Because these cells are not transformed, they display classic contact inhibition, and their proliferative activity declines at densities of greater than 10^5 per cm^2 . These cells also achieve confluence on collagen-coated 0.45μ porous membrane-bottomed Costar TransWell cell culture inserts in the 5% serum-containing Clonetics medium, especially when initially plated at high densities to keep the number of additional divisions low. This strategy for achieving confluent monolayers of microvascular endothelial cells for measurements of junctional permeability is a modification of that employed by Yamada et al. for their studies on effects of calcium channel blockers, cyclic nucleotides, and

phorbol esters on human umbilical vein endothelial permeability [37,38]. The Clonetics cells cannot be passaged excessively, and were generally used at passages 4 through 12. Immediately prior to exposure to phosgene, we replaced the serum-supplemented Clonetics medium with Hanks balanced salt solution (HBSS) or with serum-free Clonetics medium to eliminate any endogenous antioxidants in the 5% serum-containing growth medium. Even in the absence of serum, the ECGM is a highly enriched medium and is capable of sustaining the endothelial cells, although it may not support proliferation. Typically, six 24 well microplates were prepared for each experiment. The range of cell densities and numbers on multiple wells of any one plate or set of plates prepared at the same time for an experiment was low, as reflected by the range of fluorescence intensities recorded from DNA-bound ethidium homodimer-1 in wells of methanol-treated cells (cf. section G). Due to some variation in growth kinetics and times at which experiments were conducted, the absolute numbers of cells at the time of exposure could not be matched from experiment to experiment. Thus, reproducibility among multiplicate samples within a single experiment was high, but for those measurements which were sensitive to absolute cell numbers, the variability from experiment to experiment was greater.

By employing a system of endothelial cells cultured on an underlying stroma or interstitium, it was our intent to replicate more closely the structural features of these cells within the lung, i.e. to develop a more realistic "organotypic" model. We found that endothelial cells achieve confluence with excellent preservation of normal morphology when cultured in a beta-tested version of Gibco serum-free endothelial cell growth medium or a "low serum" (2%) formulation of the Clonetics medium on a substratum composed of a complete interstitial extracellular matrix formed by R22 rat smooth muscle cells in culture [17]. In these media, the endothelial cells on this interstitial matrix synthesize a basement membrane which appears to retain some of the architecture and composition of native basement membrane extracellular matrix. The confluent cells also maintain their native morphology (with a characteristic "cobblestone" appearance) over repeated passages when they adhere to the interstitial matrix (Figure 5). In our original plans, we had intended to compare effects of phosgene on endothelial cells cultured directly on plastic with data obtained from this organotypic system of endothelial cells on the interstitial extracellular matrix. However, in response to more current priorities, we have instead proposed to transfer aspects of the technology of organotypic models to evaluate mechanisms of injury and repair after exposure to sulfur mustard.

C. Methods for Culture of Type II Alveolar Epithelial Cells

We employed the method of Dobbs [18] to obtain cultures of type II alveolar cells from rat lungs. After dispersal of the lung tissue with elastase, a mixture of cell types is obtained. Type II cells can be separated from other cells by their distinctive adherence properties. Initially, the cell mixture is allowed to adhere to plates coated with rat IgG, to which contaminating macrophages and lymphocytes adhere rapidly via their Fc receptors. The type II epithelial cells are then allowed to adhere more slowly to uncoated plates over a 22 h period to separate them from nonadherent contaminating cells. For these studies, adherence-purified rat type II epithelial cells were maintained in short term culture by being plated at high densities onto uncoated 0.4 μ porous Costar TransWells in Clonetics Bronchial Epithelial Cell Growth Medium, a serum-free culture medium which supports growth of rat type II alveolar epithelial cells. Immediately prior to phosgene exposure, the medium in the inserts was removed, while the medium in the surrounding wells was left in place to prevent dehydration of the cell monolayers. After exposure to 300 ppm phosgene or 5% CO₂ in air for 3 min, medium was added to the surrounding wells and to the inserts and the levels adjusted to eliminate any hydrostatic pressure gradient.

The human alveolar cell carcinoma-derived cell line A549 was also employed in some preliminary experiments as a model of the human type II pneumocyte. The A549 cell line was

developed in the late 1970s as a stable, transformed human line which retains several distinctive features of type II pneumocytes, including the active synthesis of phosphatidylcholine containing a high percentage of saturated fatty acids (especially palmitate) via the CDP-choline pathway [30], and the development of multilamellar bodies in confluent cultured cells which can be exocytosed in response to stimulation with the calcium ionophore A23187 [19]. A549 cells also retain some of the regulatory controls on phospholipid metabolism which are characteristic of type II pneumocytes, including binding of glucocorticoids to plasma membrane receptors [20] and induction of lecithin synthesis by prostaglandins [21]. Culture of A549 cells in flasks and multiwell plates was carried out using Clonetics bronchial epithelial cell growth medium in a fashion identical to that employed for the rat type II alveolar epithelial cells. As discussed above for endothelial cells, numbers and densities of A549 cells in wells of any one plate, or among plates within a single experiment fell within a narrow range, but numbers and densities could not be so tightly controlled from experiment to experiment.

D. Method for Exposure to Phosgene

All phosgene exposures were carried out in an acrylic box of dimensions approximately 16" x 16" x 16" placed within a hood with airflow in excess of 1,000 cu ft/min. The gas inlet to the box received either 300 ppm phosgene gas in air (Matheson Corp) or 5% CO₂ in air. Gas flow was adjusted to 5 L/min at 5 psi. Once the phosgene passed through the box, it was drawn into the exhaust line along with the air entering the surrounding hood, and passed through a jet spray of Na₂CO₃ solution in an in-line "scrubber" to inactivate the toxicant before venting to the outside. The exposure chamber and room were all constructed to meet Federal safety guidelines. Exposures of cultured cells to gases within the box were generally limited to a total of 10 minutes; the time at which gas flow was transferred from the source of 300 ppm phosgene to 5% CO₂ in air is noted throughout this report. The composition of phosgene in the supply tanks was verified initially by passing 2 L of gas through impingers into 10 ml of 0.01 N NaOH. Under these conditions, each equivalent of phosgene is quantitatively converted to 2 equivalents of HCl, which neutralize a corresponding amount of NaOH. The remaining NaOH is then titrated with a standardized HCl solution. Accurate determinations of the concentration of phosgene gas within the chamber or dissolved within the culture medium above the exposed cells were not undertaken, and so the true integrated doses of phosgene to which the cells were exposed, as well as the detailed time course of phosgene concentration during the exposure remain unknown. We recognize the serious limitations which the absence of such data place on true dosing values. Since a single exposure protocol was used consistently throughout the studies reported here, times of "exposure" to 300 ppm phosgene represent durations of 5 L/min flow of 300 ppm phosgene into the acrylic box. The term "exposure" is used throughout this report to represent this duration of phosgene gas flow.

E. Junctional Integrity of Pulmonary Microvascular Endothelial Cells

We employed two different assays of the effects of phosgene on junctional integrity of monolayers of endothelial and type II alveolar epithelial cells. Endothelial cells do not develop very tight junctions in culture under the best of conditions, and measurements of electrical resistance of monolayers are not very sensitive to effects of phosgene. Our initial measurements of effects of phosgene on junctional integrity of human lung microvascular endothelial cell monolayers and subsequent measurements on junctional integrity of rat type II alveolar epithelial cell monolayers were carried out by measuring rates of permeability of mannitol, a low molecular weight solute (MW = 186). As discussed above in section B, by employing a modification of the method of Yamada et al. [37,38], in which we applied an initial high seeding density of 5×10^5 cells/cm² to collagen-coated 0.45 μ porous membrane-bottomed Costar TransWells, we ensured that cells which had been detached from flasks at or near confluence would re-establish confluence on the cell culture inserts

after overnight growth without significant additional proliferative activity. One hour prior to exposure to phosgene, the medium in the TransWells and in the surrounding wells of the microplate was removed and replaced with fresh serum-free ECGM containing 1 μ M mannitol. The medium in the TransWells was removed immediately before the cells in their microplates were exposed to 300 ppm phosgene for 3 min, followed by a 7 min washout with 5% CO₂ in air. The medium in the surrounding wells was adjusted to 1 ml, and 0.2 ml of medium containing 1 x 10⁶ cpm [¹⁴C]-mannitol was added to the inserts. These volumes were selected to eliminate any hydrostatic pressure gradient on the porous membrane-bottomed inserts. After addition of the medium containing [¹⁴C]-mannitol to the TransWells, the medium in the surrounding wells was sampled over the next four hours to determine the rate of diffusion of the radiolabel from the TransWells into the surrounding medium. Figure 6 illustrates the rate of diffusion of mannitol from the TransWells into the surrounding medium across the barrier formed by monolayers of microvascular endothelial cells exposed to 300 ppm phosgene for 3 minutes followed by 7 min washout. This diffusion rate is compared to that observed across the barrier of control monolayers of endothelial cells exposed to 5% CO₂ continuously for 10 min under the same experimental conditions. Four experiments were performed on triplicate TransWells to obtain this data; the error bars show the standard error of the mean for each treatment group. The rate of diffusion of mannitol after phosgene exposure was about 21% greater than that for the controls (1056 vs 873) with a P value of 0.03, indicating that the difference is statistically significant. Hypotheses to address the origin of this increased permeability are considered in the following section.

F. Junctional Integrity of Type II Alveolar Epithelial Cells after Exposure to Phosgene

We also examined the effects of 900 ppm·min exposure to phosgene on the junctional integrity of rat type II alveolar cell monolayers formed on Costar TransWells. The electrical resistance of the epithelial cell monolayers after exposure was determined with a Millicell ERS ohmmeter. This experiment was performed on triplicate samples. Our experimental apparatus is not compatible with resistance measurements during phosgene exposure, since the medium above the TransWells is removed while the cells are in the exposure chamber, and the shortest time between termination of the exposure and measurement of electrical resistance is about 15 min. By this time, the resistance of the rat type II alveolar epithelial cells was observed to have declined from a pre-exposure level of ~1000 ohms to ~600 ohms, as shown in Figure 7. This reduced level of electrical resistance remained remarkably constant over the next 24 h, suggesting that the nature of the alterations to the epithelial cell junctions induced by phosgene exposure is irreversible, but does not result in further deterioration of the junctional integrity. Rat type II alveolar cells which were "sham" exposed to 5% CO₂ in air maintained their initial high electrical resistance, showing that the exposure protocol itself did not adversely affect the junctional integrity of the monolayers. It is noteworthy that these rat type II alveolar cell monolayers formed much tighter junctions than the human microvascular endothelial cell monolayers, either before or after phosgene exposure, as reflected by their much greater electrical resistance.

We also prepared rat lung type II alveolar cell monolayers on TransWell cell culture inserts for quantitating effects of phosgene exposure on permeability to mannitol. We hypothesized that the relatively modest fractional increases in the already rapid diffusion of mannitol after exposure to phosgene, which we had previously observed with human microvascular endothelial cell monolayers, would not be seen in these studies on type II epithelial monolayers, with their intrinsically tighter junctions. As in the electrical resistance studies, cells were maintained in short term culture for these studies by being seeded at high initial densities directly onto 0.4 μ TransWells in Clonetics bronchial epithelial cell growth medium. The TransWells were placed in 24 well microplates for culture, and immediately prior to phosgene exposure, the medium in the inserts was removed, while

the medium in the surrounding wells was left in place to prevent dehydration of the cell monolayers. After exposure to 300 ppm phosgene or 5% CO₂ in air for 1 min or 3 min, fresh medium containing ¹⁴C-mannitol (1 x 10⁶ cpm) was added to the TransWells and the medium in the surrounding wells was sampled over the next four hours to determine the rate of diffusion of the radiolabel from the TransWells into the surrounding medium as described above in section E. This experiment was performed twice on triplicate wells for each treatment group. In our previous studies with microvascular endothelial cells, we observed that the high "baseline" rate of diffusion of radiolabeled mannitol was modestly augmented after 3 min phosgene exposure. As shown in Figure 8, the absolute permeability of type II epithelial monolayers is much lower than that of the endothelial monolayers (~20 cpm/min for type II monolayers vs ~870 cpm/min for endothelial monolayers), and the increase induced by 3 min of phosgene exposure is considerable (> five-fold increase for the type II monolayers vs ~20% increase for the endothelial monolayers). As was the case for our previous endothelial monolayer studies, the origin of this increased permeability cannot be established unequivocally by measurements of mannitol diffusion rates alone. It is possible that phosgene exposure resulted in scattered cytotoxic foci throughout the endothelial and type II epithelial cell monolayers, and increased diffusion occurred at these sites. Alternatively, phosgene may have triggered "activation" of the endothelial and type II epithelial cells resulting in gaps among the junctions. This latter interpretation is consistent with the phosgene-induced changes in cytoskeletal F-actin in endothelial cells observed by Werrlein et al. [22]. It would be necessary to test for other evidence of endothelial and type II epithelial cell activation to establish the origin of the increased rate of mannitol diffusion; such evidence is presented in following sections. In the future, studies on the permeation of higher molecular weight solutes in which rates of diffusion of a series of fluorescent dextrans across cell monolayers are measured after exposure to phosgene might provide additional clarifying results.

From our previous studies of electrical resistance, we believe that few holes of substantial size were introduced into the type II epithelial cell monolayers after 3 min of phosgene exposure, or we would have expected a more significant reduction in electrical resistance of the monolayers. We therefore do not expect that confluent type II alveolar cell monolayers would permit passage of high molecular weight solutes such as the series of fluorescent dextrans, even after phosgene exposure, whereas such high molecular weight solutes may be the only valid probes for determination of effects of phosgene on endothelial cell junctions.

A significant finding is the marked integrity of the junctions within the type II epithelial monolayers after flow of 300 ppm phosgene into the exposure chamber was limited to 1 minute. This result alone would suggest that these cells might not be significantly affected by 1 min of such "exposure", but additional measurements of alterations in cell functions, presented in the following sections, were undertaken to pursue this question. On the basis of all our results, we conclude that alterations in cell functions can be detected as a consequence of 1 min of flow of 300 ppm phosgene into the exposure box. Such alterations after 1 min of exposure may not result in outright cytotoxicity to all the cells but may manifest themselves as physiological changes in such parameters as production of reactive oxygen metabolites and eicosanoids or changes in calcium permeability which may not be apparent for several hours. While we found that the rat type II alveolar epithelial cells are especially useful for measurements of monolayer electrical conductance and permeability to low molecular weight metabolites, we planned to pursue the possibility of physiological changes in type II epithelial cells with the A549 alveolar carcinoma-derived cell line. This cell line is of human origin, and is therefore more amenable to assays of levels of cytokines released after phosgene exposure; its human source also suggests that its sensitivity to phosgene may be more reflective of the human body than any findings obtained from rat cell monolayers. While we did have the opportunity to use this cell line for studies of cytotoxic injury and mitochondrial membrane

potential changes resulting from phosgene exposure, preliminary experiments on electric resistance of A549 cell monolayers indicated that cultures which appear confluent by light microscopy do not form tight junctions. No further studies on effects of phosgene on junctional integrity of human type II alveolar epithelial cells have been undertaken at this time, but as we describe in following sections, the A549 cell line displays other functional properties which suggest that it is indeed more resistant to phosgene than human lung microvascular endothelial cells.

G. Detection of Cytotoxic Injury to Nuclear and Plasma Membranes of Microvascular Endothelial Cells Using Fluorescent Probes

In order to assess cytotoxic injury induced by phosgene exposure, we elected to employ a set of fluorescent probes which are sensitive to the integrity of nuclear and plasma membranes. Use of these probes has several advantages over such methods as Trypan Blue exclusion measurements which were previously used to distinguish "live" cells from "dead" cells. 1) It is possible to quantitate the magnitude of injury in multiple samples efficiently with a multiwell microplate spectrofluorimeter. 2) Probes for nuclear and plasma membrane integrity can be employed simultaneously. 3) Kinetics of progression of cytotoxic injury can be determined. It is important to note that cells in which nuclear and plasma membranes have been compromised may have been designated as "dead" by previous criteria for cytotoxicity but such cells may in fact retain a number of functions and may continue to carry out metabolic processes for several hours. We have therefore described the changes detected in these assays as indicative of cytotoxic *injury* rather than "cell death." We used a pair of probes which are similar to the combination of BCEF-AM and neutral red adopted by the laboratory of Robert Van Buskirk in previous Army contract work [23], but which have less sensitivity to intracytosolic pH [24]. Calcein acetoxymethyl ester (calcein-AM) is nonfluorescent and is freely permeable to the cytosol. The nonfluorescent ester is hydrolyzed to the strongly fluorescent free calcein only in cells in which the plasma membrane is intact and cytosolic nonspecific esterase activity is retained. The esterolysis of calcein-AM can be followed kinetically by measuring the rate of appearance of fluorescence from free calcein, or cells can be incubated for ~45 min - 1 h with the ester for an "endpoint" determination of extent of plasma membrane integrity. Nuclear membrane integrity can be assessed with the DNA-intercalating dye, ethidium homodimer-1, which undergoes a very marked increase in fluorescence when it binds to DNA, but which can reach the nucleus from the extracellular milieu only when the nuclear and plasma membranes are compromised. Thus, cells with no nuclear or plasma membrane injury ("live" cells, as defined in the original description of this method) develop strong green fluorescence from free calcein, but display no red fluorescence as long as ethidium homodimer-1 is excluded from the nucleus. Membrane injury is seen as a loss of green fluorescence and a gain of red fluorescence ("dead" cells, as originally designated). The hydrolysis of calcein-AM is primarily a kinetic process, the rate of which is determined by the absolute number of "live" cells, whereas spontaneous hydrolysis of the ester by "dead" cells or by medium alone takes 24 h. Thus, both the rate of increase in fluorescence intensity and the relative fluorescence intensity from calcein at the end of a fixed time interval (typically 45-60 min) are proportional to the number of "live" cells. The rate of binding of ethidium homodimer-1 to the DNA of "dead" cells is rapid, so that the "endpoint" value of ethidium fluorescence is typically achieved within the interval of time for preparing the plate and reading it in our instrumentation; the rate of entry into "live" cells is imperceptibly slow. Thus, the relative fluorescence intensity from ethidium is proportional to the number of "dead" cells. The responses of calcein-AM esterolysis and ethidium binding can generally be compared among the wells of a single plate (or batch of plates) exposed to an experimental challenge, but since each of these probes is sensitive to the absolute number of cells which are viable (capable of hydrolyzing calcein-AM) or nonviable (allow ethidium homodimer-1 to bind to DNA), comparisons of fluorescence intensity between two different

experiments, in which total cell numbers within the wells may be quite different, may not always be feasible. We have endeavored to identify circumstances under which the absolute number of cells in the wells of a particular plate contributed to the fluorescence intensity of a specific probe by treating duplicate or triplicate wells with methanol, to allow for maximum binding of ethidium homodimer-1.

The Cytofluor 2300 multiwell fluorescent microplate reader is an ideal instrument to determine the fluorescence from the two probes simultaneously. In preliminary studies, we developed standard curves for determining percentages of "live" and "dead" cells in wells of microplates after exposure to potentially cytotoxic agents. These standard curves make use of the fluorescence at 530 nm arising from calcein, and the fluorescence at 645 nm from DNA-bound ethidium homodimer-1. Using the "endpoint" method of obtaining measurements at the end of a fixed time point, the percentages of "live" and "dead" cells can be calculated from the relationships:

$$\% \text{ live cells} = \frac{\text{measured signal}_{530} - \text{minimum signal}_{530}}{\text{maximum signal}_{530} - \text{minimum signal}_{530}}$$

$$\% \text{ dead cells} = \frac{\text{measured signal}_{645} - \text{minimum signal}_{645}}{\text{maximum signal}_{645} - \text{minimum signal}_{645}}$$

Typical standard curves for R22 rat smooth muscle cells exposed to different concentrations of methanol (5%, 25%, 50%, and 75%) in medium to induce varying degrees of cytotoxic injury are illustrated in Figures 9 and 10. The results show that within 45 min, both calcein and ethidium fluorescence achieve stable values in the methanol-treated cells.

In our initial application of this method to studies on cytotoxic injury induced by phosgene exposure, we exposed bovine endothelial cells in 24 well microplates to 300 ppm phosgene in air for periods of 3 min, 5 min, 7 min, and 10 min, followed by 10 min washouts with 5% CO₂ in air. Immediately before exposure, the medium above the cells was replaced with HBSS, and immediately after removal of the cells from the exposure chamber, the HBSS was replaced with fresh endothelial cell growth medium. After additional incubation for 2 h, the medium was removed and replaced with 2 μM ethidium homodimer-1 and 3 μM calcein-AM freshly prepared in HBSS. The cells were incubated for 45 min to achieve stable levels of free calcein and DNA-bound ethidium before reading the fluorescence at 530 nm with 485 nm excitation and at 645 nm with 530 nm excitation. All measurements were made with a Cytofluor 2300 and were carried out in triplicate. Cells in control plates were not exposed either to phosgene or to air in the chamber prior to the assay, or were exposed only to air in the chamber. In each plate, a well of cells was treated with 70% methanol for 1 h prior to the incubation with calcein-AM and ethidium homodimer-1 to serve as a control for 100% cytotoxicity. Figure 11 illustrates the effect of phosgene exposure on cytotoxic injury to bovine endothelial cells. It is evident that these cells were highly resistant to cytotoxic effects of phosgene for periods of up to 10 min exposure. Minimal reduction of calcein fluorescence was detected after phosgene exposure, suggesting that plasma membrane integrity was not significantly compromised by the phosgene exposure. Some increase in nuclear membrane permeability was detectable after phosgene exposure as evidenced by an increase in ethidium homodimer-1 fluorescence. It must be emphasized that these results show only that the plasma membranes and nuclear membranes of the bovine endothelial cells did not suffer marked loss of integrity after these intervals of exposure to phosgene, and do not address any effects on intracellular metabolic processes to which these probes are not sensitive.

We then exposed human lung microvascular endothelial cells (Clonetics) in 24 well microplates to 300 ppm phosgene in air for periods of 1 min, 3 min, 6 min, and 9 min, followed by 10 min washouts with 5% CO₂ in air. As in the case of the bovine endothelial cells, all measurements on cells exposed to phosgene or 5% CO₂ only were performed in triplicate. For some measurements, we employed duplicate plates, each of which contained triplicate samples, for each exposure condition. Immediately before exposure, the ECGM above the cells was replaced with 100 μ l of HBSS per well. We have established that this volume is just sufficient to avoid drying of the wells during subsequent exposures to phosgene or air, but does not impede effective diffusion of the phosgene gas to the cells. To further reduce risk of drying, immediately after removal of the cells from the exposure chamber, the HBSS was replaced with 500 μ l fresh HBSS if cytotoxic injury measurements were made immediately, or with fresh ECGM if the cells were incubated for a significant additional interval of time prior to cytotoxicity measurements. It should be noted that HBSS contains glucose, and thus provides an energy source for some extended maintenance of cell functions. For the actual assay measurements, the medium was removed and replaced with 2 μ M ethidium homodimer-1 and 3 μ M calcein-AM freshly prepared in HBSS. The microplates were read in the Cytofluor 2300 every 15 minutes for 1 h to determine the rate of generation of free calcein and DNA-bound ethidium by recording the fluorescence at 530 nm and 645 nm. Cells in control plates were not exposed either to phosgene or to air in the chamber prior to the cytotoxicity assay, or were exposed only to air in the chamber. In each plate, a well of cells was treated with 70% methanol prior to the incubation with calcein-AM and ethidium homodimer-1 to serve as a control for 100% cytotoxicity. Figures 12 through 15 illustrate the time course of conversion of calcein-AM to the free fluorophore (closed triangles) and the extent of binding of ethidium homodimer-1 (closed squares) for human microvascular endothelial cells exposed to air only (Figure 12), or to 300 ppm phosgene for 1 min (Figure 13), 3 min (Figure 14), and 6 min (Figure 15), followed by a subsequent 2 h incubation in ECGM prior to assay. In these figures, the relatively constant low calcein fluorescence (open triangles) and the high ethidium fluorescence (open squares) of the methanol-treated cells in the "100% cytotoxicity" control wells are shown for comparison with the fluorescence from the cells in the test wells. It is evident that under these conditions, in contrast to the bovine cells, human lung microvascular endothelial cells proved to be highly sensitive to cytotoxic effects of phosgene which could be detected after a period of exposure as brief as 1 min. A marked reduction in the rate of generation of calcein fluorescence was detected after 1 min phosgene exposure, suggesting that plasma membrane integrity was significantly compromised. Additionally, a significant increase in nuclear membrane permeability was detectable after as little as 1 min phosgene exposure as evidenced by an increase in ethidium homodimer-1 fluorescence, approaching that of the methanol-treated cells. By 3 min of phosgene exposure, nearly maximum effects on loss of cytosolic esterolytic activity and increase in nuclear permeability to ethidium homodimer-1 were observed. When we performed the cytotoxicity assay on cells 10 min after exposure to phosgene, we obtained the same results, indicating that cytotoxic injury developed either during or immediately after phosgene exposure, and that subsequent incubation in ECGM in air for several hours resulted neither in exacerbation nor in reduction of cytotoxic injury. In Figure 16, the levels of esterolyzed calcein and DNA-bound ethidium after 1 h of incubation with the two probes are illustrated for human endothelial cells which had been exposed to 5% CO₂ in the chamber for 10 min but not to phosgene, and for cells which had been exposed to phosgene for 1 min, 3 min, or 6 min. These levels are expressed relative to the levels of calcein formed in endothelial cells which were incubated with calcein-AM immediately upon removal of the culture medium (100% "Live") and the levels of DNA-bound ethidium homodimer-1 in methanol-treated cells (100% "Dead"). Exposure of cells to 5% CO₂ in air only resulted in levels of calcein and DNA-bound ethidium which were within experimental error of those found in cells analyzed immediately after removal of the ECGM. The

phosgene dose dependence of calcein-AM esterolysis and ethidium binding after 1 h of incubation with the probes was fully consistent with the kinetic data we obtained by monitoring fluorescence every 15 min, but we felt it was important to have both methodologies available for studies involving use of prophylactic or therapeutic interventions.

These results confirmed the importance of conducting experiments on human cells whenever possible, since the marked species differences in sensitivity to phosgene which were previously observed with whole animals appear also to be present in cells studied *in vitro*. Additional studies on effects of phosgene exposure on the cytosolic esterase activity and nuclear permeability to dyes in human microvascular endothelial cells are presented below in conjunction with other measurements of calcium permeability and generation of intracytosolic reactive oxygen metabolites. The use of multiwell plates facilitates assay of these different functional properties on cells in different wells of the same plate, so that the results obtained with the different probes can be compared with greater confidence.

H. Detection of Phosgene-Induced Cytotoxic Injury to A549 Epithelial Cells

As indicated above, the human A549 cell line has many similarities to type II pulmonary epithelial cells with respect to metabolism [19,20,30], although its ability to form tight junctions in culture appears to be limited. We therefore employed this cell line as a model of human type II pneumocytes for studies on cytotoxic effects of phosgene exposure. A549 cells were grown to confluence in 24 well microplates and, after replacement of the culture medium with 100 μ l HBSS per well, were exposed to 300 ppm phosgene for 1 or 3 minutes in triplicate wells as described in the previous section for human microvascular endothelial cells. An additional 500 μ l HBSS was added and the cells were then immediately incubated with calcein-AM and ethidium homodimer-1 or the HBSS was replaced with fresh medium for a period of six hours prior to assay with calcein-AM and ethidium homodimer-1, as described for human endothelial cells in the previous section. Results for cells assayed by incubation with the probes for 45 min, six hours after exposure to phosgene, are shown in Figure 17; results for cells assayed immediately after phosgene exposure were identical within experimental limits. The effects of phosgene on the rate of calcein-AM hydrolysis by the A549 cells were also fully consistent with data obtained by the "endpoint" method, in which the levels of free calcein formed were determined after 45 min of incubation with the probes. It is apparent that A549 cells were sensitive to phosgene exposure, but the human type II pulmonary epithelial cell line was significantly more resistant than the microvascular endothelial cells. After 3 minutes of phosgene exposure, there was only a ~50% reduction in cytosolic nonspecific esterase activity in the A549 cells, whereas the esterase activity in the human endothelial cells was very much lower after 3 minutes of exposure. Slight, but reproducible alterations in both esterase activity and nuclear permeability to ethidium homodimer-1 were detected in the A549 cells after 1 minute of exposure to phosgene. As shown in the following sections, the mitochondrial membrane potential of A549 cells was found to be less sensitive to phosgene exposure than that of human endothelial cells; the ability of the epithelial cell line to maintain calcium pump activity was also shown to be greater than that of endothelial cells. These findings suggest the possibility that phosgene-induced injury may develop earlier and with greater severity to the pulmonary endothelium than to type II epithelial cells. Such evidence of differential sensitivity of pulmonary endothelium and epithelium to phosgene is consistent with the findings of Werrlein et al. on differential effects of phosgene on the F-actin content of pulmonary endothelial and epithelial cells [22]. However, some other distinctive features of A549 cells, such as elevated levels of intracellular glutathione [31], may contribute to their unusual phosgene resistance, and extending these results to the normal human alveolar epithelium may still be premature at this stage. Moreover, the effects of phosgene on other types of epithelial cells lining the alveolar space, as well as the large and small airways, were not

addressed in these studies, and the contribution of compromise of these components of the epithelial barrier to leakage of fluid and protein into the lung has not been investigated.

I. Effects of Phosgene Exposure on Mitochondrial Membrane Potential of Human Microvascular Endothelial Cells

We employed two techniques to probe the effects of phosgene exposure on the mitochondrial membrane potential of human microvascular endothelial cells. At the Cancer Research Institute of New York Medical College we used the lipophilic cationic dye Rhodamine 123, which accumulates in those mitochondria in which a membrane potential is maintained [25]. Endothelial cells were exposed to 300 ppm phosgene for 1 min before detachment by trypsinization and incubation with 10 μ g/ml Rhodamine 123 (R123) in Dulbecco's phosphate-buffered saline (PBS) for 30 min. The cells were then washed and resuspended in 20 μ g/ml propidium iodide (PI) in PBS before analysis by flow cytometry. Cells which were R123-positive and PI-negative were considered to be functionally normal, while cells which were R123-negative and PI-positive had compromised membranes and had lost the capacity to retain a mitochondrial potential gradient [26]. The lack of precise measures of true phosgene exposure makes these studies, as well as those on acridine orange uptake into lysosomes (cf. section *M*), somewhat difficult to compare to studies on cells in 24 well microplates, especially since the configurations of flasks and plates are so very different. However, as we show below, the qualitative patterns of response demonstrated by the two types of experiments are in good agreement.

Figure 18 illustrates the effects of 1 min of phosgene exposure on mitochondrial membrane potential as measured by this protocol. The percentage of R123-negative, PI-positive cells increased from 4.5% in the controls exposed to 5% CO₂ in air to 14.8% in cells exposed to 300 ppm phosgene for 1 min. In addition to the cells which had effectively lost all capacity to maintain a mitochondrial membrane potential after phosgene exposure, a smaller subset of cells appeared to have some partial compromise in cell functions. These cells had intermediate levels of R123 fluorescence, along with some PI uptake, suggesting a transitional state of injury. The subset of cells which exhibited this transitional state was found to be extremely small (1.1%) in the control population exposed to 5% CO₂ in air, but amounted to 5.2% of the entire population of cells exposed to phosgene for 1 min. Furthermore, within the subset of cells exhibiting very low PI fluorescence, there was also a variable decline in R123 MFI after 1 min of phosgene exposure. One example of this decline is illustrated in Figure 19, which shows a histogram of the distribution of R123 fluorescence in PI-negative cells exposed to 5% CO₂ in air or to 300 ppm phosgene for 1 min. In this experiment, the R123 MFI declined by 11% after phosgene exposure, while in other experiments the decline was only 6.7% or not detectable at all. Further studies would be required to determine whether the population of cells with reduced R123 fluorescence would go on to exhibit more severe functional compromise or would recover normal properties.

At Stony Brook, a different approach to measurement of mitochondrial membrane potential which does not involve detachment by trypsinization was employed. This method makes use of a novel probe of mitochondrial membrane potential known as JC-1, developed by the laboratory of Lan Bo Chen [27-29]. JC-1 is a lipophilic cationic cyanine dye which undergoes marked red shifts in its excitation and emission spectra when it aggregates. Chen's laboratory has shown that accumulation of JC-1 into mitochondria is accompanied by formation of these "J-aggregates" only when the mitochondrial membrane potential is maintained. When the electrochemical potential of the mitochondria is redistributed almost entirely towards a pH gradient by addition of valinomycin, the formation of J-aggregates is abolished, while addition of nigericin, which collapses the pH gradient and shifts the mitochondrial electrochemical potential to solely a membrane potential gradient, enhances J-aggregate formation. In our studies, we employed human microvascular

endothelial cells which had been exposed for 10 min to 5% CO₂ in air only or to 300 ppm phosgene for various times ranging from 1 min to 9 min. The cells were then treated directly with a solution of 10 µg/ml JC-1 in HBSS for 12 min or were maintained for 2 h in endothelial cell growth medium before the 12 min incubation with 10 µg/ml JC-1 in HBSS. JC-1 is extremely lipophilic and must be dissolved in dimethyl sulfoxide. The final working solution of JC-1 in HBSS is extremely unstable and the dye rapidly precipitates, adhering to hydrophobic surfaces such as plastic tubes, pipet tips, and microplate wells. While the lipophilicity of JC-1 made it difficult to control the actual final concentration of dye to which the cells were exposed in the various studies reported here, the use of multiwell microplate technology facilitated assay of control and experimental groups of cells simultaneously, so that in any one experiment, all wells were incubated with the same concentration of dye. After the 12 minute incubation, the JC-1 solution was aspirated and replaced with fresh HBSS alone and the fluorescence at 530 nm (arising from JC-1 monomers) and 590 nm (arising from J-aggregates) was determined simultaneously with 485 nm excitation, using the Cytofluor 2300 [28]. The same cells were then incubated in HBSS for 2 h at 37°C and the fluorescence of JC-1 monomers at 530 nm and J-aggregates at 590 nm was redetermined. Figure 20 illustrates the fluorescence from JC-1 monomers and J-aggregates after different periods of phosgene exposure or after exposure to the control atmosphere of 5% CO₂ in air. While there was an increase in the uptake of JC-1 into the cells after phosgene exposure, this increase was almost solely due to uptake of monomers, and not to intramitochondrial concentration of the dye into J-aggregates. (A light microscopic analysis of the different patterns of JC-1 uptake is discussed in section K.) The total concentration of intracellular JC-1 declined over time after replacement of the dye-containing medium with fresh HBSS, but the ratio of monomers to J-aggregates underwent relatively little further change. Control cells exposed to 5% CO₂ in air continued to take up JC-1 over time, but in this case, the uptake was associated with a much higher ratio of aggregates to monomers than was seen in the phosgene-treated cells. To emphasize the distinction between total cellular uptake and intramitochondrial concentration into J-aggregates, the ratio of fluorescence at 590 nm (J-aggregates) vs 540 nm (monomers) by control and phosgene-treated cells is illustrated in Figure 21. Cells which were "sham"-exposed to 5% CO₂ had a ratio of J-aggregates to JC-1 monomers which was greater than 1 and which persisted over 2 h, very similar to the pattern of JC-1 uptake exhibited by cells which were exposed to JC-1 directly after being maintained in ECGM. After as little as 1 min of exposure to 300 ppm phosgene, the ratio of aggregates to monomers fell to about 1:2, and persisted at this low value over 2 h. These results demonstrating marked alterations in endothelial cell physiology after an exposure to phosgene as brief as 1 minute are consistent with our observations of the effects of a 1 minute exposure to phosgene as detected by loss of calcein esterolytic activity and increased nuclear binding of ethidium homodimer-1. Additional measurements of mitochondrial membrane potential of endothelial cells after phosgene exposure which were matched with measurements of other functional properties are presented in sections K and R.

J. Effects of Phosgene Exposure on Mitochondrial Membrane Potential of the A549 Human Pulmonary Epithelial Cell Line

Unlike the marked sensitivity of human endothelial cell mitochondrial membranes to phosgene exposure, the mitochondrial membranes of A549 epithelial cells are extremely resistant to phosgene. Figure 22 illustrates the fluorescence from JC-1 monomers and aggregates in A549 cells after exposure to 5% CO₂ only or after exposure to 1 min or 3 min of 300 ppm phosgene. The ratio of aggregates to monomers, based on fluorescence intensity, is ~2:1, and is virtually unaffected by phosgene. We do not know the precise mechanism by which A549 cells achieve their resistance to phosgene, but the ability of the mitochondrial membranes in these type II pulmonary epithelial cells to maintain an electrochemical potential after exposure to a phosgene dose which induces some

changes in cell functions is consistent with the relative resistance of the nonspecific esterase activity of these cells to phosgene exposure (cf. section *H*) and the capacity of the calcium pumps in A549 cells to maintain a low intracellular calcium concentration even in the presence of calcium ionophores (cf. section *L*).

K. Intracellular Calcium Levels in Microvascular Endothelial Cells

For these studies, human microvascular endothelial cells from Clonetics Corp. were cultured in Endothelial Cell Growth Medium (ECGM) containing 5% serum as described above. Cells were plated in 24 well microplates to permit evaluation of a single plate with multiple probes, using different wells for each probe. As described above, prior to phosgene exposure, the medium was replaced with 100 μ l Hank's balanced salt solution (HBSS) in each well, and immediately after exposure, the medium was replaced again with 500 μ l fresh HBSS. For studies on cells maintained for longer than 3 hours after phosgene exposure, the HBSS was replaced with fresh ECGM. From our studies on mitochondrial membrane potential, nonspecific esterase activity, and exclusion of DNA-intercalating dyes, we concluded that control cells, not challenged with agents that might affect calcium homeostasis, would not suffer significant cytotoxic injury for intervals up to 3 hours in HBSS after sham exposure to 5% CO₂, and, when ECGM was added, for periods in excess of 12 hours after sham exposures.

We selected the probe fluo-3 for measurements of intracellular calcium levels because its excitation and emission spectra overlap closely those of fluorescein, calcein, and related fluorophores, thereby facilitating measurements with the Cytofluor 2300 as well as with the flow cytometer [26]. Since the literature on use of fluo-3 for measurements of intracellular calcium with our instrumentation was somewhat limited, we first confirmed the response of the dye to an agent known to act as a calcium ionophore, ionomycin, as illustrated in Figure 23. Six wells of HMVEC were initially incubated with 10 μ M fluo-3 acetoxymethyl ester for 30 min in HBSS to allow the calcium probe to enter the cytosol where nonspecific esterases remove the protecting group, trapping the probe in the cytosol. Even though this buffer contains about 1.5 mM calcium, as long as the membranes and calcium pumps of the cells are not perturbed, the calcium pumps maintain the intracellular calcium at low levels, and since the acetoxymethyl ester does not bind calcium, background fluorescence is relatively low after replacement of the extracellular medium with fresh HBSS. This initial fluorescence at 530 nm is indicated by the "pre" bars in Figure 23. The cells in three wells were treated with 10 μ M ionomycin or, in the other three wells, with a corresponding volume of HBSS and the fluorescence at 530 nm recorded again ("post"). Addition of this ionophore to human endothelial cells led to an increase in fluo-3 fluorescence which is faster than we could detect with the Cytofluor 2300 (the shortest time between exposure to the stimulus and reading of fluorescence is about 2 minutes with this instrument). At a lower concentration of ionomycin, we could follow the kinetics of other cellular responses to the increase in intracytosolic calcium induced by the ionophore. Figures 24 and 25 show the effects of 1.5 μ M ionomycin on HMVEC. The increase in intracytosolic calcium was detected immediately, whereas a calcium-induced generation of intracellular reactive oxygen species, as measured by oxidation of dihydrodichlorocarboxyfluorescein, was not complete until six minutes after addition of the ionophore (cf. section *P*). The increase in intracytosolic calcium eventually resulted in cytotoxic injury to HMVEC, as shown in Figure 25. Because of the rapidity with which cytotoxic injury appears to follow upon intracytosolic calcium accumulation, it was not feasible to use calcein-AM as a probe of such injury, but progressive failure of the membranes to exclude ethidium bromide could be followed at regular intervals after addition of ionomycin. A final concentration of 2 μ M ethidium bromide was added to triplicate wells of HMVEC in HBSS on the same plate as other sets of triplicate wells which had been preincubated for 30 min with fluo-3-AM or with CDCFH-AM for 30 min (cf. section *P*). All cells were then

challenged with 1.5 μM ionomycin and the plate placed immediately into the Cytofluor 2300 for repetitive reading. By 6 minutes after addition of 1.5 μM ionomycin, ethidium homodimer-1 began to enter the nuclei of HMVEC and bind to DNA, a diagnostic mark of loss of cell membrane integrity. This loss of membrane integrity progressed over the next several minutes. This cytotoxicity may have also limited the capacity of the cells to release reactive oxygen metabolites. A similar pattern of rapid calcium uptake as detected by fluo-3 fluorescence, followed subsequently by cytotoxic injury, was also reported by Jiang et al. [26] in their studies on ionomycin-treated rat renal cells.

We then evaluated the effect of a known "activating" agent, phorbol myristate acetate (PMA) on the intracytosolic calcium levels of HMVEC with fluo-3 as a probe. Figure 26 illustrates a two-phase response of increasing intracytosolic calcium levels after stimulation of HMVEC with 1 μM PMA. Cells in triplicate wells were first pre-incubated with 10 μM fluo-3-AM to "load" the cytosol with the calcium probe, washed with HBSS, and then treated with the phorbol ester. A small but significant and reproducible increase in intracytosolic calcium was seen within the resolution time of the Cytofluor 2300, but a much larger increase occurred about 2 hours after the initial stimulus. This later increase in intracytosolic calcium occurred at approximately the same time as an increase in the release of arachidonic acid metabolites, and is consistent with the hypothesis that changes in calcium homeostasis which occur at this time coincide temporally with activation of gene transcription and subsequent expression of such gene products as the enzymes of the eicosanoid biosynthetic pathway. It must be noted that fluo-3 fluorescence from unstimulated HMVEC cultures also increases by 2 hours after initial "loading," but the increase from PMA-stimulated cells is significantly greater. In view of the absence of other evidence of cytotoxic injury in unstimulated HMVEC for periods of up to 3 hours in HBSS, we have no satisfactory explanation for the increase in fluo-3 fluorescence from unstimulated HMVEC cultures. A possible mechanism involves active pumping of the intracellular hydrolyzed fluo-3 anion from the intracellular compartment to the extracellular medium. Such pumping of anionic dyes has been reported for human macrophages [32]. Fluorescence microscopy studies in the presence and absence of an anti-fluorescein antibody (which quenches extracellular fluo-3 fluorescence) could help to resolve this issue.

Figure 27 shows the time course of increase of intracytosolic calcium after exposure of triplicate wells of HMVEC to 300 ppm phosgene for 1 minute, 3 minutes, or 6 minutes. As before, cells were loaded with 10 μM fluo-3-AM for 30 min and then washed in HBSS prior to phosgene exposure. It must be emphasized that transient increases in intracytosolic calcium which might have occurred during or immediately after phosgene treatment could not be detected by this method. It is clear from the data that a more gradual increase in intracytosolic calcium could be detected earliest in HMVEC which were exposed to phosgene for 1 minute. Longer exposures to phosgene resulted in a much slower increase in fluo-3 fluorescence, but, as we show in the following figures, cells which were exposed to phosgene for 3 minutes or longer also failed to generate reactive oxygen metabolites as detected by oxidation of dihydrodichlorocarboxyfluorescein (cf. section *P*). Moreover, as we have previously described, after exposure to phosgene for 3 minutes or longer, HMVEC suffer marked loss of mitochondrial membrane potential as measured by the J-aggregate to monomer ratio of fluorescence of JC-1, and show marked evidence of cytotoxic injury as reflected in increased binding of ethidium homodimer-1 to DNA and decreased esterolysis of calcein-AM. We believe that the increase in intracytosolic calcium seen in HMVEC exposed to phosgene for 1 minute may elicit in at least some of the cells a response similar to that seen after PMA treatment, i.e. an "activation" response in the absence of massive direct cytotoxic injury.

By 3 hours or more after exposure, intracytosolic calcium levels appeared to increase in all wells of HMVEC which were exposed to phosgene as well as those which were sham exposed to 5% CO_2 , raising the possibility that some of the manipulations performed on the cells, including

replacement of medium, might have been sufficient to trigger an "activation" response, or, less likely, to have introduced some cytotoxic injury. We therefore undertook to carry out simultaneous measurements on effects of phosgene exposure on fluo-3 fluorescence, nonspecific esterase activity towards calcein-AM, nuclear permeability to ethidium homodimer-1, and formation of intramitochondrial aggregates of JC-1. As shown in Figure 28 (data performed on a different plate of cells than those used in Figure 27), the fluo-3 fluorescence was still highest in cells exposed to phosgene for 1 minute; this fluorescence intensity was about twice that of sham exposed cells. Sham exposure to 5% CO₂ also resulted in increased fluo-3 fluorescence when compared with cells maintained continuously in HBSS. Figure 29 illustrates the effects of sham exposure or phosgene exposure on the capacity of the HMVEC to hydrolyze calcein-AM and exclude ethidium homodimer-1, our standard measures of cell injury. (It should be noted that intracytosolic esterolysis of fluo-3-AM occurred during the pre-incubation prior to phosgene exposure, whereas treatment with calcein-AM was carried out after phosgene exposure.) As was observed in previous experiments, sham exposure to 5% CO₂ had no significant effect on esterase activity or nuclear exclusion of ethidium homodimer-1, showing that, in the absence of phosgene, neither the manipulations of the plates involved in the exposure protocol, nor the subsequent incubation of the plates for as long as 3 hours after exposure, resulted in cytotoxic injury. Significant, but not complete, injury to HMVEC was apparent after 1 minute of phosgene exposure, as previously noted in section G. After 3 minutes of phosgene exposure, cytosolic nonspecific esterase activity was lost, and after 6 minutes of exposure, maximum levels of ethidium homodimer-1 binding to nuclear DNA could be detected.

Figures 30 and 31 illustrate the effects of phosgene exposure on the mitochondrial membrane potential of the same plate of HMVEC. As in previous studies, we added the cationic cyanine dye JC-1 after phosgene exposure to probe mitochondrial membrane potential. It is important to note that the cells used for the measurements in Figures 28 through 31 were all from different triplicate sets of wells on the same microplate. As seen in Figure 31, even 1 minute of phosgene exposure was sufficient to markedly lower mitochondrial membrane potential, seen as a decrease in the J-aggregate-to-monomer ratio. Figure 30, which illustrates the fluorescence intensity of monomers and J-aggregates, shows that especially after 6 minutes of phosgene exposure, the total levels of intracellular JC-1 accumulated after a 12 minute incubation with JC-1 were significantly increased, but these increases reflected predominantly increased concentrations of intracellular monomeric dye. In order to interpret these results more clearly, we examined the cells exposed to phosgene for different intervals under the microscope, using epifluorescence to visualize both green and orange fluorescence. The results with this method were extremely striking: sham exposed cells showed all the JC-1 within the mitochondria which fluoresced bright orange, confirming the intrinsic resistance of the HMVEC monolayers to the incubation protocol in the absence of phosgene treatment. After 1 minute of phosgene exposure, the dye was still predominantly within the mitochondria, but fluoresced green with greater intensity and orange with less intensity. The JC-1 was no longer concentrated within the mitochondria in cells exposed to phosgene for 3 minutes, but was diffusely distributed. After 6 minutes of exposure, the greatest accumulation of the dye was within the nucleus of the cells; no mitochondrial accumulation could be detected against the diffuse monomer fluorescence. (Extra-mitochondrial JC-1 does not aggregate.)

We conclude from these studies that brief (~1 minute) exposure of HMVEC to 300 ppm phosgene results in a different state in at least some of the cells than 3 minutes or 6 minutes of exposure. The shorter exposure times of no longer than 1 minute can lead to an "activation" response characterized by increased intracellular calcium levels and decline in the mitochondrial membrane potential, whereas the longer exposures produce more serious immediate cell injury, in which metabolic processes are more profoundly compromised. In sham-exposed cells, the slow gain of fluo-3 fluorescence may reflect some low level of "activation" or loss of calcium pump activity, in

addition of the possibility of leakage of the dye into the extracellular space, aided by an anion pump [32].

L. Intracellular Calcium Levels in the A549 Human Type II Alveolar Epithelial Cell Line

Preliminary studies on the intracellular calcium levels of A549 cells indicated that the type II alveolar epithelial cells have calcium pumps which can maintain a low intracellular calcium level even in the presence of the calcium ionophore, ionomycin. A549 cells were pre-loaded with 10 μM fluo-3-AM for 30 minutes prior to removal of the extracellular probe and addition of the calcium ionophore. Separate wells of A549 cells in the same plate were pre-incubated with 4 μM ethidium homodimer-1 for 30 minutes prior to addition of the same concentration of calcium ionophore. In the presence of 10 μM ionomycin, the influx of calcium into human endothelial cells and the development of cytotoxic injury had been too fast to be resolved by the Cytofluor 2300. At this same concentration of calcium ionophore, a slow gradual increase in intracellular calcium concentration could be observed in A549 cells over a 45 minute period of measurement, as shown in Figure 32. During this period of time, no changes in intracellular calcium levels could be observed in A549 cells maintained in medium alone. The development of cytotoxic injury to the A549 cells was correlated with the influx of calcium, as was observed in endothelial cells, but, again this injury developed much more slowly in the A549 cells in the presence of 10 μM ionomycin than we had observed with endothelial cells. By 15 minutes after addition of 10 μM ionomycin, very little binding of ethidium homodimer-1 to DNA had occurred in the A549 cells, and complete loss of the capacity of the plasma and nuclear membranes to exclude the dye had not yet occurred by 45 minutes after introduction of the ionophore (Figure 32). These results demonstrate a substantially greater capacity of the calcium pumps in A549 cells to maintain a low intracellular calcium concentration in the presence of a calcium ionophore than the pumps in human microvascular endothelial cells. This increased calcium pump activity in A549 cells after challenge with ionomycin appears to be correlated with the relative resistance of A549 cells to cytotoxic injury after phosgene exposures which induce extensive injury in endothelial cells. At the time of termination of this research, no studies on effects of phosgene exposure on intracellular calcium levels in A549 cells had been completed. It is possible that accumulation of calcium generally precedes development of cytotoxic injury in cells after an insult such as phosgene exposure, and that the ability to maintain calcium homeostasis predicts resistance to cytotoxic injury, but the detailed mechanisms by which A549 cells exclude calcium and resist phosgene-induced injury remain to be elucidated, and the two processes in A549 cells are linked at this time only by our correlative observations.

M. Effects of Phosgene on Acidification of Lysosomes by Proton Pumps

Accumulation of acridine orange (AO) into the lysosomes of normal cells is associated with an intense red fluorescence [33]. Failure to acidify the lysosomal compartment as a result of loss of proton pumping activity is seen as a marked reduction in the intensity of the red fluorescence from AO. While this loss of lysosomal pump activity is not a direct measure of cytotoxicity, it is usually highly correlated with cellular changes which lead to cell death. Acridine orange can also intercalate into nucleic acids, especially in nucleoli, where it emits in the green. Human microvascular endothelial cells were exposed as adherent monolayers in T-75 tissue culture flasks to 300 ppm phosgene for 3 min and then flushed with 5% CO_2 in air for 7 min. Our lack of quantitative measures of phosgene exposure to cells, either in T flasks or in multiwell plates, has already been noted (cf. section I), and the true exposure times must therefore be regarded as only approximations. Control cultures were exposed to 5% CO_2 only. Some flasks were then employed directly for the lysosomal acidification assay, while others received fresh medium (RPMI 1640 + 10% serum) and were incubated in a 5% CO_2 atmosphere for 3 h prior to the acidification assay.

After exposure, a fraction of the endothelial cells detached spontaneously from the flasks. The remaining adherent cells were then detached by trypsinization. In those cultures which were assayed immediately after exposure, the spontaneously detached cells and the adherent cells which were detached by trypsinization were pooled prior to incubation with AO. In those cultures which were allowed to incubate for 3 h prior to assay, the spontaneously detached cells and the trypsinized adherent cells were assayed separately. The lysosomal acidification assay was carried out by replacing all media with HBSS and incubating the cells with 1 $\mu\text{g/ml}$ AO in HBSS for 5 min prior to analysis by flow cytometry. Flow cytometric assay has the advantage of permitting quantitative measurement of the distribution of lysosomal acidifying activities of the individual cells. The analyzed data were presented as dual channel contour plots, in order to visualize changes in nucleic acid intercalation or lysosomal acidifying activity in the cells. A typical contour plot of the pooled cells collected immediately after exposure to phosgene, incubated with AO, and analyzed by flow cytometry within 1 h of exposure is shown in Figure 33. Measurements on adherent cells using the Cytofluor 2300 could only provide estimates of the average levels of AO accumulation in lysosomes and nucleic acid intercalation, but, unlike flow cytometric analyses, could not reveal whether such averages reflect a mixture of highly active and inactive cells or a broad range of activities. The results on AO accumulation into lysosomes of the pooled cells which were collected immediately after exposure as well as measurements on the separate subsets of spontaneously detached and trypsinized adherent cells 3 h after exposure are presented in Table I. (The total time elapsed between exposure and flow cytometry of cells which were not subsequently incubated is approximately 1 h.) Cells which were analyzed immediately after exposure to 5% CO_2 alone were 98% strongly positive for red fluorescence from accumulated AO in acidified lysosomes. Cells isolated after a 3 min exposure to phosgene were only 60% strongly positive for red fluorescence. A more detailed analysis of the trypsinized adherent and spontaneously detached subsets of cells separately incubated with AO 3 h after exposure suggests that the loss of lysosomal acidifying activity was especially dramatic in the spontaneously detached cells, in either control cultures (63% weakly fluorescent) or phosgene-exposed cultures (44% weakly fluorescent). Phosgene exposure increased the percentage of spontaneously detached cells from 4.7% to 15.6%. In the trypsinized adherent subset of cells which had been previously exposed to phosgene, about 24% of the cells failed to acidify their lysosomal compartment, while only 1% of the control trypsinized adherent cells failed to acidify their lysosomes. These results suggest that cytotoxic effects of phosgene on human microvascular endothelial cells in culture in T75 flasks are associated with spontaneous detachment and apparent lysosomal proton pump failure. The subset of endothelial cells which remained adherent to plastic after phosgene exposure, on the other hand, was more resistant to phosgene, and only about 24% of these adherent cells lost the capacity to acidify their lysosomes after trypsinization and flow cytometry. Those cells which remained adherent 3 h after exposure to phosgene but which displayed weak red fluorescence also had reduced intensity of green fluorescence, suggesting some loss of DNA into which AO can intercalate. This loss of DNA is consistent with necrotic cell death, but this interpretation must be viewed with some caution, as it has been argued that the bulk of chromatin in living cells may not be accessible to intercalation with AO [34].

In additional measurements of lysosomal proton pump activity, the effect of incubating the cells in fresh medium after phosgene exposure was investigated. We exposed human microvascular endothelial cells as adherent monolayers in T-75 tissue culture flasks to 300 ppm phosgene for 1 min or 3 min, followed by flushing with 5% CO_2 in air for 7 min. Control cultures were exposed to 5% CO_2 only as previously described. Some flasks were then employed directly for the lysosomal acidification assay as previously described, while others received fresh endothelial cell growth medium and were incubated in a 5% CO_2 atmosphere for additional periods ranging from 3 h to 24 h prior to the acidification assay. The lysosomal acidification assay was carried out by detaching

adherent cells by trypsinization, replacing all media with HBSS, and incubating the cells with 1 $\mu\text{g/ml}$ AO in HBSS for 5 min prior to dual channel fluorescence analysis by flow cytometry. We confirmed our initial observations that after exposure to phosgene, a fraction of the endothelial cells detach spontaneously from the flasks without trypsin treatment. The spontaneously detached cells generally had much lower lysosomal pump activity than those cells which remained adherent after exposure either to phosgene or to 5% CO_2 in air and which had to be trypsinized for flow cytometric analysis (Figure 34). The size of the spontaneously detached subset was a function of phosgene exposure time: in our studies, about 20.5% of the cells detached after 1 min of phosgene exposure (Figure 35), while about 40% detached after 3 min exposure (cf. Figure 34). Only about 3% of the cells exposed to 5% CO_2 alone spontaneously detached (cf. Figures 33 and 35). As also shown in Figure 35, a 3 h period of incubation in culture medium after exposure to phosgene resulted in only a modest increase (of marginal statistical significance) in the fraction of cells with marked reduction in lysosomal pump activity, supporting the conclusions reached from our studies with calcein and ethidium homodimer-1 that for several hours, endothelial cells do not undergo exacerbation or resolution of the pathophysiologic changes induced by phosgene exposure. This result was also seen with cells that had been incubated in culture medium 24 h after phosgene exposure.

Within the subset of cells that remained adherent after phosgene treatment, some more subtle changes in lysosomal pump activity could be detected. Figure 36 illustrates the histogram analysis of the distribution of red fluorescence intensity of the subset of endothelial cells which retained their capacity to acidify lysosomes after exposure to 5% CO_2 in air or to 1 min of phosgene. The mean fluorescence intensity (MFI) of the AO-positive subset was 47.5 ± 1.6 , while the MFI of the cells which remained AO-positive after 1 min of phosgene exposure declined slightly to 41.6 with a markedly non-normal distribution ($\text{SD} = 4.5$). The MFI of cells which remained AO-positive after 3 min of phosgene exposure declined even more, and was only about 71.1% of the MFI of the AO-positive control cells. It appears that the progressive skewing of the distribution of lysosomal pump activity of AO-positive cells after increasing times of exposure to phosgene reflects a more subtle change in cell physiology induced by the oxidant gas than the more serious alterations in cell function which resulted in spontaneous detachment. Preliminary indications from measurements on cells allowed to incubate in culture medium after exposure to phosgene suggest that these more subtle changes in lysosomal pump activity are also relatively stable for several hours after the cells have been subjected to phosgene.

The relative stability of the changes in lysosomal proton pumping activity in phosgene-exposed HMVEC suggests that this toxicant may have multiple effects on membranes in these cells. It will be recalled that significant, but not total loss of mitochondrial membrane potential and nonspecific esterase activity, and increased permeability of nuclei to ethidium homodimer-1 also characterize HMVEC exposed to phosgene, especially for brief (~ 1 minute) durations. We would expect that those cells in which all mitochondrial activity was abrogated would deplete their energy stores, resulting in a progressive loss of all ATP-driven membrane pumping activities. However, our results demonstrate temporally stable and limited declines in lysosomal proton pumping activity in viable HMVEC exposed to phosgene. These results are insufficient to discriminate between reduction, but not exhaustion, of energy stores and ATP-generating capacity, leading to a new steady state of reduced activity of energy-dependent pumps, versus direct effects of phosgene on the pumps and/or the membranes on which they are located.

N. Effects of Phosgene on Release of Arachidonic Acid Metabolites

Our studies on release of arachidonic acid mediators were also carried out on human microvascular endothelial cells (Clonetics Corp.) cultured in Endothelial Cell Growth Medium (ECGM) containing 5% serum. For measurements of eicosanoid release, cells were maintained as

adherent monolayers in Falcon 24 well microplates. With an initial seeding density of 5×10^5 cells/cm², the cells achieved confluence after overnight growth in a 5% CO₂ atmosphere at 37°C. Immediately prior to exposure to phosgene, the medium was removed and replaced with 200 µl fresh serum-free ECGM per well. As previously noted, although this medium lacks serum (and endogenous antioxidants that might be present in serum and complicate studies on eicosanoid metabolism), it is supplemented and will support maintenance (but not proliferation) of confluent HMVEC. The cells in their microplates were exposed to 300 ppm phosgene for 3 min, followed by a 7 min washout with 5% CO₂ in air. Again, because of the differences in medium composition and volume between these and other studies on cells in 24 well plates, the true times of exposure of the cells to phosgene are only approximated by these reported times of 5 L/min flow of 300 ppm phosgene into the exposure chamber. Fresh serum-free medium was added to each well to bring the total volume to 1 ml, the plates were returned to the 37°C incubator, and the entire supernatant was removed from individual wells at hourly intervals from 1 h to 4 h post-exposure for determination of eicosanoid release by ELISA [8]. At the end of 4 h, the medium in each of the remaining wells was replaced with 1 ml of fresh serum-free ECGM and the plates were incubated for an additional 20 h, at which time the supernatants were removed for determination of the levels of released eicosanoids. This experiment was performed on quadruplicate wells for each exposure group, with duplicate aliquots removed from each well for ELISA determinations. Kits for leukotrienes C₄, D₄, and E₄ (the three leukotrienes cross react with the antibody in the kit and cannot be measured individually by ELISA), for 6-keto-prostaglandin F₁α, and for thromboxane B₂ were obtained from Cayman Laboratories.

Figure 37 illustrates the time course of the release of 6-keto-PGF₁α from human lung microvascular endothelial cells. This prostanoid is a stable metabolite of PGI₂ (prostacyclin), and provides a measure of vasodilatory mediator activity. The levels of 6-keto-PGF₁α in the control wells, which were exposed to air only, remained relatively constant, while the levels of this eicosanoid increased sharply 2 hours after exposure to phosgene, and continued to increase over the next 22 h post-exposure. A somewhat similar pattern is seen in Figure 38 for the time course of release of thromboxane B₂, an eicosanoid with vasoconstrictor activity. The results shown are for two experiments, each of which employed quadruplicate wells for each exposure group, as described above. An increase in the levels of released TxB₂ was seen 2 h after phosgene exposure. A further increase was detected in the 24 h sample, but the spontaneous release of TxB₂ from the control samples collected 24 h after exposure to air only was also markedly elevated, suggesting that the extended time in culture alone may have been sufficient to stimulate the cells to release this arachidonic acid metabolite. While the percentage increase in 6-keto-PGF₁α after phosgene exposure clearly exceeded the percentage increase in TxB₂, it would be premature to suggest that this *in vitro* result is indicative of an overall vasodilatory action of phosgene on the pulmonary circulation *in vivo*. Time course studies of leukotriene C₄, D₄, and E₄ release from the endothelial cells after exposure to phosgene or air only are illustrated in Figure 39. The spontaneous release of these products of the lipoxygenase pathway from the control cells increased with time, especially in the 24 h sample, but the levels of leukotrienes released from cells 2 h or longer after exposure to phosgene were uniformly higher than the control levels, with a P value of less than 0.05. These results were consistent with preliminary results we had obtained, showing that levels of eicosanoids released by endothelial cells after phosgene exposure are increased. The results also indicated that the actual duration of phosgene exposure to the endothelial cells in this study was not so destructive that their capacity to synthesize arachidonic acid metabolites was compromised, and reiterates our conclusions that there are levels of phosgene exposure which induce alterations in cell functions, rather than causing outright necrotic cell death.

O. Effects of Phosgene on Cytokine Release

From our studies on release of eicosanoids from human microvascular endothelial cells exposed to different cumulative doses of phosgene, we concluded that the time course of eicosanoid release was consistent with a model in which some cells are not killed by phosgene, but instead undergo changes in functional properties consistent with a shift to an "activated" state. These markers of activation did not appear until ~2 hours after phosgene exposure, consistent with a model in which the machinery for their synthesis was mobilized. The lag in mediator release suggested that the activation response was not achieved simply by release of stored mediators, but required *de novo* synthesis. We then examined the release of a cytokine, interleukin-6 (IL-6) by type II epithelial cells and microvascular endothelial cells exposed to phosgene. Human microvascular endothelial cells (Clonetics Corp) were cultured in Clonetics ECGM containing 5% serum for all these studies. Cells were plated in 24 well microplates. Prior to phosgene exposure, the medium was replaced with HBSS which was replaced with fresh ECGM immediately after exposure. Supernatants from the wells were collected 2 h after phosgene exposure and IL-6 levels were assayed by an ELISA (R & D, Minneapolis MN). Unlike the eicosanoids, which were released at increased levels 2 h after exposure to 300 ppm phosgene for 3 min, decreased levels of IL-6 were released over a 2 h period after phosgene exposure, as shown in Figure 40. By assaying control wells which contained known amounts of IL-6 standard but no cells, we confirmed that the apparent decrease in IL-6 levels did not result from direct destruction of the immunoreactivity of the cytokine by phosgene or its breakdown products. While the ELISA detected no IL-6 release from the rat type II epithelial cells before or after exposure to phosgene, the ability of the monoclonal antibodies in this immunoassay to recognize the rat cytokine is unknown, and may be limiting. We also encountered some cultures of human microvascular endothelial cells which released levels of IL-6 below the limits of detection by the ELISA regardless of phosgene exposure, so the significance of the suppression of IL-6 release from these cells after phosgene exposure remains uncertain and should be investigated further.

P. Methods to Detect Generation of Reactive Oxygen Metabolites

In these studies we evaluated the best means of detecting the generation of reactive oxygen metabolites both intracellularly and extracellularly. Unlike neutrophils or macrophages, human endothelial and epithelial cells do not release significant levels of reactive oxygen metabolites into the extracellular milieu. Nevertheless, these cells generate intracellular reactive oxygen species which may be critical for triggering the complex responses of the cells to phosgene exposure. It has been argued that intracellular reactive oxygen species, especially hydroxyl radicals and hydrogen peroxide but not superoxide anions, play a critical role in destroying the I κ B- α subunit of the NF- κ B complex in the cytosol and in modulating AP-1 levels, thereby activating the transcription of a number of genes associated with cell responses to cytotoxic injury [10]. We selected carboxydichlorodihydrofluorescein diacetate acetoxyethyl ester (CDCFH-DA-AM) and dichlorodihydrofluorescein diacetate (DCFH-DA) as our probes of intracytosolic generation of reactive oxygen species. These molecules diffuse freely into the cytosol from the extracellular milieu, and are hydrolyzed by cytosolic nonspecific esterases. The free anion forms of hydrolyzed acetate and acetoxyethyl ester probes are trapped within the cytosol. The esterolyzed dyes are nonfluorescent until they are oxidized by reactive oxygen species (especially hydrogen peroxide and hydroxyl radicals) to carboxydichlorofluorescein or dichlorofluorescein [35]. As was the case for the probe fluo-3-AM, cells were incubated with a 4 μ M solution of the diacetate acetoxyethyl ester or the diacetate of the corresponding reduced fluorescein probe for 30 minutes prior to stimulation or phosgene exposure.

Studies on the chemistry of oxidation of dihydrofluorescein derivatives to their corresponding fluorescein derivatives have indicated that superoxide anions are incapable of serving as oxidants for

this reaction, although some enzymes which can generate superoxide, such as xanthine oxidase, can use dihydrofluorescein derivatives as substrates [35]. In order to confirm the nature of the response of the nonfluorescent precursor probe DCFH-DA to oxidants, we incubated it with neutrophils and macrophages for 30 min to allow for hydrolysis and intracytosolic trapping, followed by stimulation with 100 nM phorbol myristate acetate to induce a respiratory burst. These leukocytes generate substantial quantities of both intracellular and extracellular reactive oxygen species. Conversion of the hydrolyzed probe into its oxidized fluorescent product was completely insensitive to the addition of superoxide dismutase to the extracellular milieu, as shown in Figure 41 (data obtained on PMA-stimulated human neutrophils). Conversely, the reduction of ferricytochrome c in the medium by the human neutrophils was completely abolished by the addition of superoxide dismutase (Figure 42), confirming that DCFH-DA (and CDCFH-DA-AM) can be used as probes of intracellular generation of reactive oxygen species, including hydrogen peroxide and hydroxyl radicals, but not superoxide anions. We had previously employed lucigenin-enhanced chemiluminescence as a probe to detect generation of reactive oxygen species in the extracellular milieu [36], and showed that phosgene inhibits the generation of lucigenin-enhanced chemiluminescence from the human macrophage-like cell line, U937, after stimulation with PMA (Figure 43).

As previously indicated in Figure 25, an increase in intracellular calcium resulting from addition of ionomycin to HMVEC was correlated with generation of intracellular reactive oxygen species which could be detected by oxidation of the nonfluorescent reduced forms of CDCFH or DCFH. The reduced acetoxyethyl esters of these dyes were loaded for 30 minutes into cells at a concentration of 4 μM as described above. The extracellular medium was then replaced with fresh HBSS. Generation of reactive oxygen species was clearly linked temporally to changes in intracellular calcium levels. Figure 44 illustrates the levels of intracellular reactive oxygen species generated by HMVEC after treatment with 1 μM phorbol myristate acetate: this data was obtained with cells on the same plate as those used to generate the data on intracellular calcium levels in Figure 26. Some increase in reactive oxygen species could also be detected after 3 hours of sham treatment. We have already shown that after 3 hours, there was some evidence of spontaneous activation of HMVEC which had been manipulated but not treated with known activating agents. However, a much more marked increase in generation of reactive oxygen species was seen in the PMA-treated cells. This increase corresponded to the increase in intracellular calcium levels seen in Figure 26. In Figure 45, the time course of generation of intracellular reactive oxygen species after 1 minute, 3 minutes, and 6 minutes of phosgene exposure is illustrated, using cells from the same plate as was used to generate the data in Figure 27. The levels of reactive oxygen species began to increase in all samples by 3 hours, but a earlier significant increase in reactive oxygen species could be seen in the cells exposed to phosgene for 1 minute (filled squares) as soon as 45 minutes after exposure. In a separate experiment, shown in Figure 46, on cells from the same plate as those used to generate the intracellular calcium data in Figure 28, the levels of intracellular reactive oxygen species capable of oxidizing the probes increased markedly by 3 hours after a 1 minute exposure to phosgene. Only relatively modest increases were seen in cells treated for 3 minutes or 6 minutes, suggesting that the immediate injury to these cells exposed to phosgene for longer durations limited their capacity to generate reactive oxygen species.

Q. Protection by Antioxidants - N-acetyl Cysteine

We undertook initial experiments to test antioxidants as possible candidates for intervention in reducing injury resulting from phosgene exposure. Intratracheally instilled N-acetyl cysteine has been recently investigated as a therapeutic agent for lowering the levels of arachidonic acid metabolites released by isolated perfused rabbit lungs after *in vivo* exposure to 1500 ppm \times min phosgene [39]. We tested the ability of 6.25 mg/ml N-acetyl cysteine (38 mM) to control the

generation of arachidonic acid metabolites after exposure of HMVEC to phosgene. As previously carried out for measurements of eicosanoid release, cells were maintained as adherent monolayers in Falcon 24 well microplates. With an initial seeding density of 5×10^5 cells/cm², the cells achieved confluence after overnight growth in a 5% CO₂ atmosphere at 37°C. Immediately prior to exposure to phosgene, the medium was removed and replaced with 200 μ l fresh serum-free ECGM per well. Cells were pre-incubated with N-acetyl cysteine for 30 minutes prior to phosgene exposure. The cells in their microplates were then exposed to 300 ppm phosgene for 3 min, followed by a 7 min washout with 5% CO₂ in air. Fresh serum-free medium was added to each well to bring the total volume to 1 ml, the plates were returned to the 37°C incubator, and the entire supernatant was removed from individual wells at hourly intervals from 1 h to 4 h post-exposure for determination of eicosanoid release by ELISA. At the end of 4 h, the medium in each of the remaining wells was replaced with 1 ml of fresh serum-free ECGM and the plates were incubated for an additional 20 h, at which time the supernatants were removed for determination of the levels of released eicosanoids. Kits for leukotrienes C₄, D₄, and E₄ (the three leukotrienes cross react with the antibody in the kit), for 6-keto-prostaglandin F₁ α , and for thromboxane B₂ were obtained from Cayman Laboratories.

Figure 47 illustrates the percentage suppression by 38 mM N-acetyl cysteine of the release of 6-keto-PGF₁ α , TXB₂, and LTC₄, D₄, and E₄ from HMVEC as a function of time after a 3 minute exposure to 300 ppm phosgene. As discussed previously, these eicosanoids were selected because 6-keto-PGF₁ α is a stable metabolite of PGI₂, and provides a measure of vasodilatory mediator activity; thromboxane B₂ is an eicosanoid with vasoconstrictor activity; and leukotrienes C₄, D₄, and E₄ represent products of the lipoxygenase pathway. As also indicated in previous sections, the levels of these arachidonic acid metabolites rise most markedly about 2 hours after phosgene exposure, with a second rise by 24 hours which is also seen in cells exposed to 5% CO₂ only. By 2 hours after the 3-minute phosgene exposure, the levels of 6-keto-PGF₁ α released by N-acetyl cysteine-treated cells were found to be only 63% of those from "unprotected" cells. The 6-keto-PGF₁ α levels were 49% of unprotected controls after 3 hours, 45% after 4 hours, and 37% after 24 hours. Similar levels of suppression of TXB₂ and leukotrienes were also seen. The P values for these levels of suppression were all below 0.05. These results indicate that N-acetyl cysteine may have a prophylactic protective effect on arachidonic acid metabolism elicited by phosgene exposure which is similar to its mode of action on cells challenged with t-butyl peroxide. Of interest, the agent ETYA which also had been shown to have a protective role in suppressing eicosanoid release after t-butyl peroxide challenge, had no protective role in suppressing release of arachidonic acid metabolites after phosgene exposure (data not shown).

We also tested the effects of two concentrations of N-acetyl cysteine (38 mM and 5 mM) on the increased permeability of type II epithelial cell monolayers to [¹⁴C]-mannitol induced by exposure to 300 ppm phosgene for 3 min. While the increase in permeability was consistently smaller in phosgene-exposed monolayers maintained in the presence of N-acetyl cysteine than the increase in permeability of phosgene-exposed monolayers maintained in medium alone, the difference in the rates of mannitol diffusion did not achieve statistical significance. Further studies would be required to determine whether this antioxidant can preserve junctional integrity of type II epithelial cells after exposure to phosgene.

R. Effects of Antioxidants on Phosgene-Mediated Responses - Pyrrolidine Dithiocarbamate

We also examined the protective effect of a somewhat more selective antioxidant, pyrrolidine dithiocarbamate (PDTTC). This scavenger has been shown to be especially effective in suppressing the activation of κ B-regulated genes in cells by preventing the oxidative destruction of I κ B- α , a cytosolic inhibitor of the transcriptional activator, NF- κ B [10]. More recently, however, observations have appeared which suggest that PDTTC can possess pro-oxidant activity under certain circumstanc-

es. In a communication from the Karolinska Institute [40], PDTC was shown to prevent apoptosis in thymocytes challenged with various toxicants (etoposide or thapsigargin) over a time course of 8 h, while by 24 h treatment with even relatively low doses of PDTC alone induced apoptosis. The authors of this study suggested that the protective and the cytotoxic effects were actually related, and were associated with increases in the ratio of oxidized to reduced glutathione induced by the dithiocarbamate, which normally functions as a reducing agent, not as an oxidant. This specific shift in the glutathione redox state was attributed to the transport of copper into the cells by PDTC, where it participates in glutathione oxidation. In another recent communication from the Weizmann Institute [41], PDTC as well as another supposed antioxidant, butylated hydroxyanisole, were shown to induce expression of genes under the control of both NF- κ B and AP-1 through a pro-oxidant mechanism. Such dual activities may account for apparently paradoxical accounts from the same laboratory of inhibition of stromelysin (MMP-3) expression by PDTC in mesangial cells [42] but inhibition of expression of gelatinase-B (MMP-9) in the same cells via the apparently same NF- κ B- and AP-1-dependent pathway [43].

In order to evaluate the effect of prophylaxis with PDTC on resistance of HMVEC to phosgene exposure, we pre-incubated the endothelial cells in multiwell plates with 100 μ M - 1 mM PDTC in HBSS for 30 minutes prior to exposure to phosgene. If PDTC was left in the medium for 24 hours after exposure, it appeared to be cytotoxic, and we therefore replaced the PDTC-containing HBSS with fresh ECGM 30 minutes after exposure. We saw neither significant protective effect nor cytotoxicity of 100 μ M PDTC in this experiment (data not shown), but higher concentrations of PDTC did appear to have some significant protective effects on nonspecific cytosolic esterase activity. Figure 48 shows the levels of conversion of calcein-AM to free calcein, seen as appearance of fluorescence, in triplicate wells of HMVEC exposed to phosgene for 1 or 3 minutes, or sham exposed to air only, and then incubated for 6 hours in ECGM prior to assay. PDTC had little effect on the cytosolic esterase activity of the sham-exposed cells. Cells exposed to phosgene for 1 minute lost about 40% of their cytosolic esterase activity in the absence of PDTC, and about 55% of their esterase activity in the presence of 200 μ M PDTC, but only ~10% loss in esterase activity was detected in the cells which had been pre-incubated with 500 μ M or 1 mM PDTC, followed by 1 minute of phosgene exposure. After 3 minutes of phosgene exposure, virtually all the esterase activity was destroyed in HMVEC which had not been pre-incubated with the antioxidant. Low, but measurable levels of esterase activity were preserved in the 3 minute-exposed cells treated with 200 μ M, 500 μ M or 1 mM PDTC. Figure 49 shows the binding of ethidium homodimer-1 to nuclear DNA in the same plate of HMVEC employed for esterase activity determinations in Figure 48. As in Figure 48, ethidium binding was assayed 6 hours after phosgene exposure. Low levels of ethidium binding were seen for sham-exposed cells, and this low level was not markedly affected by PDTC. Ethidium binding increased markedly when determined 6 hours after the 1 minute exposure and was actually lower 6 hours after a 3 minute exposure to phosgene, reflecting lower levels of DNA in the wells of the plate exposed for 3 minutes (we have already established that cells exposed to phosgene for 3 minutes incur extensive immediate cytotoxic injury and fail to exclude ethidium, as shown in section G). The reduced levels of ethidium binding in 3 minute-exposed cells could reflect DNA degradation accompanying cell death, or simply an anomalously low cell count in the plate employed for the 3 minute exposure. The levels of ethidium binding to DNA were also higher in cells exposed to phosgene for 1 minute in the presence of 200 μ M PDTC than in the absence of PDTC, consistent with a slightly lower level of esterase activity in cells exposed to phosgene for 1 minute in the presence of 200 μ M PDTC than in the absence of PDTC. As discussed further below, such observations suggest that PDTC may have some cytotoxic effects of its own on HMVEC. Levels of DNA-bound ethidium were reduced by about 20% in the cells which were exposed to phosgene for 1 minute in the presence of 500 μ M or 1 mM PDTC, compared with levels for 1 minute-exposed cells

in the absence of PDTC, consistent with increased levels of cytosolic esterase activity in these 1-minute exposed cells at the higher PDTC concentrations. PDTC had very little effect on the high levels of ethidium binding to DNA in cells exposed to phosgene for 3 minutes, consistent with the cytotoxicity of this duration of phosgene exposure (cf. section G). However, as discussed below, since the percentages of uninjured cells under these conditions are so low, small changes in ethidium binding could still be consistent with measurable increases in the numbers of uninjured cells. Nonspecific esterase activity is a more sensitive measure of such effects in the setting of extensive cytotoxicity.

An interesting observation, shown in Figure 50, is that the 500 μM and 1 mM concentrations of PDTC which appeared to offer some protection against phosgene-induced cytotoxic injury, as reflected by calcein generation from its acetoxymethyl ester and ethidium homodimer-1 binding to DNA, had no protective effect on the loss of mitochondrial membrane potential. Significant loss of membrane potential, seen as a decline in the ratio of fluorescence from JC-1 aggregates vs monomers, occurred after as little as 1 minute of phosgene exposure, with still greater loss after 3 minutes of exposure. Concentrations of PDTC as high as 1 mM had no effect on the decline in the J-aggregate:monomer emission intensity ratios, suggesting that the effects of phosgene on mitochondrial membrane potential might have been immediate, and could not be blocked by this antioxidant.

The apparently paradoxical cytotoxic behavior of PDTC was also investigated more closely in light of recent reports in the literature describing both protective and cytotoxic actions of PDTC and other dithiocarbamates. We observed a very similar pattern of response of human microvascular endothelial cells to PDTC, with evidence of cytotoxicity, especially at higher doses of the dithiocarbamate in the absence of phosgene, but measurable (although modest) dose-dependent dithiocarbamate-mediated protection against the most cytotoxic levels of phosgene. To evaluate protection, we continued to employ the assay of cytosolic esterase activity based on calcein-AM hydrolysis. The fluorescence from free calcein was measured in the Cytofluor 2300 fluorescent microplate reader as described above. Figure 51 illustrates the protective effect of PDTC in a second experiment on human pulmonary microvascular endothelial cells exposed to 300 ppm phosgene for 3 min, a dose which routinely results in marked cell injury. As can be seen from the figure, doses of PDTC from 100 μM to 500 μM with which the cells were incubated for a total of 1 h (30 min prior to exposure in the chamber and 30 min post exposure) produced measurable progressive loss of esterase activity after sham exposure to 5% CO_2 in air only, indicating some inherent cytotoxicity of these doses of PDTC in the absence of phosgene. Doses of 200 μM and 500 μM PDTC provided measurable protection against the injury produced by a 900 ppm-min cumulative phosgene dose, which is qualitatively consistent with the dose-dependent protection by PDTC after the less cytotoxic phosgene exposure of 300 ppm-min shown in Figure 48, although in that study no protection by doses of PDTC lower than 500 μM could be detected. It is important to note that the sensitivity of the Cytofluor microplate fluorimeter was increased to detect the calcein signals from the phosgene-exposed cells, because the extent of injury introduced by a 900 ppm-min cumulative dose was so high and the corresponding levels of esterase activity were low. Without this increase in sensitivity, the calcein signals from all the phosgene-exposed cells would be near the lower limit of detection. It is unfortunately not possible to relate the sensitivity scales on the Cytofluor 2300 by a uniform multiplicative factor, but each incremental increase in the gain for the photomultiplier tube represents approximately an eight- to ten-fold increase in sensitivity. The more recent model of the Cytofluor (Cytofluor II™) is designed to provide more quantitation of fluorescence intensities over extended ranges of sensitivity. Figure 52 illustrates the protective effect of these same doses of PDTC on endothelial cells exposed to phosgene for only 1 min (a cumulative dose of 300 ppm-min), as well as 3 min (900 ppm-min) in another study. The 100 μM dose of PDTC offered

no protection against cytotoxic injury produced by this lower level of phosgene exposure and actually appeared to display some synergistic cytotoxicity, as we had previously seen for a 200 μM dose of PDTC in the experiment shown in Figure 48. However, the 200 μM and 500 μM doses of PDTC provided statistically significant protection against phosgene-induced loss of esterase activity. In this experiment, protection against the even greater loss of esterase activity produced by the higher cumulative phosgene dose of 900 ppm·min was seen in cells treated with all three doses of PDTC. Again, it should be noted that the sensitivity of the fluorimeter was increased to detect the very low levels of esterase activity remaining after the 900 ppm·min cumulative phosgene dose. Finally, in Figure 53, we illustrate the effects of higher doses of PDTC on endothelial cells. The cells were maintained in the presence of doses of PDTC ranging from 500 μM to 2 mM for only one hour as previously, but the levels of esterase activity were not determined until six hours after the cells had been exposed to phosgene. As can be seen in this figure, there was still significant protection by the 1 mM and 2 mM doses of PDTC against the near total loss of esterase activity produced by 900 ppm·min phosgene cumulative exposure, although this protection was not as great as that provided by the 500 μM dose. However, especially after these longer incubation times, there was significant loss of esterase activity in the endothelial cells sham exposed to 5% CO_2 in air only, especially after treatment with 2 mM PDTC. Again, it should be noted that cytotoxicity to all endothelial cells exposed to 900 ppm·min cumulative phosgene was extensive, and the sensitivity of the fluorimeter was increased to detect the protective effect of PDTC on the low levels of residual esterase activity in these cells.

From these results we conclude that PDTC has effects on endothelial cells which resemble those described by Nobel et al. [40] on thymocytes. The dithiocarbamate can provide statistically significant, although modest, protection against severe cytotoxic injury produced by an exogenous toxicant, but at higher doses, it introduced some injury on its own. In order to confirm the reported paradoxical simultaneous expression of pro- and anti-oxidant activities by PDTC we used a test human cell system which has an especially great capacity to generate reactive oxygen metabolites. For these purposes we used human neutrophils rather than endothelial cells, because their capacity to generate reactive oxygen metabolites is so much higher. Figures 54a and 54b illustrate the effects of 100 μM and 500 μM doses of PDTC on the intracellular reactive oxygen metabolite levels of two separate preparations of human neutrophils challenged with 500 μg *E. coli*/10⁶ cells. Intracellular H_2O_2 and other reactive oxygen metabolites capable of oxidizing reduced fluorescein derivatives in the neutrophils were measured by the oxidation of dichlorodihydrofluorescein (DCFH) to its fluorescent product, dichlorofluorescein (DCF), as we had previously employed for measuring reactive oxygen metabolites in human microvascular endothelial cells exposed to phosgene. It is evident from these figures that PDTC effectively suppressed the respiratory burst response of the neutrophils to the potent stimulus of *E. coli*. On the other hand, the spontaneous capacity of the neutrophils to oxidize the reduced fluorescein derivative appeared to be increased by PDTC, especially at the higher 500 μM dose. As shown in Figures 55a and 55b, two separate preparations of neutrophils exhibited higher spontaneous levels of oxidation of dichlorodihydrofluorescein to its fluorescent product in the presence of the dithiocarbamate. It should be noted that the sensitivity of the fluorimeter was not changed for measurements of respiratory burst activity in the presence and absence of *E. coli*, and the measurements in the presence and absence of this activating agent were carried out simultaneously in 24 well microplates. It is evident from inspection of the intensity of fluorescence from the *E. coli*-stimulated cells vs. that from the unstimulated cells that the anti-oxidant effects of PDTC were most pronounced when the respiratory burst activity of the neutrophils was very high, but the pro-oxidant effects were more easily seen when the spontaneous respiratory burst activity was low. We conclude from these studies that PDTC has significant anti-oxidant activity, especially in cells which have been exposed to strong pro-oxidant stimuli. However, in the

absence of such exogenous stimuli, the dithiocarbamate shows some pro-oxidant activity of its own. It should be recognized that dithiocarbamates have been employed extensively in pharmaceutical applications, ranging from treatment of various pathogenic bacteria and fungi to use in experimental therapies for AIDS. They have also been employed in treatment of nickel and copper poisoning and, in the case of disulfiram, even in therapy for chronic alcoholism. Thus, their toxicities have been well established in humans. The possible uses of those dithiocarbamates which have already been approved as pharmaceutical agents for this new application of management of phosgene poisoning should be further considered. We believe it is especially noteworthy that some indications of therapeutic benefit of high doses of ibuprofen have been previously reported in models of oxidant injury. Although the chemistry of this drug is different from that of the dithiocarbamates, it is also a good metal chelator, and may be functioning similarly to regulate intracellular levels of redox-active metals.

IV. Conclusions

Although all of our originally planned studies on the effects of phosgene were not completed within the first eighteen months of our contract with the USAMRMC, we have made sufficient progress to draw some conclusions about the effects of phosgene on human pulmonary microvascular endothelial cells and type II epithelial cells. *First*, these two cell types exhibit significantly different sensitivities to phosgene exposure: doses of phosgene which lead to extensive cytotoxic damage to endothelial cells induce relatively minimal cytotoxicity in the A549 type II pulmonary epithelial cell line. Among the features of type II epithelial cells which illustrate a greater resistance to phosgene-induced cytotoxic damage are a relatively small change in electrical resistance, maintenance of a high electrochemical gradient across the mitochondrial membrane, and relatively little loss of cytosolic esterase activity at phosgene doses which markedly depress this activity in endothelial cells. Our studies on the capacity of the two cell types to maintain a calcium gradient in the presence of ionomycin, a calcium ionophore, suggest that this gradient is far more resistant to collapse in the A549 cells. The basis of the differential sensitivity of endothelial cells and type II alveolar epithelial cells to phosgene remains unknown, although evidence summarized by Jiang et al. [26] indicates that substantial collapse of the calcium gradient across the plasma membrane leads to cytotoxicity, and data summarized by Kang and Enger [31] demonstrate especially high intracytosolic levels of the antioxidant glutathione in A549 type II alveolar epithelial cells. *A second* conclusion is that cytotoxic injury which does not result in cell death appears to convert phosgene-exposed cells to an "activated" state. This state is marked by increased release of eicosanoids, generation of reactive oxygen species, and a slow influx of calcium ions. Doses of phosgene which produce more severe cytotoxicity appear to damage cells so extensively that reactive oxygen metabolites are not produced, and no influx of calcium into the cytosol can be detected subsequent to phosgene exposure (immediate influx during phosgene exposure could not be resolved by our instrumentation). Other properties of the more severely injured cells exposed to cytotoxic phosgene levels include a loss of attachment and some possible evidence of necrotic changes in the nuclear DNA, which is accessible to intercalating dyes such as propidium iodide and ethidium homodimer-1. The concept of a sub-lethal "activated" state of those "injured" phosgene-exposed cells which still retain some functions has important implications for possible therapeutic interventions. On the basis of the rates of production of eicosanoids and reactive oxygen species, it would appear that these products of "activated" cells do not accumulate until about 2 hours after exposure to phosgene. This 2 hour period may represent a "window" for therapeutic intervention, but it is important to recognize that the cascade of intracellular signalling events which leads to production of eicosanoids and reactive oxygen species may not be amenable to interruption once it is triggered by phosgene. *A third* conclusion from our results is that some of the changes in endothelial cells which are induced by phosgene exposure can be blocked by

antioxidants. N-acetyl cysteine at a concentration of 38 mM appears to be capable of reducing the levels of eicosanoids which are released after exposure to sub-lethal levels of phosgene, and pyrrolidine dithiocarbamate at concentrations in the low 10^{-4} M range appears to preserve some cytosolic esterase activity and almost quantitatively quenches intracellular levels of hydrogen peroxide and/or hydroxyl radicals. These two antioxidants may have applications in therapeutic interventions to deal with phosgene exposure. The original model for the therapeutic efficacy of antioxidants, which was based on their capacity to neutralize extracellular reactive oxygen species, may require revision for interpreting their role in protection against phosgene toxicity. The ability of pyrrolidine dithiocarbamate, and possibly of N-acetylcysteine as well, to preserve cell functions in phosgene-exposed cells may also be related to their capacity to modulate the activities of the two major "inflammatory" transcription factors, AP-1 and NF- κ B [10]. Once these factors are activated or, in the case of NF- κ B, liberated from its complex with a cytosolic inhibitor, they can enter the nucleus and activate transcription of a number of genes involved in such inflammatory responses as cytokine release and eicosanoid synthesis. Thus, appropriate antioxidants may block an "activation" response of those phosgene-exposed cells which have not suffered lethal injury, specifically by acting at the level of transcriptional regulation.

V. Future Directions

Although our work is no longer in progress, we believe that future studies on the basic mechanisms of control of the "activated" state in phosgene-exposed cells should be considered. We would suggest that the mechanisms we have suggested for the mode of action of some antioxidants may also be applicable in other settings in which a sub-lethal injury to cells is triggered by exposure to toxicants. For example, we would propose that the use of such antioxidants as pyrrolidine dithiocarbamate, in combination with N-acetyl cysteine or high dose ibuprofen, may be of therapeutic benefit in cases of exposure to toxicants such as sulfur mustard which are not strictly oxidants themselves but which can trigger formation of intracellular reactive oxygen species in injured cells. In an analogy to one proposed mechanism by which PDTC protects against phosgene-induced injury, high dose ibuprofen has been suggested to function as an iron chelator and could thereby block formation of reactive oxygen species which would form via the Fenton reaction. This agent could be of use in management of injury from phosgene, and possibly from exposure to other toxicants as well. We also would recommend additional studies on the differential sensitivity of endothelial and type II epithelial cells to toxicants. Such studies may clarify issues such as the tendency of other toxicants, such as sulfur mustard, to evoke an infiltrating inflammatory response under conditions in which the cytotoxic injury to the epithelium has not fully developed. This pattern could reflect unusual sensitivity of endothelial cells to lose junctional integrity and to participate in extravasation of inflammatory leukocytes, either after direct cytotoxic injury from toxicants or after indirect "activation" through mediators released by other tissues after toxicant exposure. Finally, the mechanisms of cell death after exposure to phosgene and other toxicants should be investigated, in view of evidence that increases in intracellular calcium levels and formation of intracellular reactive oxygen species are often correlated with initiation of the pathway that leads to apoptosis or programmed cell death. The relative contributions of necrotic cell death and apoptotic cell death after exposure to cytotoxic levels of phosgene are important for assessing the course of post-injury repair processes. Such studies on apoptosis are likely to be very useful in evaluating the course of injury and repair after exposure to other toxicants of military importance as well.

References

1. Gilchrist, H.L., and Matz, P.B. (1933) The residual effects of warfare gases: the use of chlorine gas, with report of cases. *Med. Bull. V.A.* 9:229-270.
2. National Institute for Occupational Safety and Health (1976) Occupational exposure to phosgene. Publ. 76-137(NIOSH), U.S. Dept. of Health, Education, and Welfare, U.S. Government Printing Office, Washington, D.C., pp. 1-129.
3. Currie, W.D., Hatch, G.E., and Frosolono, M.F. (1987) Pulmonary alterations in rats due to acute phosgene inhalation. *Fund. Appl. Toxicol.* 8:107-114.
4. Ghio, A.J., Kennedy, T.P., Hatch, G.E., and Tepper, J.S. (1991) Reduction of neutrophil influx diminishes lung injury and mortality following phosgene inhalation. *J. Appl. Physiol.* 71:657-665.
5. Hatch, G.E., Slade, R., Stead, A.G., and Graham, J.A. (1986) Species comparison of acute inhalation toxicity of ozone and phosgene. *J. Toxicol. Environ. Health* 19:43-53.
6. Kennedy, T.P., Michael, J.R., Hoidal, J.R., Hasty, D., Sciuto, A.M., Hopkins, C., Lazar, R., Bysani, G.K., Tolley, E., and Gurtner, G.H. (1989) Dibutyl cAMP, aminophylline, and beta-adrenergic agonists protect against pulmonary edema caused by phosgene. *J. Appl. Physiol.* 67:2542-2552 (1989).
7. Kennedy, T.P., Rao, N.V., Noah, W., Michael, J.R., Jafri, M.H. Jr, Gurtner, G.H., and Hoidal, J.R. (1990) Ibuprofen prevents oxidant lung injury and in vitro lipid peroxidation by chelating iron. *J. Clin. Invest.* 86:1563-1573.
8. Guo, Y.L., Kennedy, T.P., Michael, J.R., Sciuto, A.M., Ghio, A.J., Adkinson, N.F. Jr, and Gurtner, G.H. (1990) Mechanism of phosgene-induced lung toxicity: role of arachidonate mediators. *J. Appl. Physiol.* 69:1615-1622.
9. Abate, C., and Gurtner, G.H. (1991) Species differences in susceptibility to inhalation of toxic gas. *Am. Rev. Resp. Dis.* 143:A544.
10. Meyer, M. Pahl, H.L., and Baeuerle, P.A. (1994) Regulation of the transcription factors NF-kappa B and AP-1 by redox changes. *Chem.-Biol. Inter.* 91:91-100.
11. Alternatives to the use of live vertebrates in biomedical research and testing: a bibliography with abstracts (1996) Hudson, V.W., ed. *Toxicology and Environmental Health Information Program, National Library of Medicine.*
12. Tyson, C.A., and Stacey, N.H. (1992) In vitro technology, trends, and issues, in *In Vitro Toxicity Testing: Applications to Safety Evaluation*, Frazier, J.M., ed. New York: Marcel Dekker. pp. 13-4312.
13. Massey, T.E. (1989) Isolation and use of lung cells in toxicology, in *In Vitro Toxicology: Model Systems and Methods*, McQueen, C.A., ed. New Jersey: Telford Press, pp. 35-6613.

14. Roth, R.A., and Bassett, D.J.P. (1989) The isolated perfused lung in toxicological studies, in *In Vitro Toxicology: Model Systems and Methods*, McQueen, C.A., ed. New Jersey: Telford Press, pp. 3-33.
15. Pino, M.V., Stovall, M.Y., Levin, J.R., Devlin, R.B., Koren, H.S., and Hyde, D.M. (1992) Acute ozone-induced lung injury in neutrophil-depleted rats. *Toxicol. Appl. Pharm.* **114**:268-276.
16. Ghio, A.J., and Hatch, G.E. (1996) Tolerance to phosgene is associated with a neutrophilic influx into the rat lung. *Am. J. Respir. Crit. Care Med.* **153**:1064-1071.
17. Roemer, E.J., Stanton, K.J., and Simon, S.R. (1994) *In vitro* assay systems for cell interactions with interstitial extracellular matrix. *In Vitro Toxicol.* **7**:209-224.
18. Dobbs, L.G. (1990) Isolation and culture of alveolar type II cells. *Am. J. Physiol.* **258**:L134-L147.
19. Shapiro, D.L., Nardone, L.L., Rooney, S.A., Motoyama, E.K., and Munoz, J.L. (1978) Phospholipid synthesis and secretion by a cell line (A549) which resembles type II alveolar epithelial cells. *Biochim. Biophys. Acta* **530**:197-207.
20. Ballard, P.L., Mason, R.J., and Douglas, W.H. (1978) Glucocorticoid binding by isolated lung cells. *Endocrinology* **102**:1570-1575.
21. Colacicco, G., Basu, M.K., Ray, A.K., Wittner, M., and Rosenbaum, R.M. (1977) Effects of prostaglandins E2 and F2alpha on lecithin biosynthesis by cultured lung cells. *Prostaglandins* **14**:283-294.
22. Werrlein, R.J., Madren-Whalley, J.S., and Kirby, S.D. (1994) Phosgene effects on F-actin organization and concentration in cells cultured from sheep and rat lung. *Cell Biol. Toxicol.* **10**:45-58.
23. Essig-Marcello, J.S., and Van Buskirk, R.G. (1990) A double label in situ cytotoxicity assay using the fluorescence probes neutral red and BCEF-AM. *In Vitro Toxicol.* **3**:219-225.
24. Poole, C.A., Brookes, N.H., and Clover, G.M. (1993) Keratocyte networks visualized in the living cornea using vital dyes. *J. Cell Sci.* **106**:685-691.
25. Rahn, C.A., Bombick, D.W., and Doolittle, D.J. (1991) Assessment of mitochondrial membrane potential as an indicator of cytotoxicity. *Fund. Appl. Toxicol.* **16**:435-438.
26. Jiang, T., Grant, R.L., and Acosta, D. (1993) A digitized fluorescence imaging study of intracellular free calcium, mitochondrial integrity and cytotoxicity in rat renal cells exposed to ionomycin, a calcium ionophore. *Toxicol.* **85**:41-65.
27. Reers, M., Smith, T.W., and Chen, L.B. (1991) J-aggregate formation of a carbocyanine as a quantitative fluorescent indicator of membrane potential. *Biochemistry* **30**:4480-4486.

28. Smiley, S.T., Reers, M., Mottola-Hartshorn, C., Lin, M., Chen, A., Smith, T.W., Steele, G.D. Jr., and Chen, L.B. (1991) Intracellular heterogeneity in mitochondrial membrane potentials revealed by a J-aggregate forming lipophilic cation, JC-1. *Proc. Natl. Acad. Sci. U.S.A.* **88**:3671-3675.
29. Cossarizza, A., Baccarani-Contri, M., Kalashnikova, G., and Franceschi, C. (1993) A new method for the cytofluorometric analysis of mitochondrial membrane potential using the J-aggregate forming lipophilic cation 5,5',6,6'-tetrachloro-1,1',3,3'-tetraethylbenzimidazolcarbocyanine iodide (JC-1). *Biochem. Biophys. Res. Comm.* **197**:40-45.
30. Smith, B.T. (1977) Cell line A549: a model system for the study of alveolar type II cell function. *Am. Rev. Respir. Dis.* **115**:285-293.
31. Kang, Y.J., and Enger, M.D. (1990) Glutathione and growth in A549 human lung carcinoma cells. *Exp. Cell Res.* **187**:177-179.
32. Cao, C., Steinberg, T.H., Neu, H.C., Cohen, D., Horwitz, S.B., Hickman, S., and Silverstein, S.C. (1993) Probenecid-resistant J774 cell expression of enhanced organic anion transport by a mechanism distinct from multidrug resistance. *Infect. Agents Dis.* **2**:193-200.
33. Moriyama, Y., Takano, T., and Ohkuma, S. (1982) Acridine orange as a fluorescent probe for lysosomal proton pump. *J. Biochem.* **92**:1333-1336.
34. Delic, J., Coppey, J. Magdelenat, H., and Coppey-Moisan, M. (1991) Impossibility of acridine orange intercalation in nuclear DNA of the living cell. *Exp. Cell Res.* **194**:147-153.
35. Zhu, H., Bannenberg, G.L., Moldeus, P., and Shertzer, H.G. (1994) Oxidation pathways for the intracellular probe, 2',7'-dichlorofluorescein. *Arch. Toxicol.* **68**:582-587.
36. Paky, A., Michael, J.R., Burke-Wolin, T.M., Wolin, M.S., and Gurtner, G.H. (1993) Endogenous production of superoxide by rabbit lungs: effects of hypoxia or metabolic inhibitors. *J. Appl. Physiol.* **74**:2868-2874.
37. Yamada, Y., Furumichi, T., Furui, H., Yokoi, T., Ito, T., Yamauchi, K., Yokota, M., Hayashi, H., and Saito, H. (1990) Roles of calcium, cyclic nucleotides, and protein kinase C in regulation of endothelial permeability. *Arteriosclerosis* **10**:410-420.
38. Yamada, Y., Yokota, M., Furumichi, T., Furui, H., Yamauchi, K., and Saito, H. (1990) Protective effects of calcium channel blockers on hydrogen peroxide induced increases in endothelial permeability. *Cardiovasc. Res.* **24**:993-997.
39. Sciuto, A.M., Strickland, P.T., Kennedy, T.P., and Gurtner, G.H. (1995) Protective effects of N-acetylcysteine treatment after phosgene exposure in rabbits. *Am. J. Respir. Crit. Care Med.* **151**:768-772.
40. Nobel, C.S.I., Kimland, M., Lind, B., Orrenius, S., and Slater, A.F.G. (1995) Dithiocarbamates induce apoptosis in thymocytes by raising the intracellular level of redox-active copper. *J. Biol. Chem.* **270**:26202-26208.

41. Pinkus, R., Weiner, L.M., and Daniel, V. (1996) Role of oxidants and antioxidants in the induction of AP-1, NF-kappa-B, and glutathione S-transferase gene expression. *J. Biol. Chem.* **271**:13422-13429.
42. Yokoo, T., and Kitamura, M. (1996) Antioxidant PDTC induces stromelysin expression in mesangial cells via a tyrosine kinase-AP-1 pathway. *Am. J. Physiol.* **39**:F806-F811.
43. Yokoo, T., and Kitamura, M. (1996) Dual regulation of IL-1 β -mediated matrix metalloproteinase-9 expression in mesangial cells by NF- κ B and AP-1. *Am. J. Physiol.* **39**:F123-F130

TABLE I

Treatment	Time h	Low Red Lumin		High Red Lumin	
		%	Mean	%	Mean
Control	1	2.0	14.9	98.0	41.2
Phosgene	1	39.7	10.6	60.3	41.6
Control (adher)	3	1.1	10.7	98.9	39.2
Phosgene (adher)	3	23.9	8.8	76.1	38.5
Control (super)	3	63.2	10.3	36.8	38.3
Phosgene (super)	3	44.2	12.0	55.8	37.8

Histogram analysis of acridine orange accumulation into acidified lysosomes as detected by flow cytometric measurements of red fluorescence from pooled human endothelial cells after detachment by trypsinization or spontaneous detachment (1 h). Cells were incubated in medium for 3 h after exposure to phosgene and spontaneously detached (super) and trypsinized cells (adher) were separately analyzed by flow cytometry after incubation with acridine orange.

Figure 1: Percentage of neutrophils in differential count from peripheral blood samples of rats pretreated with normal rabbit serum or anti-rat neutrophil antiserum and exposed to 300 ppm phosgene or to air containing 5% CO₂ for one minute, as described on pp.6-7. "phos+ANS", phosgene-exposed after pretreatment with anti-neutrophil antiserum; "phos+NRS", phosgene exposed after pretreatment with normal serum; "ANS", sham exposed to air after pretreatment with anti-neutrophil antiserum; "NRS", sham exposed to air after pretreatment with normal serum. The anti-neutrophil antiserum renders the animals neutropenic.

phos-blood neutrophil %

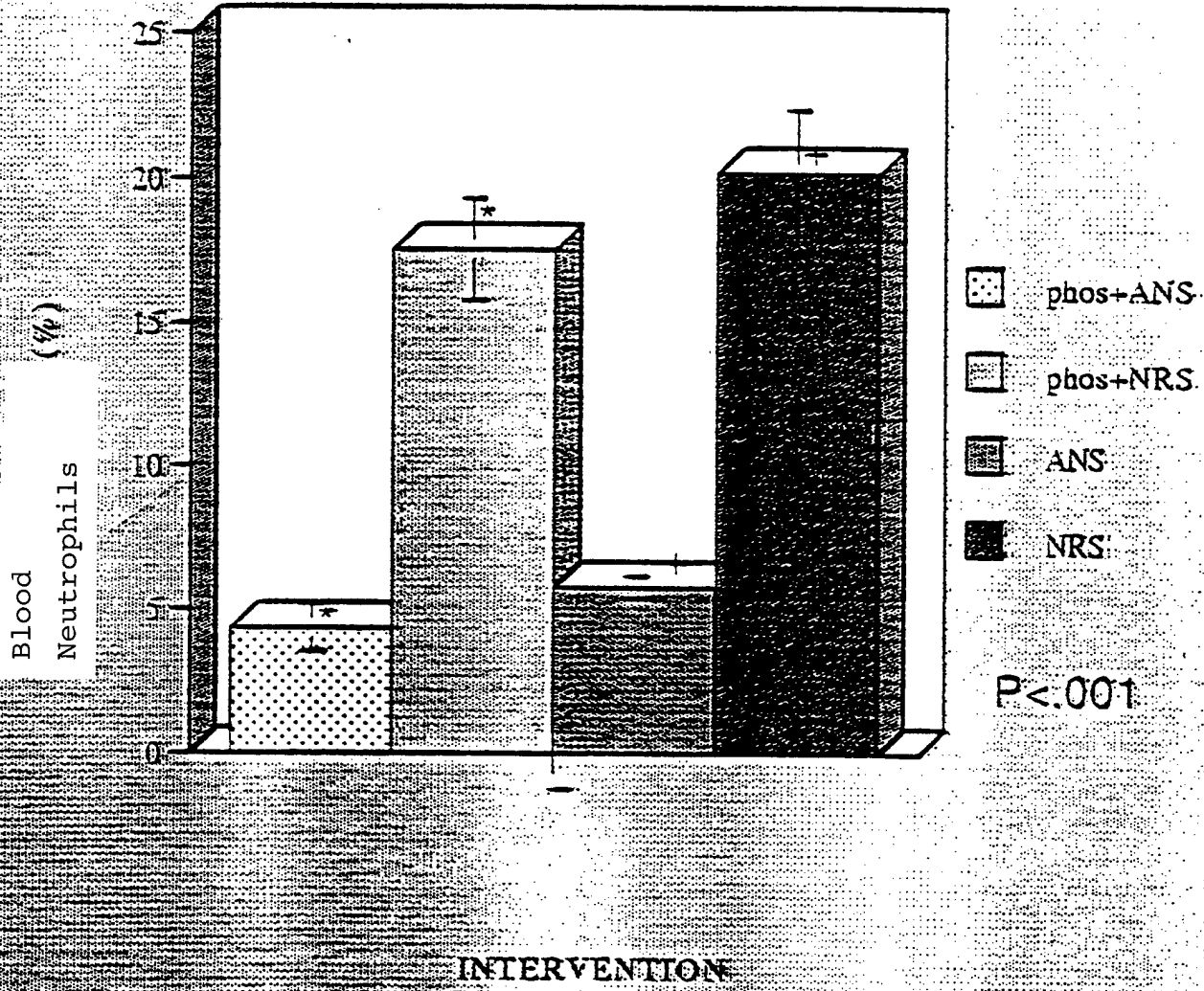
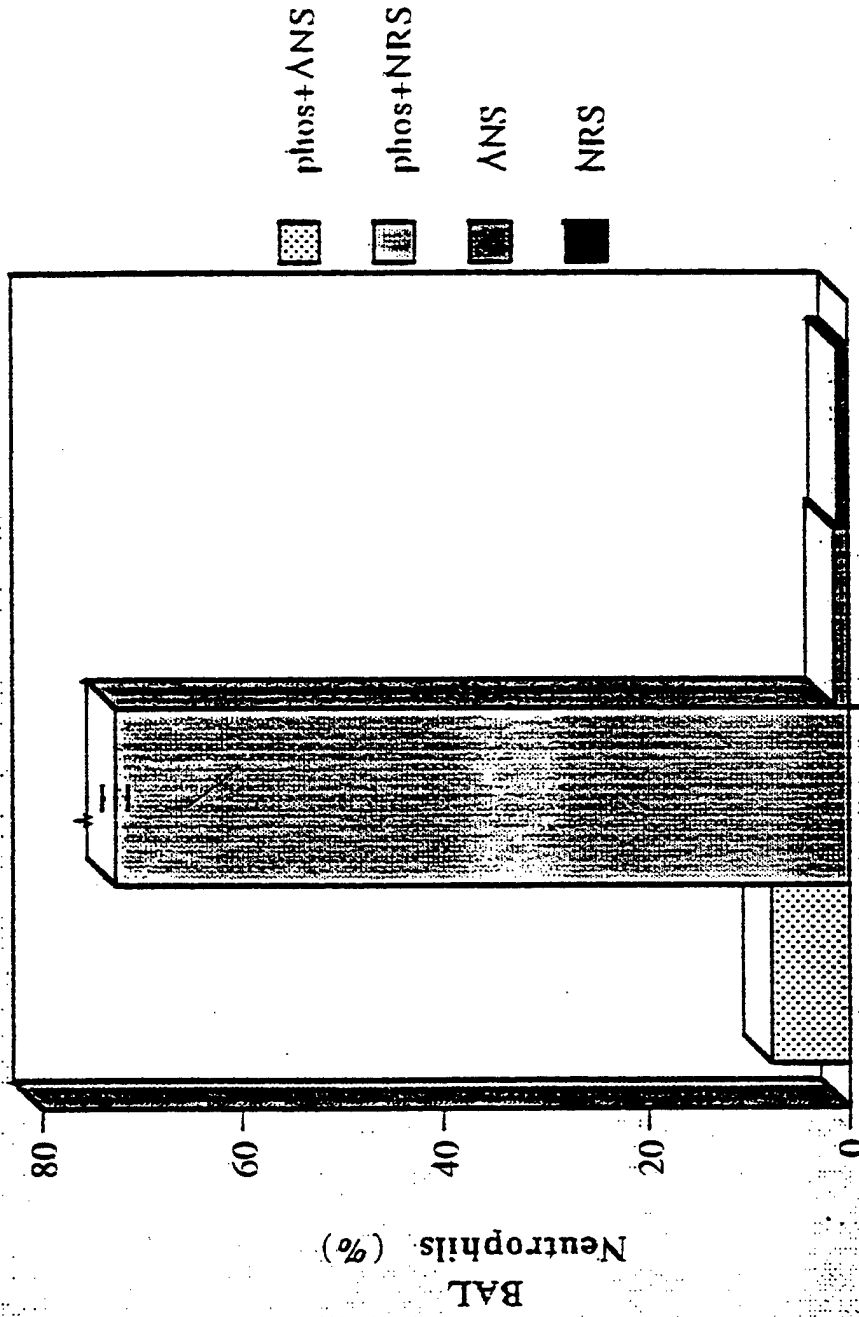


Figure 2. Percentage of neutrophils in the bronchoalveolar lavage fluid of rats pretreated with normal rabbit serum or anti-rat neutrophil antiserum and exposed to 300 ppm phosgene or to air containing 5% CO₂ for one minute, as described on pp.6-7. "phos+ANS", phosgene-exposed after pretreatment with anti-neutrophil antiserum; "phos+NRS", phosgene exposed after pretreatment with normal serum; "ANS", sham exposed to air after pretreatment with anti-neutrophil antiserum; "NRS", sham exposed to air after pretreatment with normal serum. Exposure to phosgene results in marked neutrophil influx into the alveolar space, but pretreatment with anti-neutrophil antiserum reduces this influx markedly.

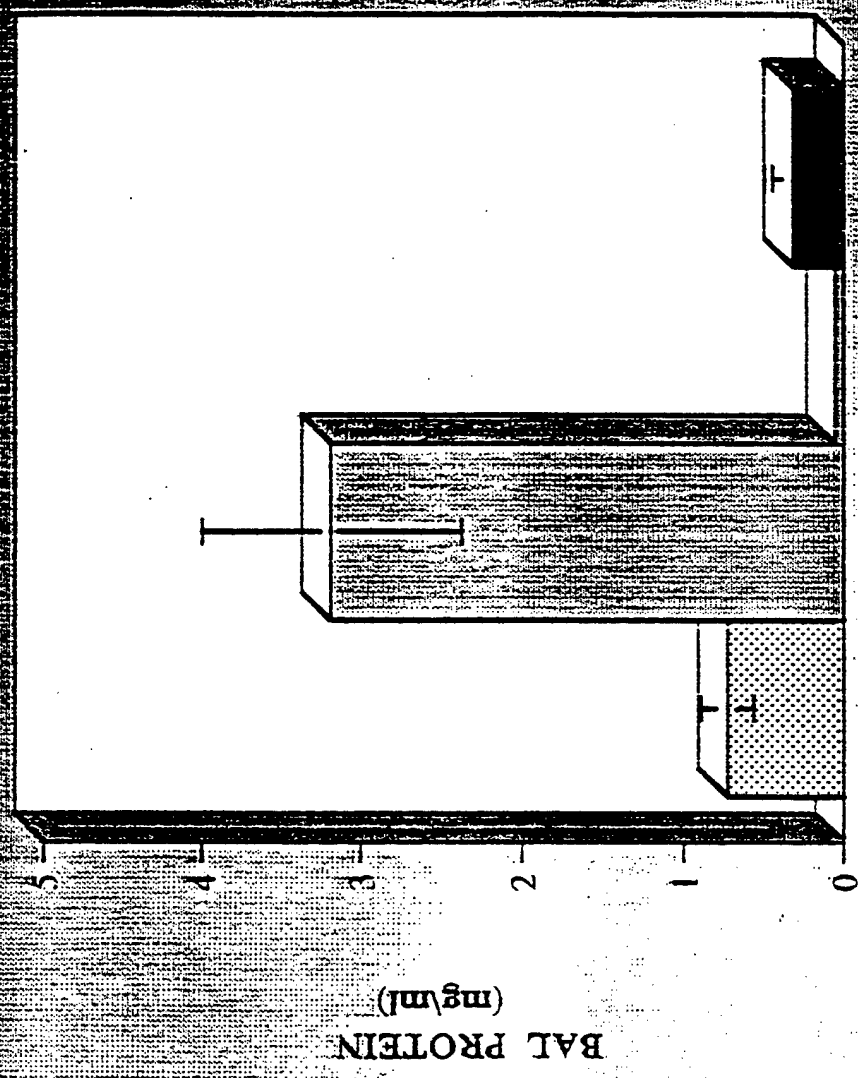
phos bal neutrophils (%)



INTERVENTION

Figure 3. Levels of BCA-reactive protein in the bronchoalveolar lavage fluid of rats pretreated with normal rabbit serum or anti-rat neutrophil antiserum and exposed to 300 ppm phosgene or to air containing 5% CO₂ for one minute, as described on pp.6-7. "phos+ANS", phosgene-exposed after pretreatment with anti-neutrophil antiserum; "phos+NRS", phosgene exposed after pretreatment with normal serum; "ANS", sham exposed to air after pretreatment with anti-neutrophil antiserum; "NRS", sham exposed to air after pretreatment with normal serum. Exposure to phosgene results in marked protein leakage into the alveolar space, but pretreatment with anti-neutrophil antiserum reduces this leakage markedly.

phos rat bal protein



phos+ANS

phos+NRS

ANS

NRS

INTERVENTION

Figure 4. Wet-to-dry weight ratio of lungs excised from rats pretreated with normal rabbit serum or anti-rat neutrophil antiserum and exposed to 300 ppm phosgene or to air containing 5% CO₂ for one minute, as described on pp.6-7. "phos+ANS", phosgene-exposed after pretreatment with anti-neutrophil antiserum; "phos+NRS", phosgene exposed after pretreatment with normal serum; "ANS", sham exposed to air after pretreatment with anti-neutrophil antiserum; "NRS", sham exposed to air after pretreatment with normal serum. Exposure to phosgene results in only a small increase in the weight ratio, which is nevertheless abrogated by pretreatment with antineutrophil antiserum.

PHOS RAT LUNG W/D#1

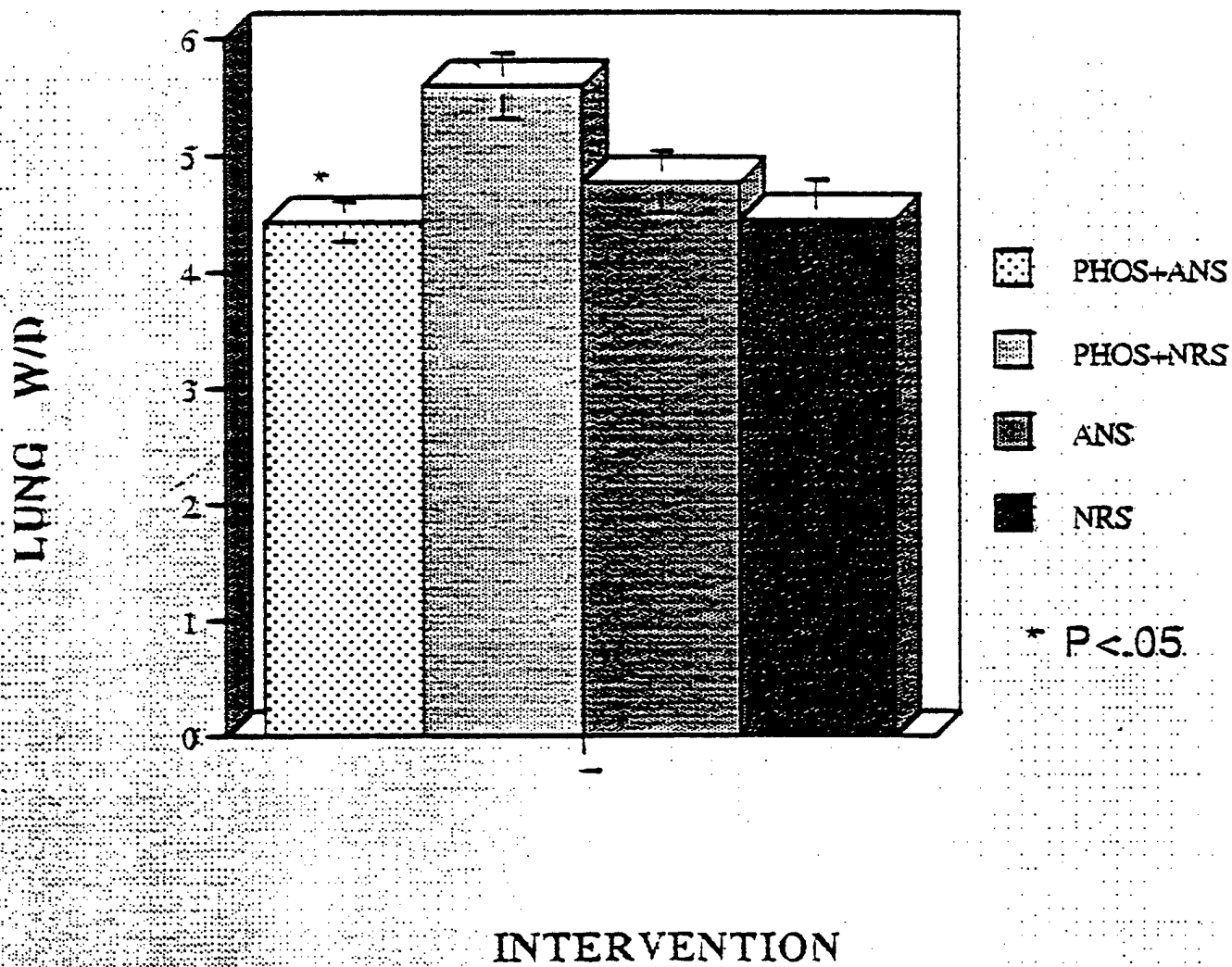
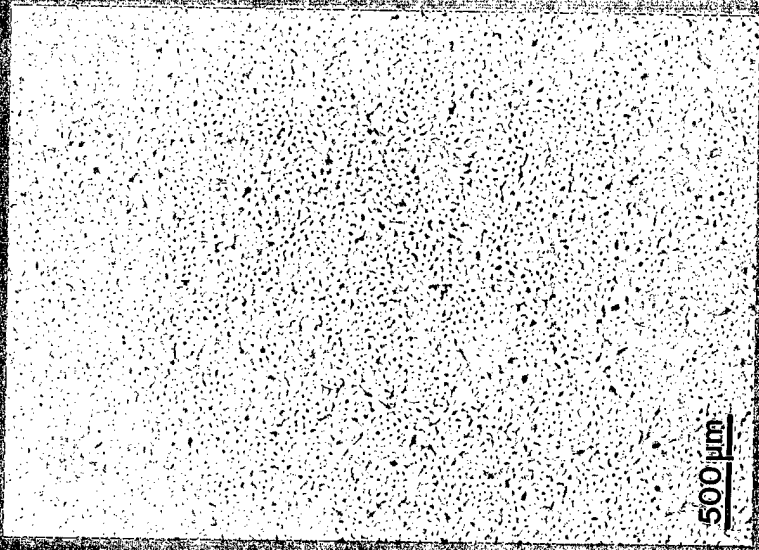
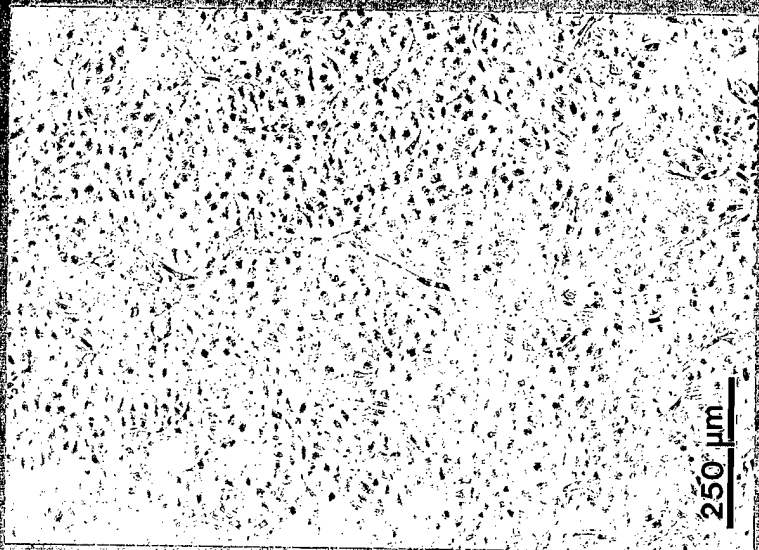
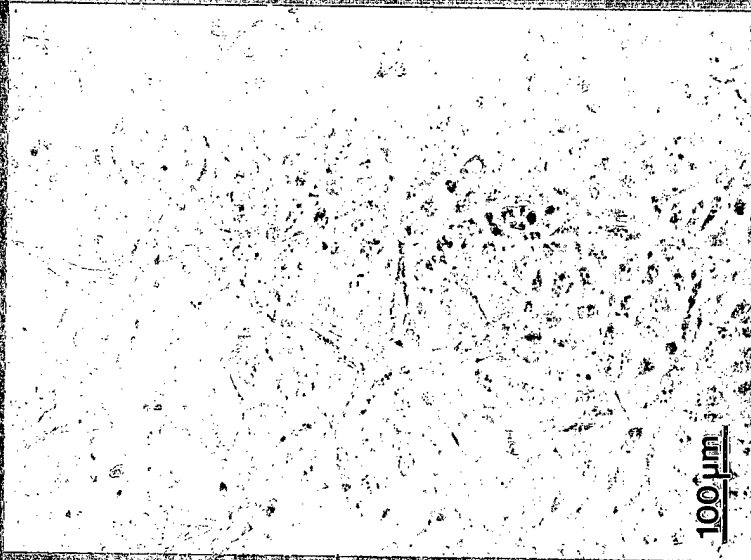
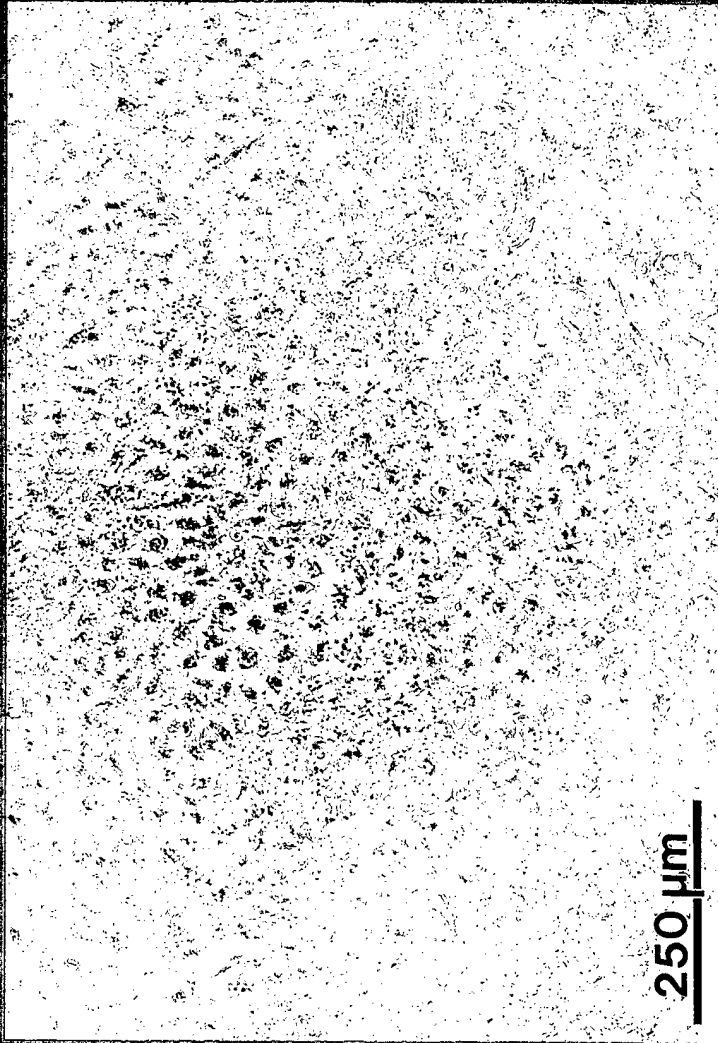


Figure 5a. Phase contrast images of human umbilical vein endothelial cells cultured on their fifth passage to confluence on a gelatin-coated polystyrene T25 flask using a beta-tested formulation of Gibco serum-free endothelial cell growth medium.



© 2000
L. W. J. J. J.

Figure 5b. Phase contrast image of human umbilical vein endothelial cells cultured on their fifth passage to confluence on a 48-well polystyrene multiplate on which an interstitial extracellular matrix had been formed by R22 smooth muscle cells as described on pp.7-8. The confluent cells appear to be all in complete close contact with one another, giving rise to a characteristic "cobblestone" appearance.



Phase contrast image of confluent passage 5 HUVEC grown in Gibco serum free human endothelial cell growth medium on R22 interstitial ECM coated 48 well plate.

Bar = 250 μ

Figure 6. Effects of a 3 minute exposure to 300 ppm phosgene on the permeability of HMVEC monolayers to mannitol. The rate of diffusion of ¹⁴C-mannitol across confluent monolayers of HMVEC on Costar TransWells was measured after exposure to phosgene or to air only as described on pp.9-10. The results shown are the mean of four experiments, each employing triplicate wells. Error bars represent standard error of the means. Phosgene exposure increases the permeability of these monolayers to mannitol.

EFFECTS OF 900 PPM·MIN PHOSGENE EXPOSURE ON PERMEABILITY OF
HMVEC MONOLAYERS TO ¹⁴C-MANNITOL

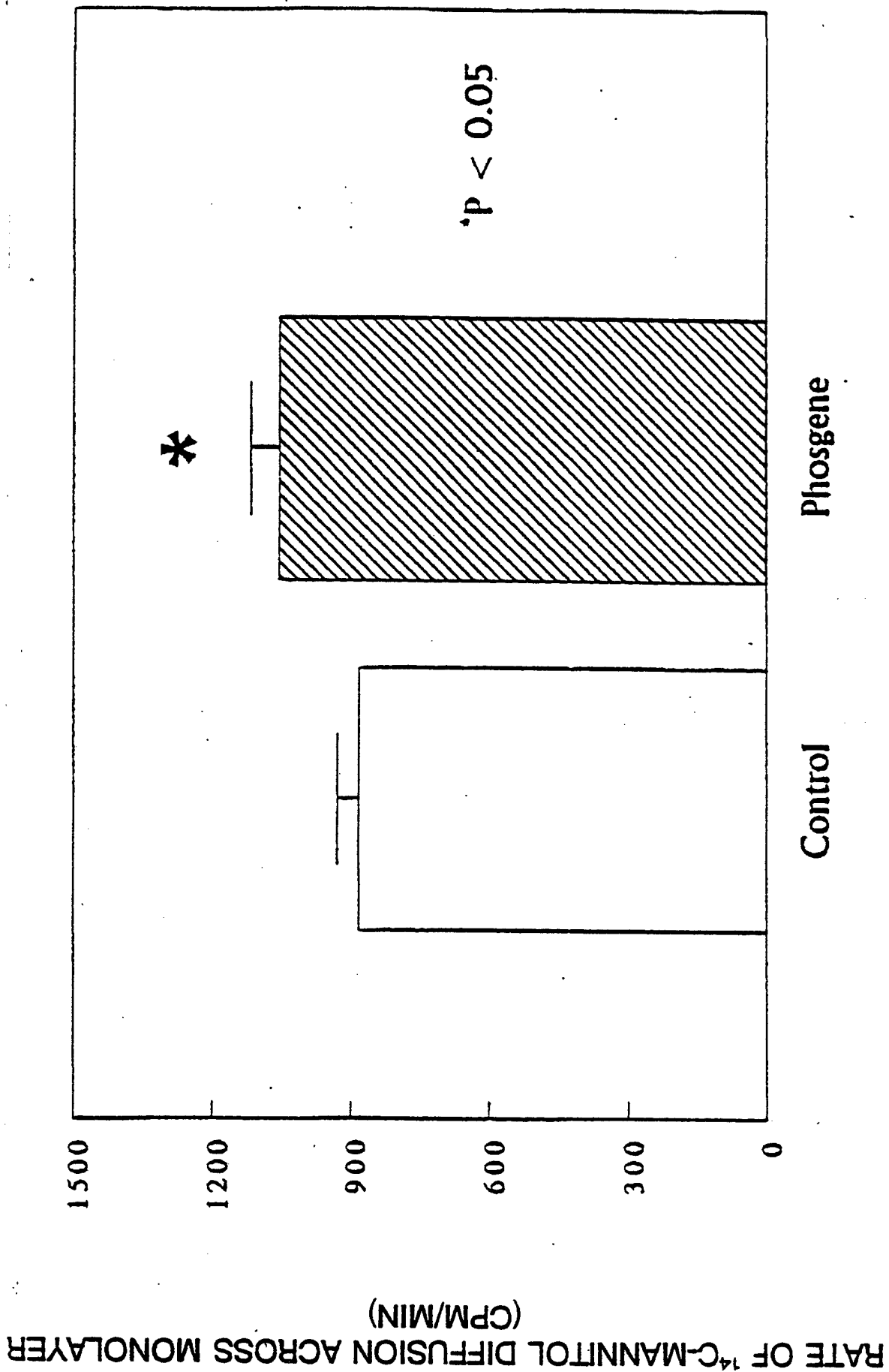


Figure 7. Effects of a 3 minute exposure to 300 ppm phosgene on the electrical resistance of confluent rat type II alveolar epithelial cell monolayers on Costar TransWells, as measured in a Millicell ERS ohmmeter. This experiment was performed on triplicate wells, as described on p.10.

ELECTRICAL RESISTANCE OF RAT TYPE II ALVEOLAR EPITHELIAL CELLS AFTER EXPOSURE TO PHOSGENE FOR 3 MINUTES

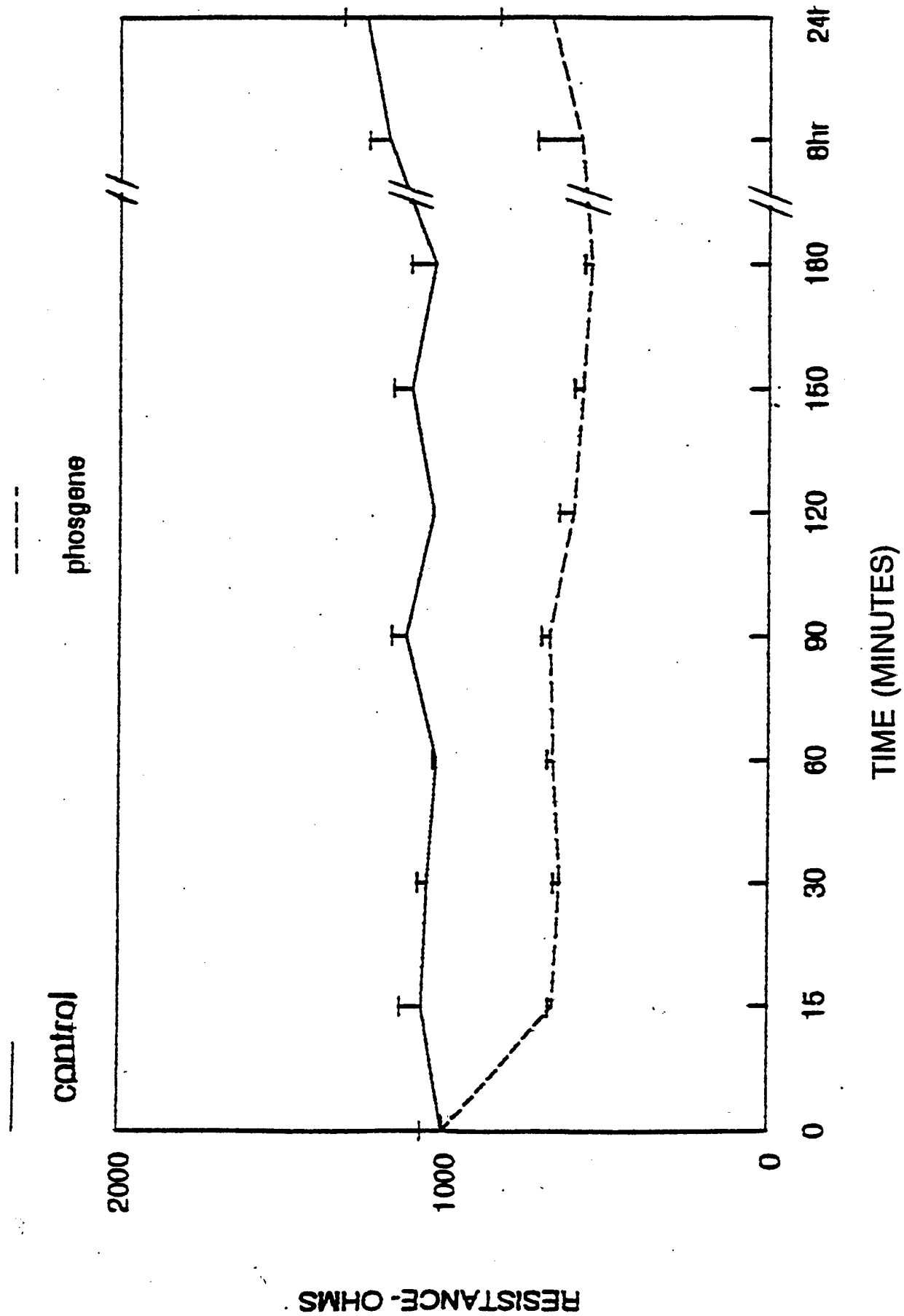


Figure 8. Effects of 1 minute or 3 minute exposures to 300 ppm phosgene on the permeability of rat type II alveolar epithelial cell monolayers to mannitol. The rate of diffusion of ^{14}C -mannitol across confluent monolayers of rat type II epithelial cells on Costar TransWells was measured after exposure to 300 ppm·min or 900 ppm·min phosgene or to air only as described on pp.10-11. The results shown are the mean of two experiments, each employing triplicate wells. Error bars represent standard error of the means. Phosgene exposure increases the permeability of these monolayers to mannitol, as seen for HMVEC in Figure 6, but the junctional integrity of sham-exposed alveolar epithelial cells is tighter than that of the endothelial cells. The epithelial cell junctions are not significantly affected by 300 ppm·min phosgene exposure, but permeability increases by five-fold after exposure to 900 ppm·min phosgene.

EFFECTS OF PHOSGENE EXPOSURE ON PERMEABILITY OF RAT TYPE II
ALVEOLAR EPITHELIAL CELL MONOLAYERS TO ¹⁴C-MANNITOL

RATE OF ¹⁴C-MANNITOL DIFFUSION ACROSS MONOLAYER
(CPM/MIN)

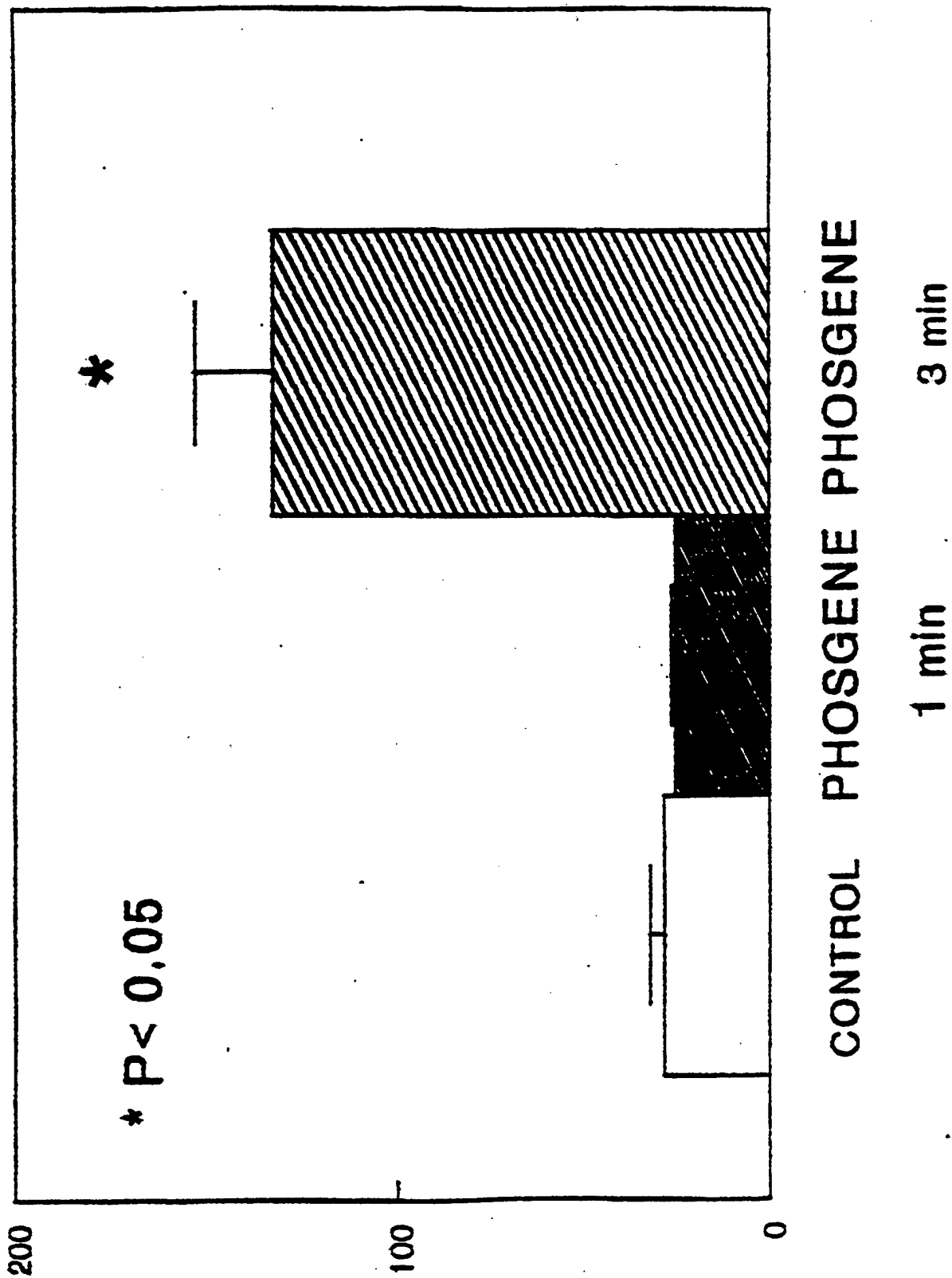


Figure 9. Evaluation of calcein-AM esterolysis as a measure of cytotoxicity. Quadruplicate wells of R22 smooth muscle cells in 24 well microplates were challenged with different concentrations of methanol to introduce different degrees of cytotoxic injury before incubation with 3 μ M calcein-AM and 2 μ M ethidium homodimer-1 as described on pp.12-13. Conversion of calcein-AM to calcein was measured by recording fluorescence at 530 nm with excitation at 485 nm. Increasing cytotoxicity is seen as less development of calcein fluorescence. Error bars show SD (n=4).

LIVE / DEAD CYTOFLUOR ASSAY

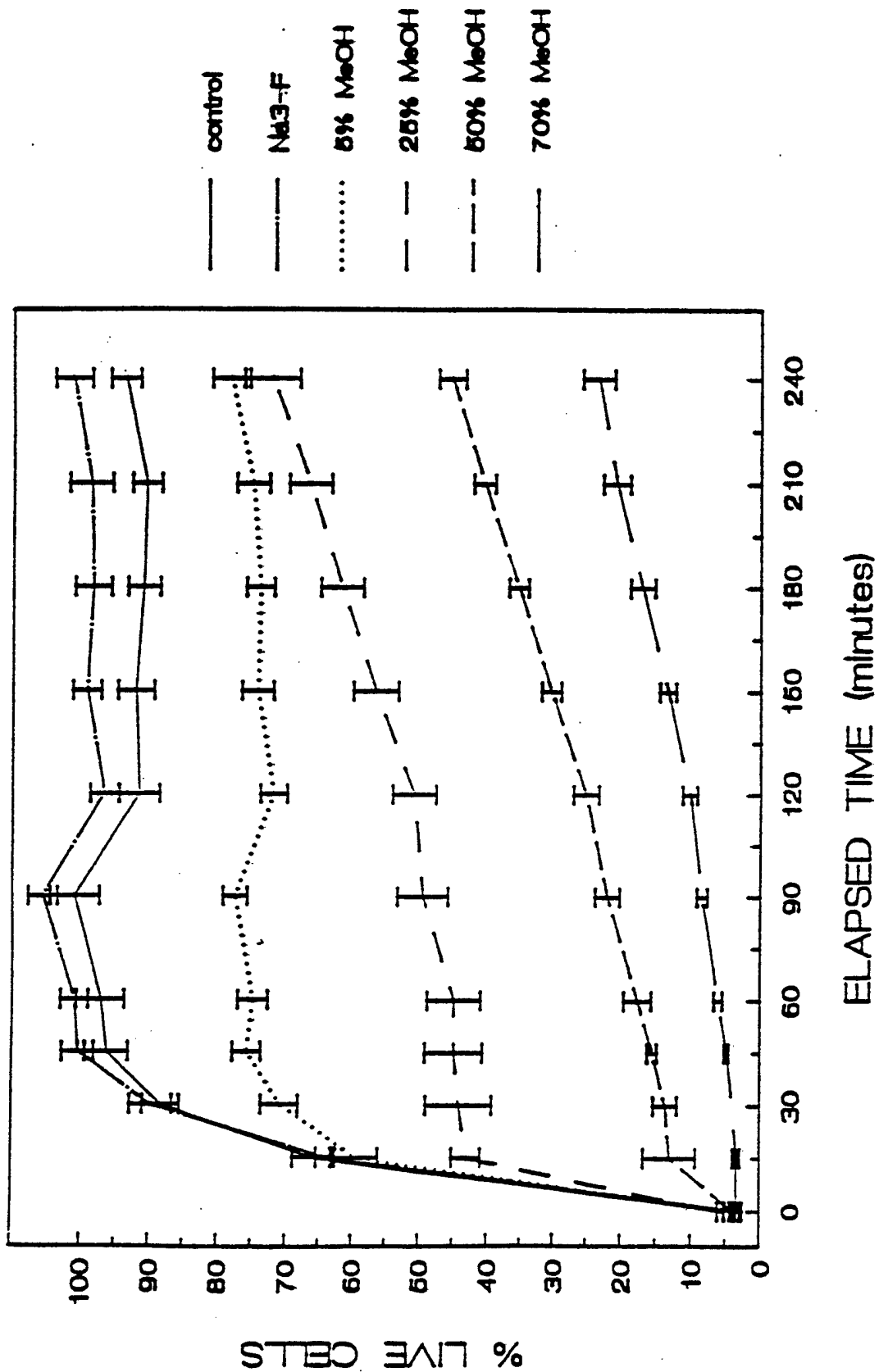


Figure 10. Evaluation of ethidium homodimer-1 binding to DNA as a measure of cytotoxicity. Quadruplicate wells of R22 smooth muscle cells in 24 well microplates were challenged with different concentrations of methanol to introduce different degrees of cytotoxic injury before incubation with 3 μ M calcein-AM and 2 μ M ethidium homodimer-1 as described on pp.12-13. Binding of ethidium homodimer-1 to DNA was measured by recording fluorescence at 645 nm with excitation at 530 nm. Increasing cytotoxicity is seen as greater development of ethidium homodimer-1 fluorescence. Error bars, SD (n=4).

LIVE / DEAD CYTOFLUOR ASSAY

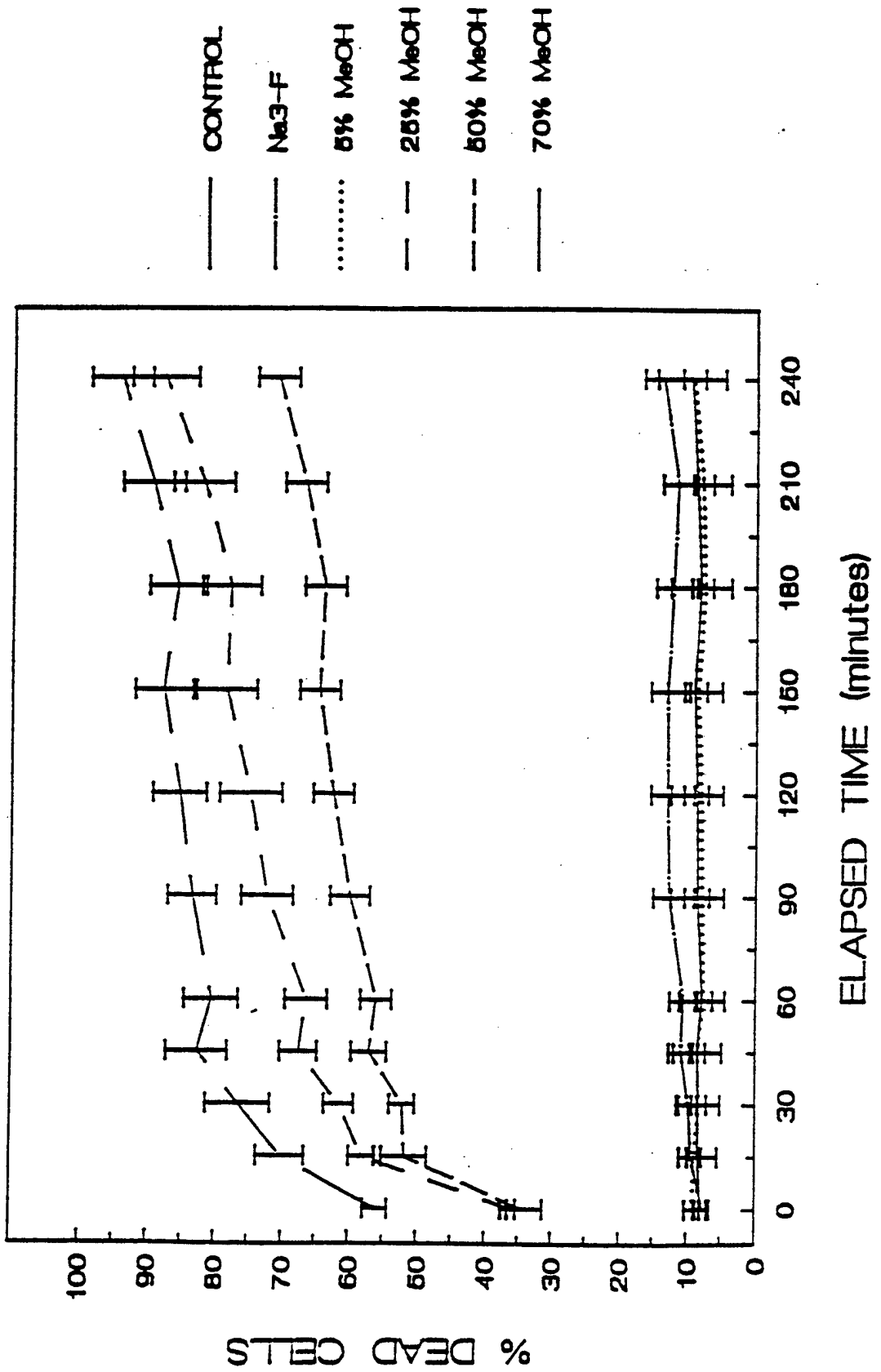


Figure 11. Effect of exposure to 300 ppm phosgene on cytotoxic injury to bovine pulmonary endothelial cells as evaluated with calcein-AM and ethidium homodimer-1, as described on p.13. This experiment was carried out on triplicate wells. Times of exposure to 300 ppm phosgene are noted on the X-axis. Calculations of "% live" and "% dead" were carried out according to the relationships described on p. 13. These cells appear to be resistant to significant cytotoxic injury from phosgene exposure. Error bars, SD (n=3).

Effects of Phosgene on BPEC "Live/Dead" Cytotoxicity Assay

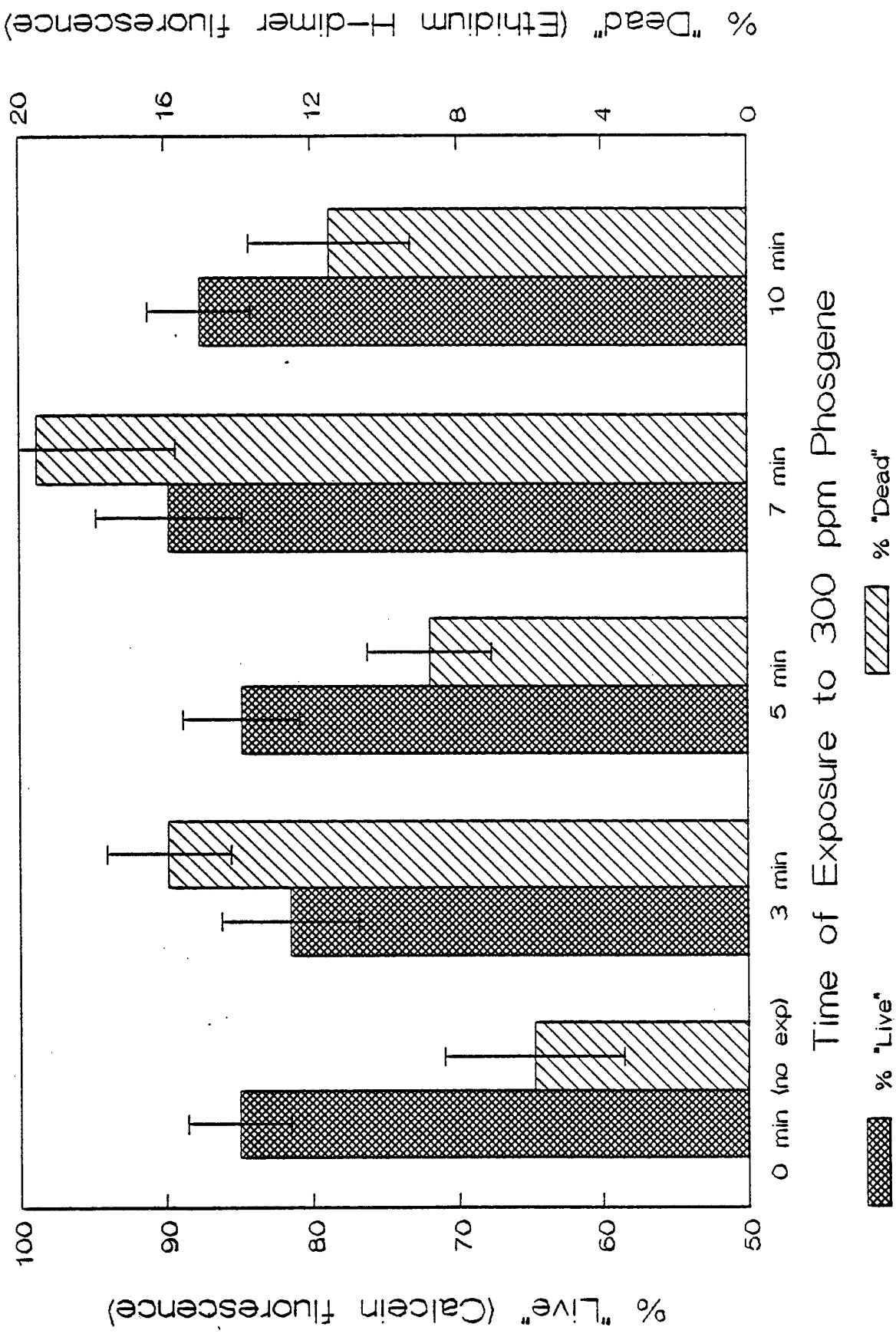


Figure 12. Effect of sham exposure to 5% CO₂ in air on cytotoxic injury to human microvascular endothelial cells as evaluated with calcein-AM and ethidium homodimer-1, as described on p.14. The fluorescence at 530 nm from calcein and at 645 nm from DNA-bound ethidium homodimer-1 was recorded every 15 minutes, starting 15 minutes after initial addition of reagents to triplicate wells of HMVEC in 24 well microplates. Closed symbols, fluorescence from sham exposed cells; open symbols, fluorescence from cells treated with 70% methanol to induce maximum cytotoxic injury.

HMVEC Exposed 6 min to Air (control) "Live/Dead" Cytotoxicity Assay

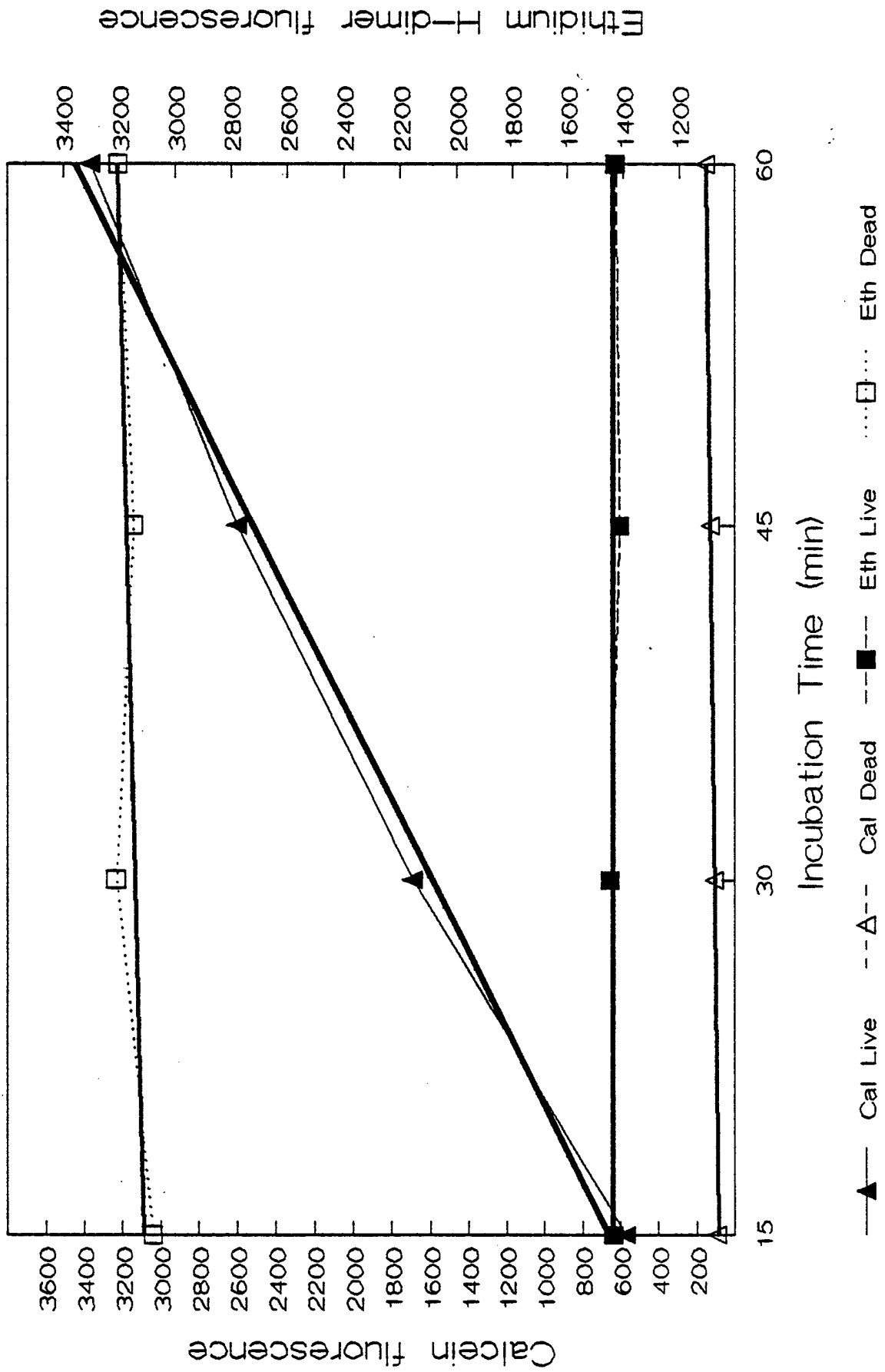


Figure 13. Effects of 1 min exposure to 300 ppm phosgene on cytotoxic injury to human microvascular endothelial cells as evaluated with calcein-AM and ethidium homodimer-1, as described on p.14. The fluorescence at 530 nm from calcein and at 645 nm from DNA-bound ethidium homodimer-1 was recorded every 15 minutes, starting 15 minutes after initial addition of reagents to triplicate wells of HMVEC in 24 well microplates. Closed symbols, fluorescence from sham exposed cells; open symbols, fluorescence from cells treated with 70% methanol to induce maximum cytotoxic injury.

HMVEC Exposed 1 min to 300 ppm Phosgene "Live/Dead" Cytotoxicity Assay

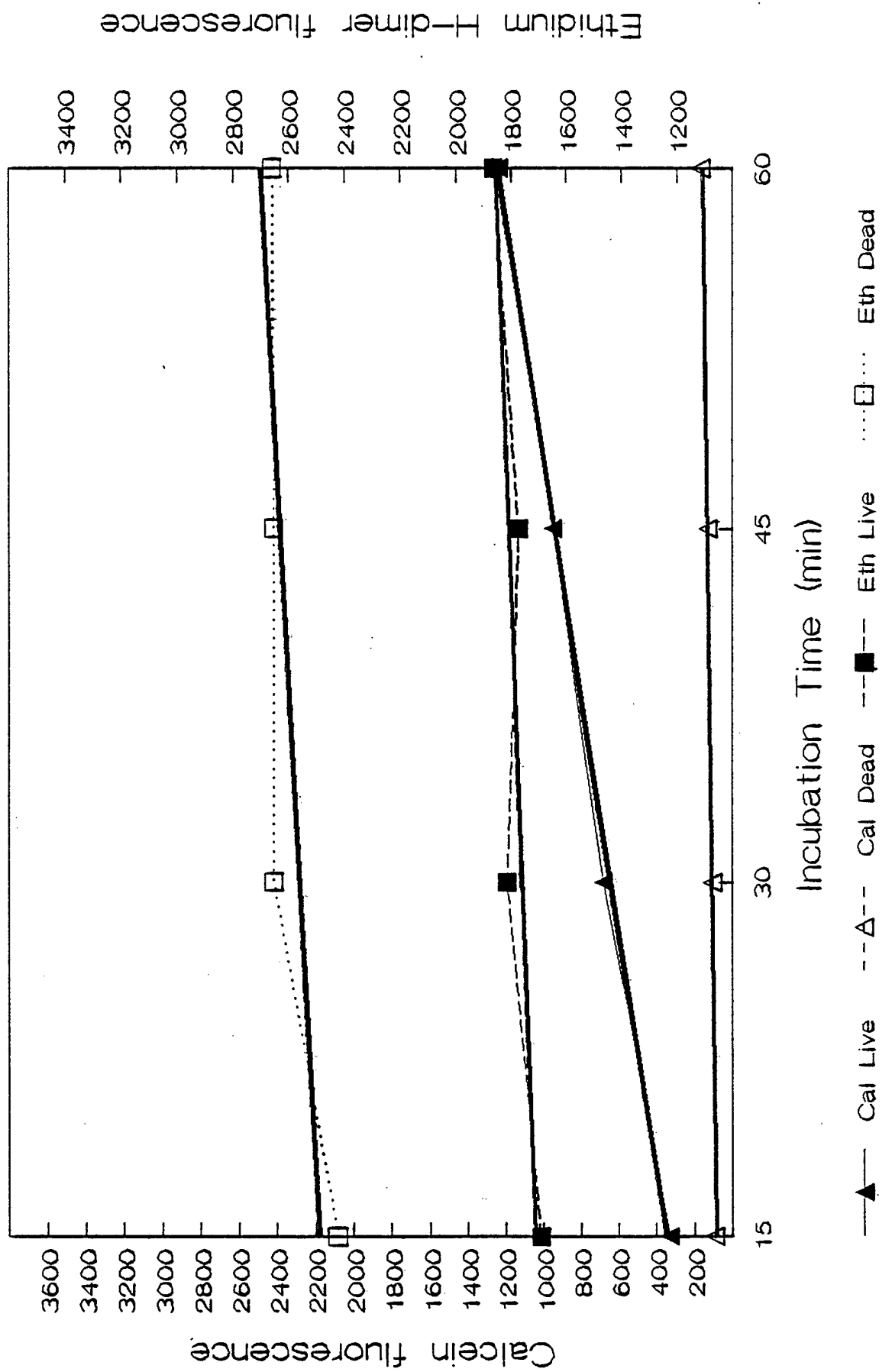


Figure 14. Effects of 3 min exposure to 300 ppm phosgene on cytotoxic injury to human microvascular endothelial cells as evaluated with calcein-AM and ethidium homodimer-1, as described on p.14. The fluorescence at 530 nm from calcein and at 645 nm from DNA-bound ethidium homodimer-1 was recorded every 15 minutes, starting 15 minutes after initial addition of reagents to triplicate wells of HMVEC in 24 well microplates. Closed symbols, fluorescence from sham exposed cells; open symbols, fluorescence from cells treated with 70% methanol to induce maximum cytotoxic injury.

HMVEC Exposed 3 min to 300 ppm Phosgene "Live/Dead" Cytotoxicity Assay

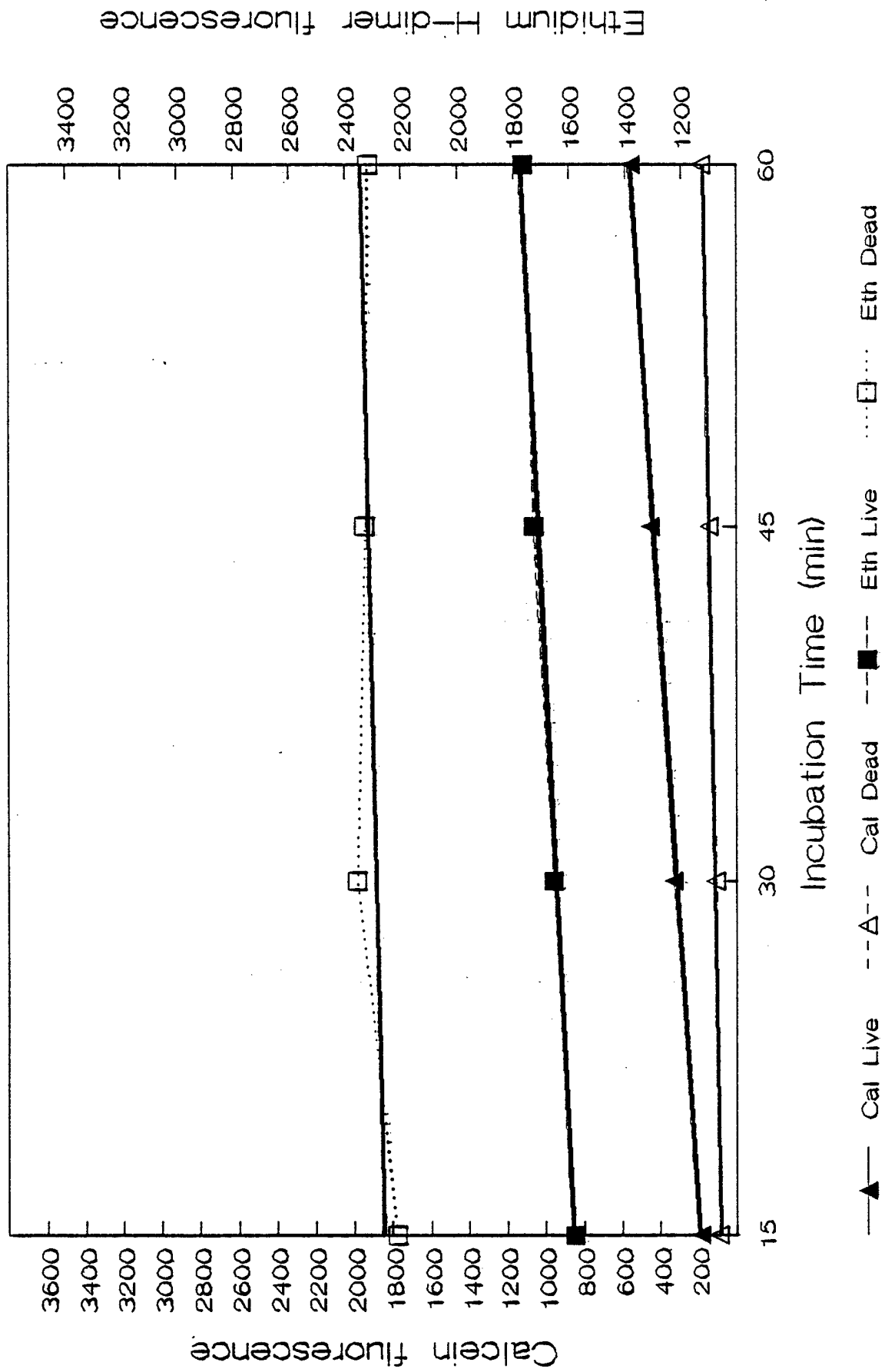


Figure 15. Effects of 6 min exposure to 300 ppm phosgene on cytotoxic injury to human microvascular endothelial cells as evaluated with calcein-AM and ethidium homodimer-1, as described on p.14. The fluorescence at 530 nm from calcein and at 645 nm from DNA-bound ethidium homodimer-1 was recorded every 15 minutes, starting 15 minutes after initial addition of reagents to triplicate wells of HMVEC in 24 well microplates. Closed symbols, fluorescence from sham exposed cells; open symbols, fluorescence from cells treated with 70% methanol to induce maximum cytotoxic injury.

HMVEC Exposed 6 min to 300 ppm Phosgene "Live/Dead" Cytotoxicity Assay

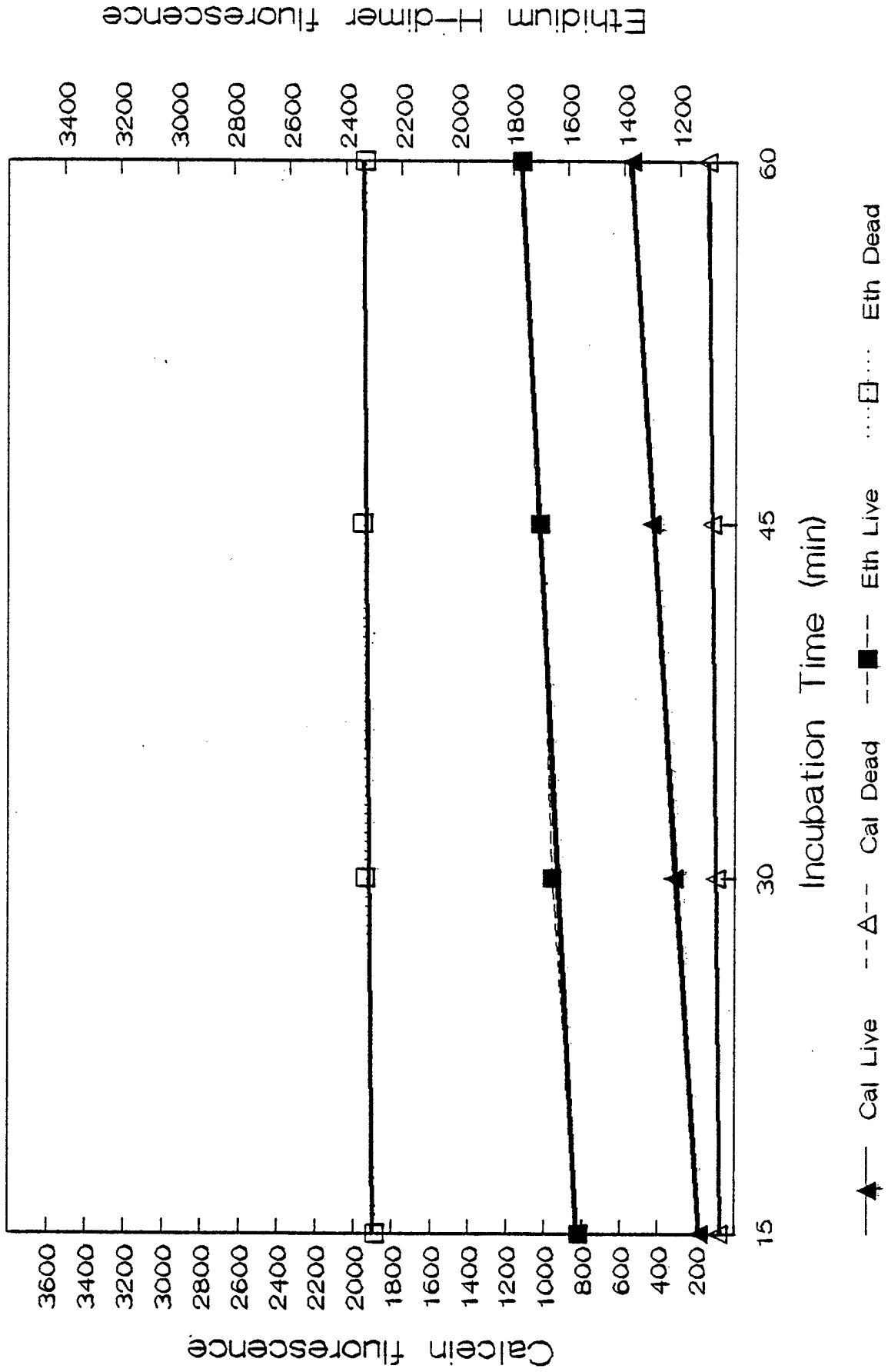


Figure 16. Effects of different periods of exposure to 300 ppm phosgene or sham exposure to 5% CO₂ in air on cytotoxic injury to HMVEC as evaluated with calcein-AM and ethidium homodimer-1, as described on pp.15-16. The fluorescence at 530 nm from calcein and at 645 nm from DNA-bound ethidium homodimer-1 was recorded 1 hour after addition of the two probes to triplicate wells of HMVEC in 24 well plates. The fluorescence intensities from phosgene- or air- exposed cells were compared to the intensities from triplicate wells of cells on a separate plate from the same batch which received no exposure ("100% live") or which had been treated with 70% methanol ("100% dead"). Error bars, SD (n=3).

Effects of Phosgene on HMVEC "Live/Dead" Cytotoxicity Assay

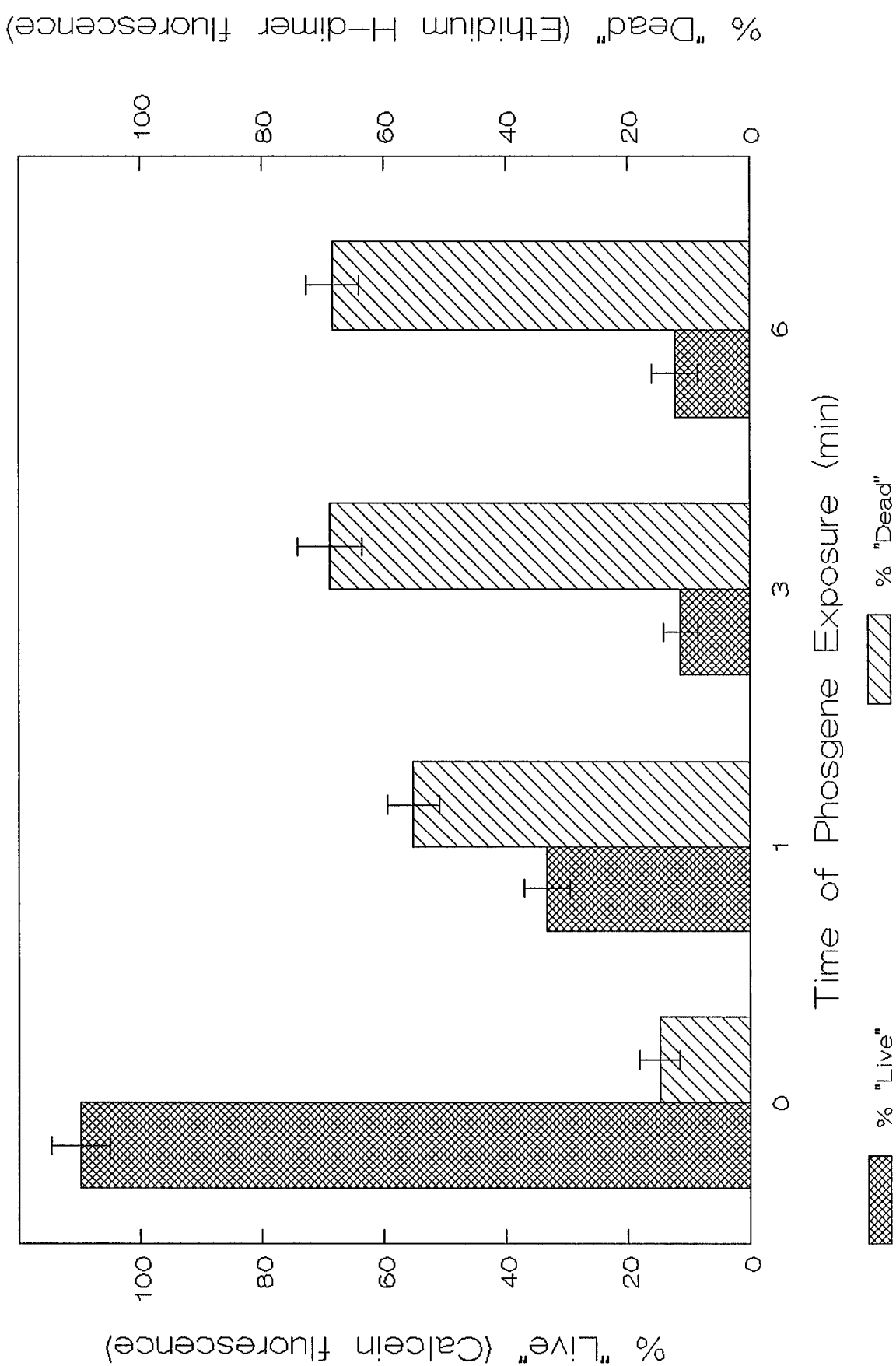


Figure 17. Effects of different periods of exposure to 300 ppm phosgene or sham exposure to 5% CO₂ in air on cytotoxic injury to A549 cells as evaluated from calcein-AM and ethidium homodimer-1, as described on p.15. Six hours after exposure of plates to phosgene or air, the two probes were added to triplicate wells of cells and fluorescence intensities at 530 nm and 645 nm were determined after an additional incubation of 45 minutes. Unlike HMVEC, A549 cells are quite resistant to cytotoxic injury from 1 minute of exposure to phosgene, and continue to display residual cytosolic esterase activity even after 3 minutes of exposure. Error bars, SD (n=3).

Effects of Phosgene on A549 Cells Cytotoxicity Assay

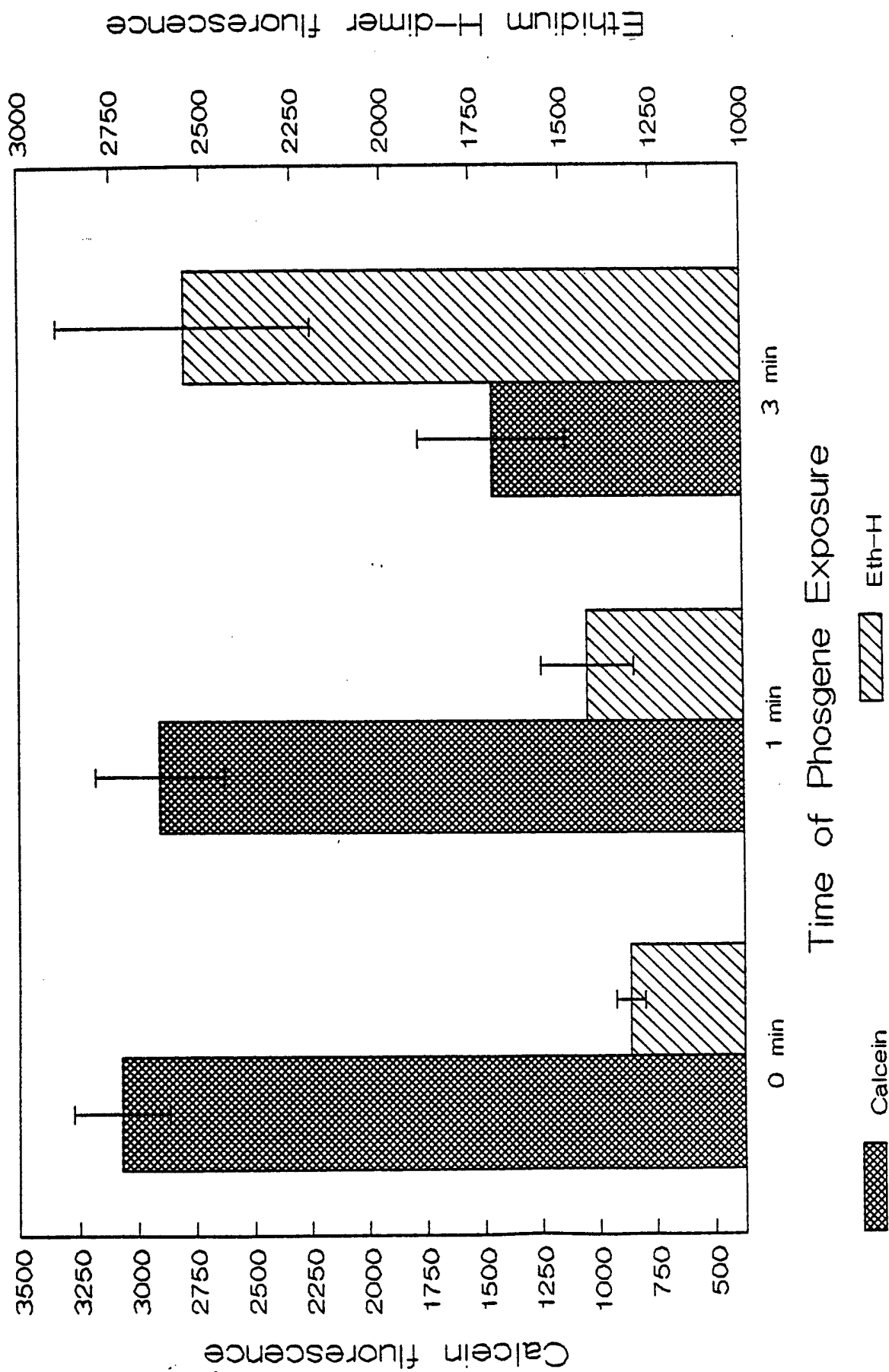


Figure 18. Effects of 1 minute of exposure of HMVEC to 300 ppm phosgene on uptake of rhodamine 123 (R123) into mitochondria, as described on p.18. After exposure to phosgene or to 5% CO₂ in air ("control"), HMVEC were trypsinized and incubated sequentially with R123 and propidium iodide (PI) before analysis by flow cytometry. The fluorescence intensities from the two probes in individual cells are displayed in two-channel scatter plots. In addition to an increase in the fraction of cells in which loss of mitochondrial membrane potential had resulted in low R123 uptake and loss of nuclear membrane integrity had resulted in binding of PI to DNA, a subset of cells in which partial loss of mitochondrial membrane potential and partial failure to exclude PI from the nucleus could also be seen after phosgene exposure.

Membrane Integrity/Mitochondrial Potential Human Endothelial Cells

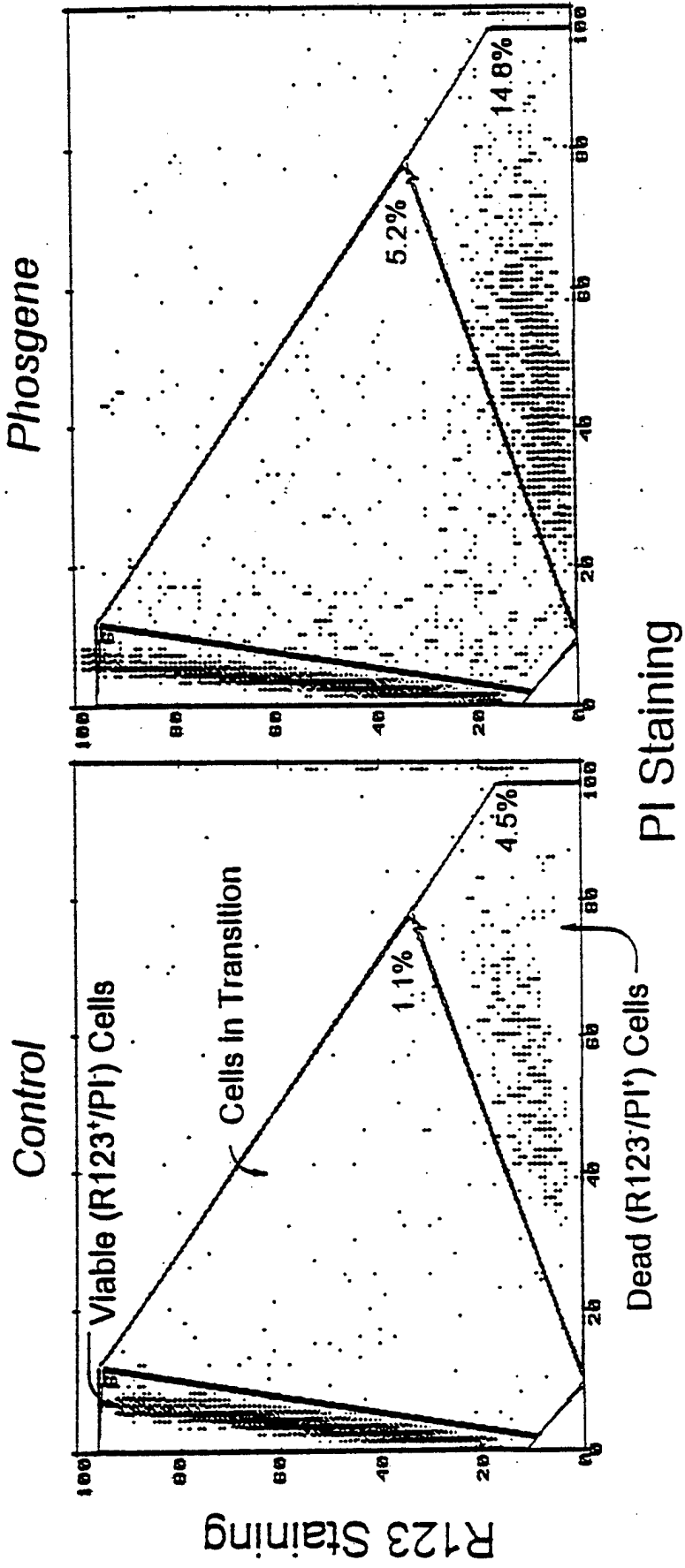


Figure 19. Effects of 1 minute of exposure of HMVEC to 300 ppm phosgene on uptake of rhodamine 123 (R123) into mitochondria, as described on p.18. A histogram analysis of R123 fluorescence intensity from PI-negative cells after exposure to phosgene or 5% CO₂ in air is shown. The distribution of apparent mitochondrial membrane potentials in cells which still exclude PI appears to be skewed to lower potential values after phosgene exposure, consistent with a transitional state of cell injury.

Mitochondrial Transmembrane Potential

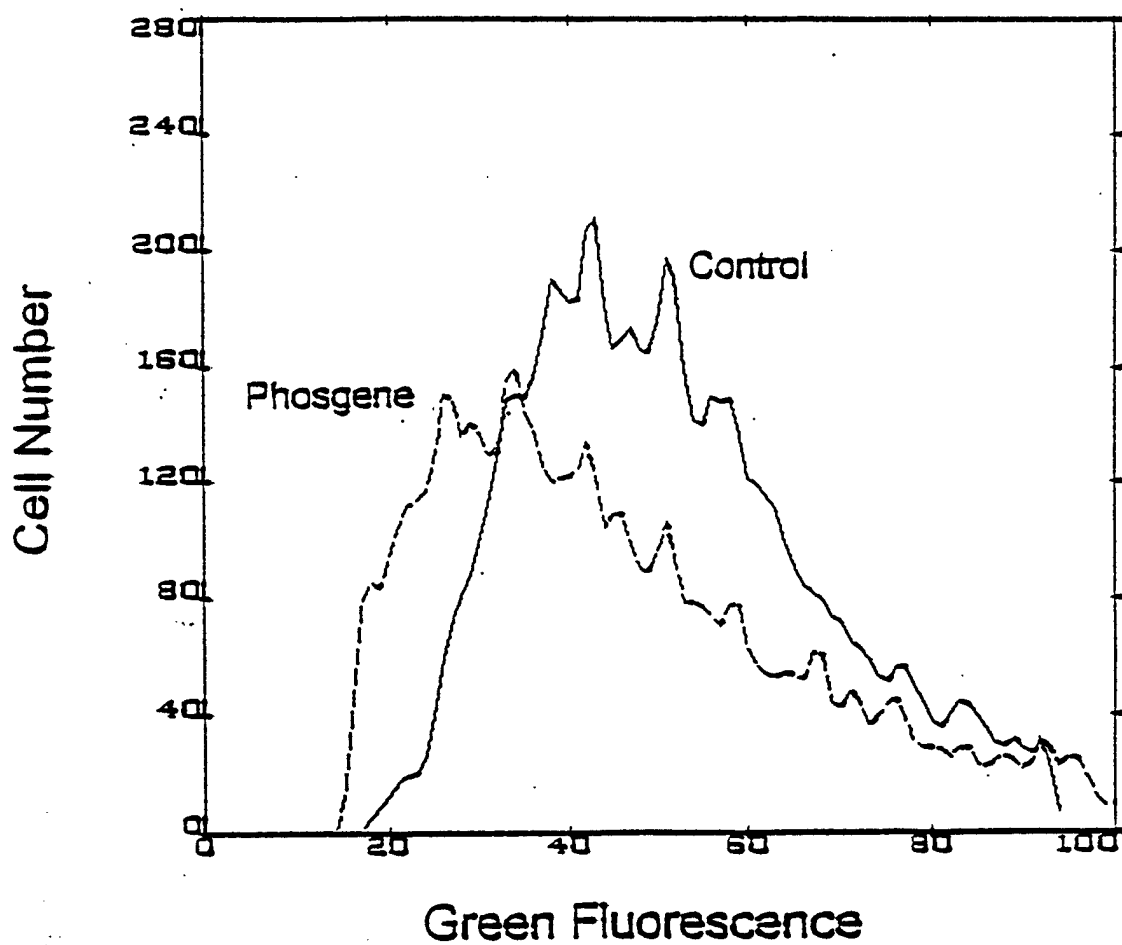


Figure 20. Uptake of the cyanine dye JC-1 into mitochondria of HMVEC exposed to 5% CO₂ in air only (0 min phosgene exposure), or to 300 ppm phosgene for different periods, as described on pp.16-17. Control cells received no exposure. Cells in triplicate wells were incubated with JC-1 for 12 minutes and then, after replacement of the dye with HBSS, the fluorescence of dye monomers at 530 nm and of J-aggregates at 590 nm was recorded immediately (0.2 h) or after an additional 108 minutes (2.0 h). Some loss of intracellular dye appears to occur after the extended incubation in HBSS. The ratio of J-aggregate to monomer fluorescence is displayed in the next Figure.

Effects of Phosgene on HMVEC

JC-1 Uptake - Monomers and J-Aggregates

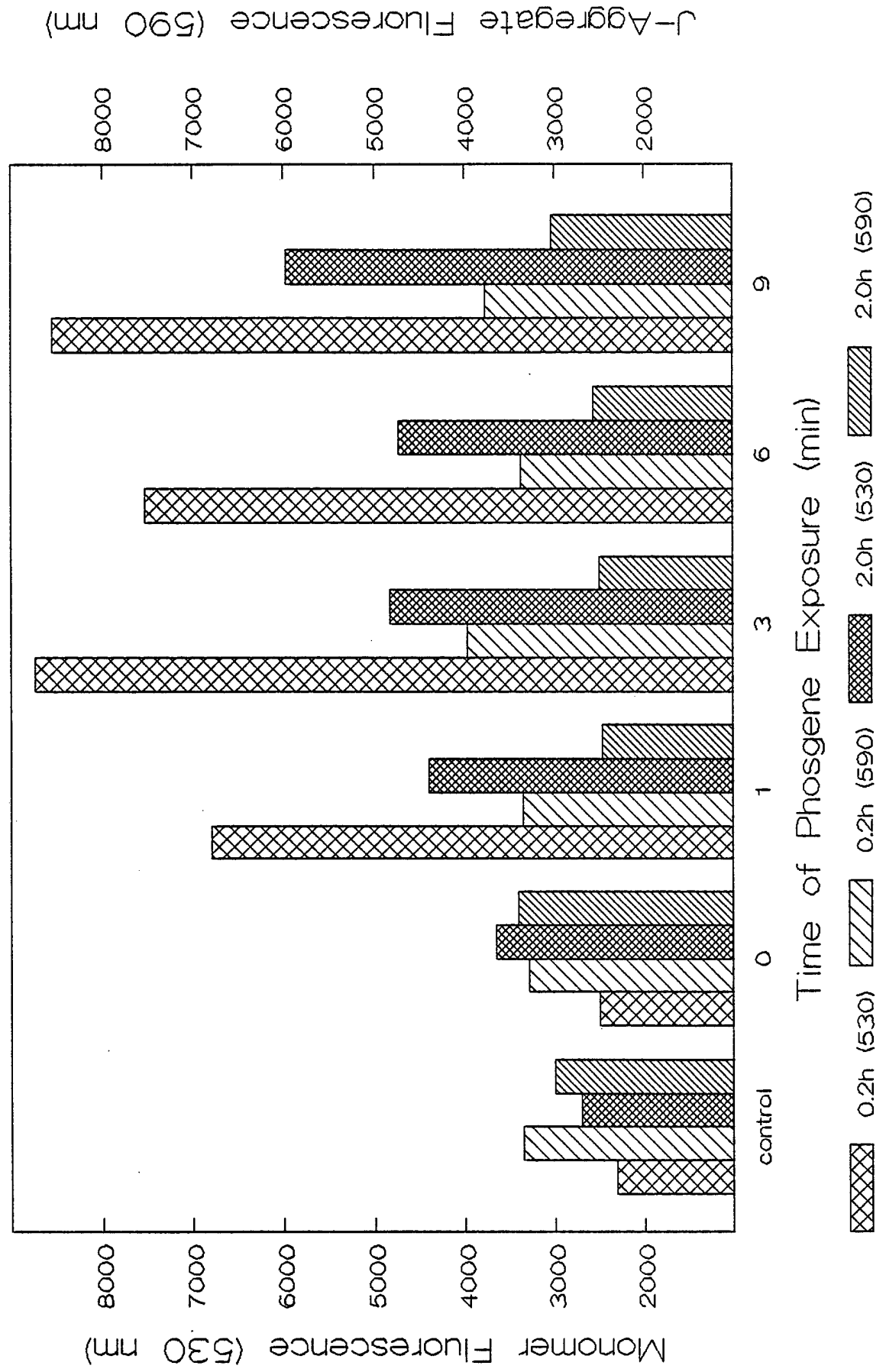


Figure 21. Ratio of the fluorescence of intra-mitochondrial J-aggregates to extra-mitochondrial monomers of the cyanine dye JC-1 in HMVEC exposed to 5% CO₂ in air only (0 min phosgene exposure), or to 300 ppm phosgene for different periods, as described on pp.16-17, and in the previous Figure 20 on p.78-79. The ratio of J-aggregate to monomer fluorescence was greater than 1 in cells which were not exposed in the chamber at all or were exposed to 5% CO₂ in air only, whereas the fluorescence ratio was less than 1 in all phosgene exposed cells, consistent with a loss of mitochondrial membrane potential after phosgene exposure.

Effects of Phosgene on HMVEC JC-1 Uptake - J-Aggregate/Monomer Ratio

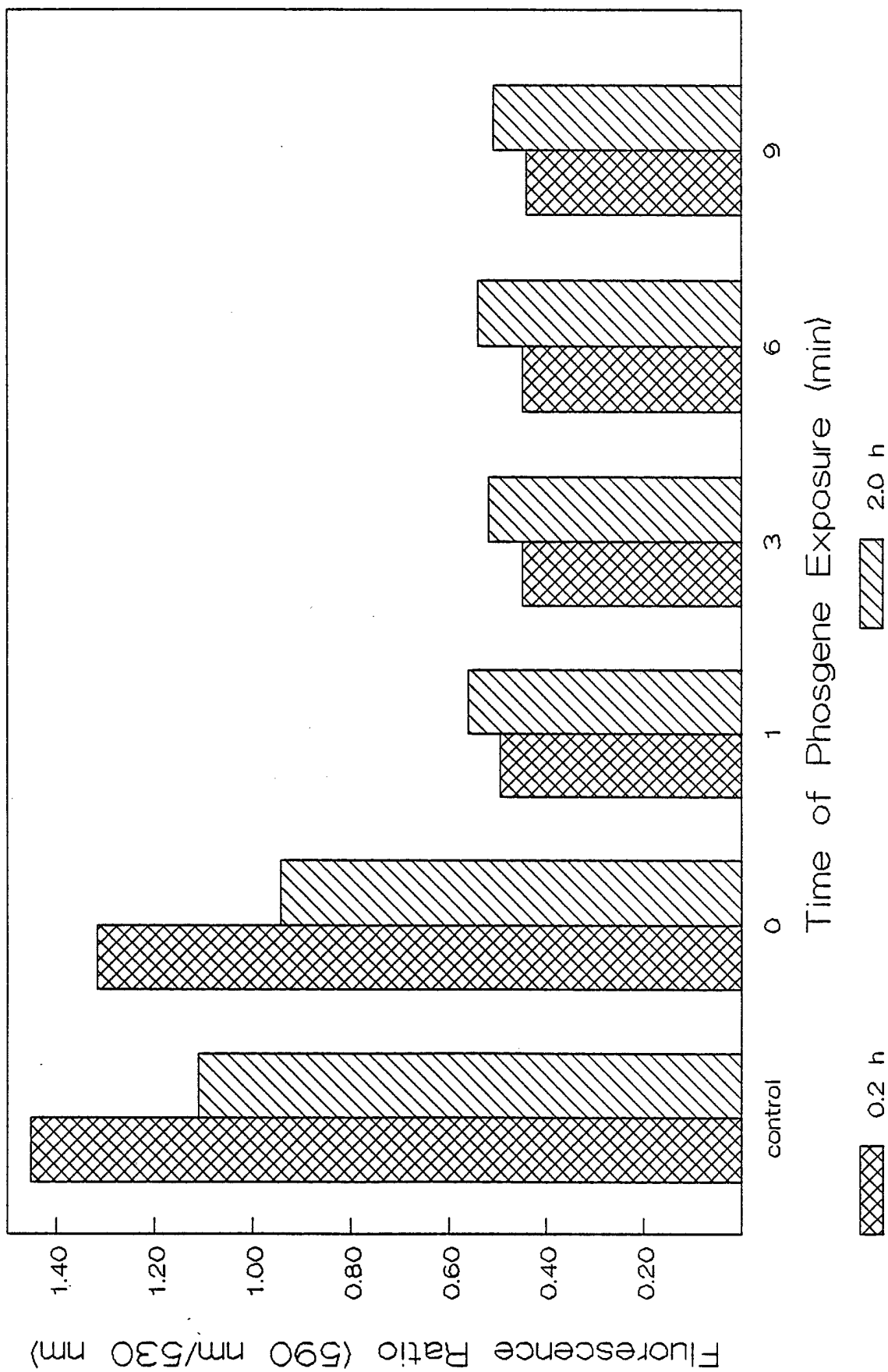


Figure 22. Uptake of the cyanine dye JC-1 into mitochondria of A549 cells exposed to 5% CO₂ in air only (0 min phosgene exposure), or to 300 ppm phosgene for different periods, as described on pp.17-18. Cells in triplicate wells were incubated with JC-1 for 12 minutes and then, after replacement of the dye with HBSS, the fluorescence of dye monomers at 530 nm and of J-aggregates at 590 nm was recorded immediately. These cells appear to retain their mitochondrial membrane potential after exposure to phosgene, as evidenced by a ratio of J-aggregate to monomer fluorescence of greater than 1. Error bars, SD (n=3).

Effects of Phosgene on A549 Cells Mitochondrial Membrane Potential - JC1

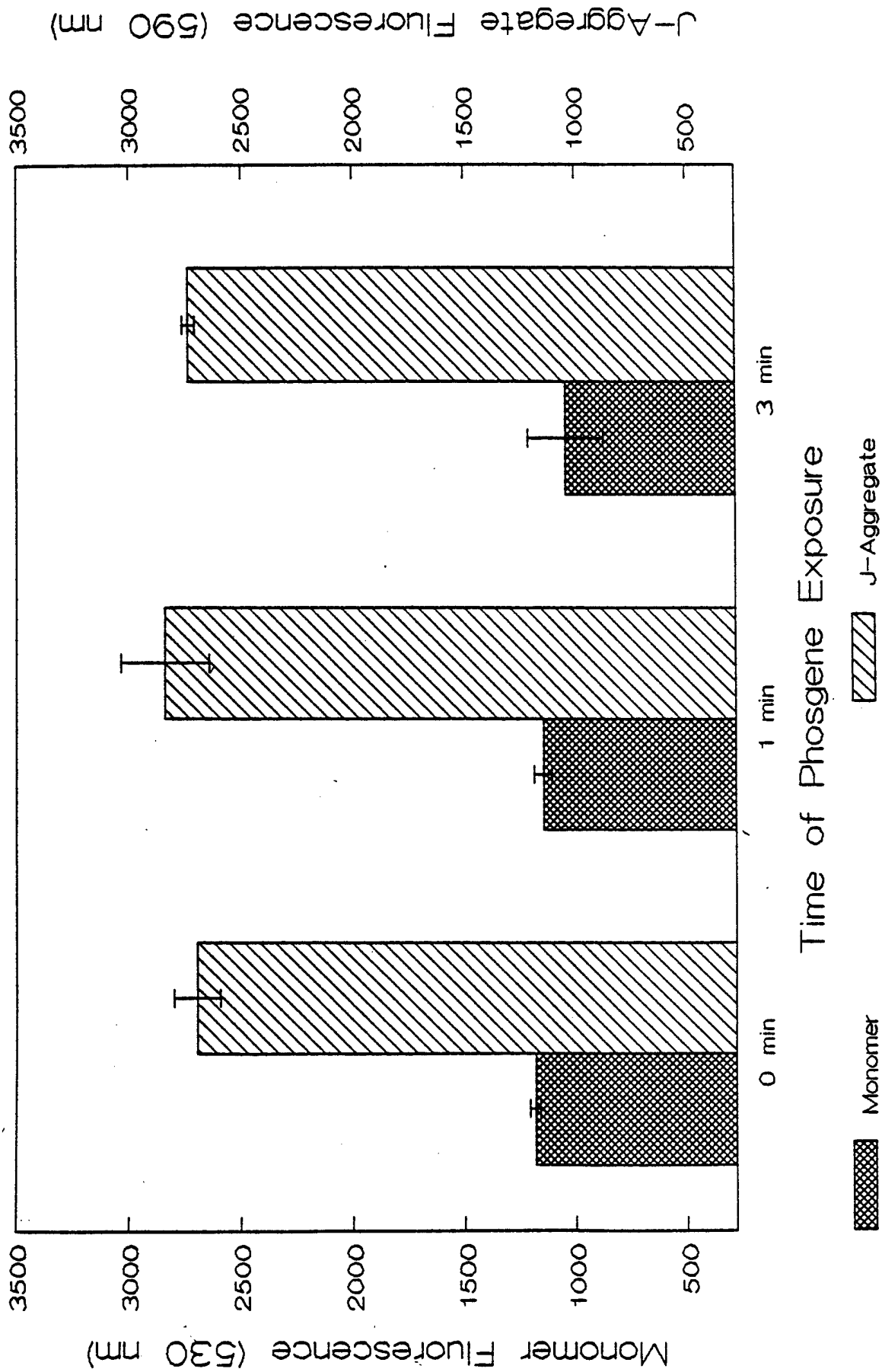


Figure 23. Evaluation of fluo-3 as a probe of intracellular calcium concentration in HMVEC. After loading HMVEC with fluo-3-AM for 30 min, triplicate wells of cells were treated with 10 μ M ionomycin or HBSS, and fluorescence from fluo-3 was recorded at 530 nm, as described on p. 18. The rise in intracellular calcium detected by fluo-3 after addition of 10 μ M ionomycin is too fast to be resolved on the Cytofluor 2300. Error bars, SD (n=3).

Effect of Ionomycin on HMVEC Intracellular Calcium - Fluo-3

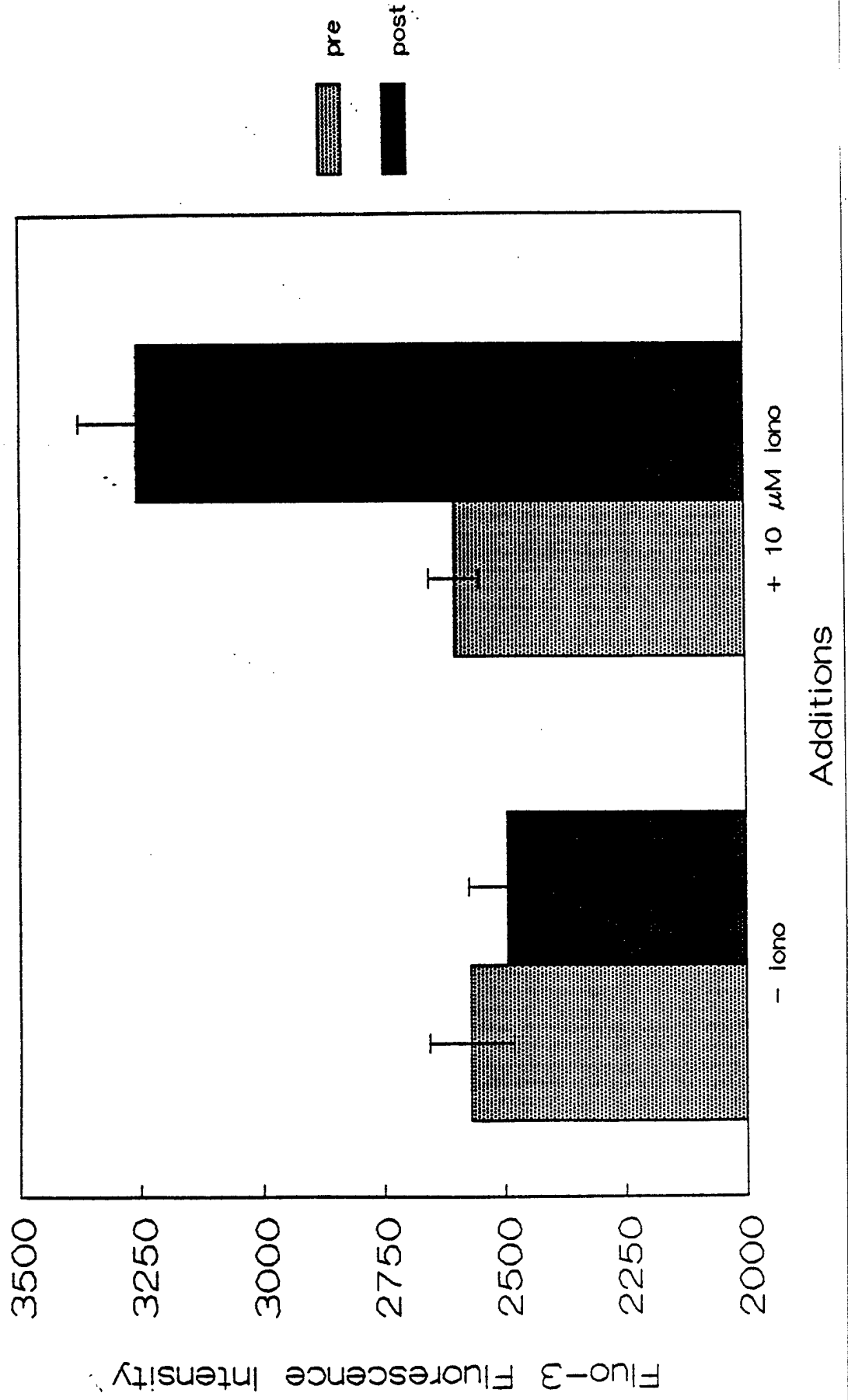


Figure 24. Kinetics of rise in intracellular calcium, as detected by fluo-3 fluorescence, and generation of intracellular reactive oxygen metabolite formation, as detected by oxidation of the fluorogenic probe CDCFH, in separate sets of triplicate wells of HMVEC exposed to 1.5 μ M ionomycin. After HMVEC were loaded for 30 min with fluo-3 AM or CDCFH-DA-AM, ionophore was added and the 24 well microplate was scanned repeatedly in the Cytofluor 2300. Whereas CDCFH oxidation to its fluorescent product CDCF could be followed over the time course of 6 minutes after exposure to the ionophore, the rise in intracellular calcium levels as detected by fluo-3 fluorescence was still too fast to be resolved on the Cytofluor 2300.

Effects of 1.5 μ M Ionomycin on HMVEC Intracellular Calcium and ROS

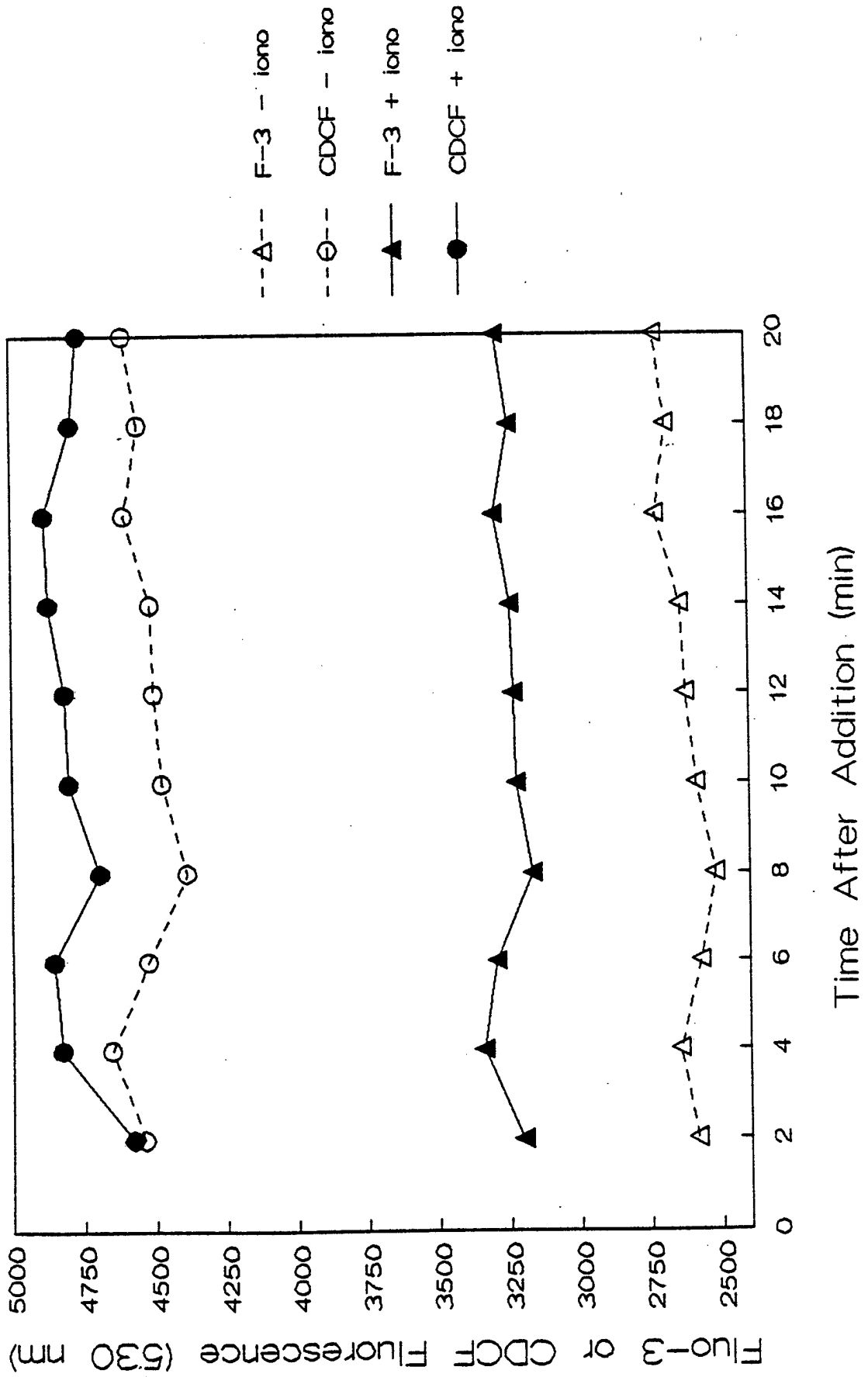


Figure 25. Kinetics of binding of ethidium homodimer-1 to DNA in HMVEC treated with 1.5 μM ionomycin in the same 24 well microplate as was used to follow rise in intracellular calcium and generation of intracellular reactive oxygen metabolite formation, shown in the previous Figure 24 and described on pp.18-19. Duplicate wells of HMVEC received 2 μM ethidium homodimer-1 before addition of 1.5 μM ionomycin and repeated scanning in the Cytofluor 2300. Fluorescence intensities from individual wells are shown. The rise in intracellular calcium and generation of intracellular reactive oxygen species precedes progressive failure to exclude ethidium homodimer-1 from the nuclear DNA, indicating development of cytotoxic injury.

Effects of 1.5 μ M Ionomycin on HM Cytotoxicity

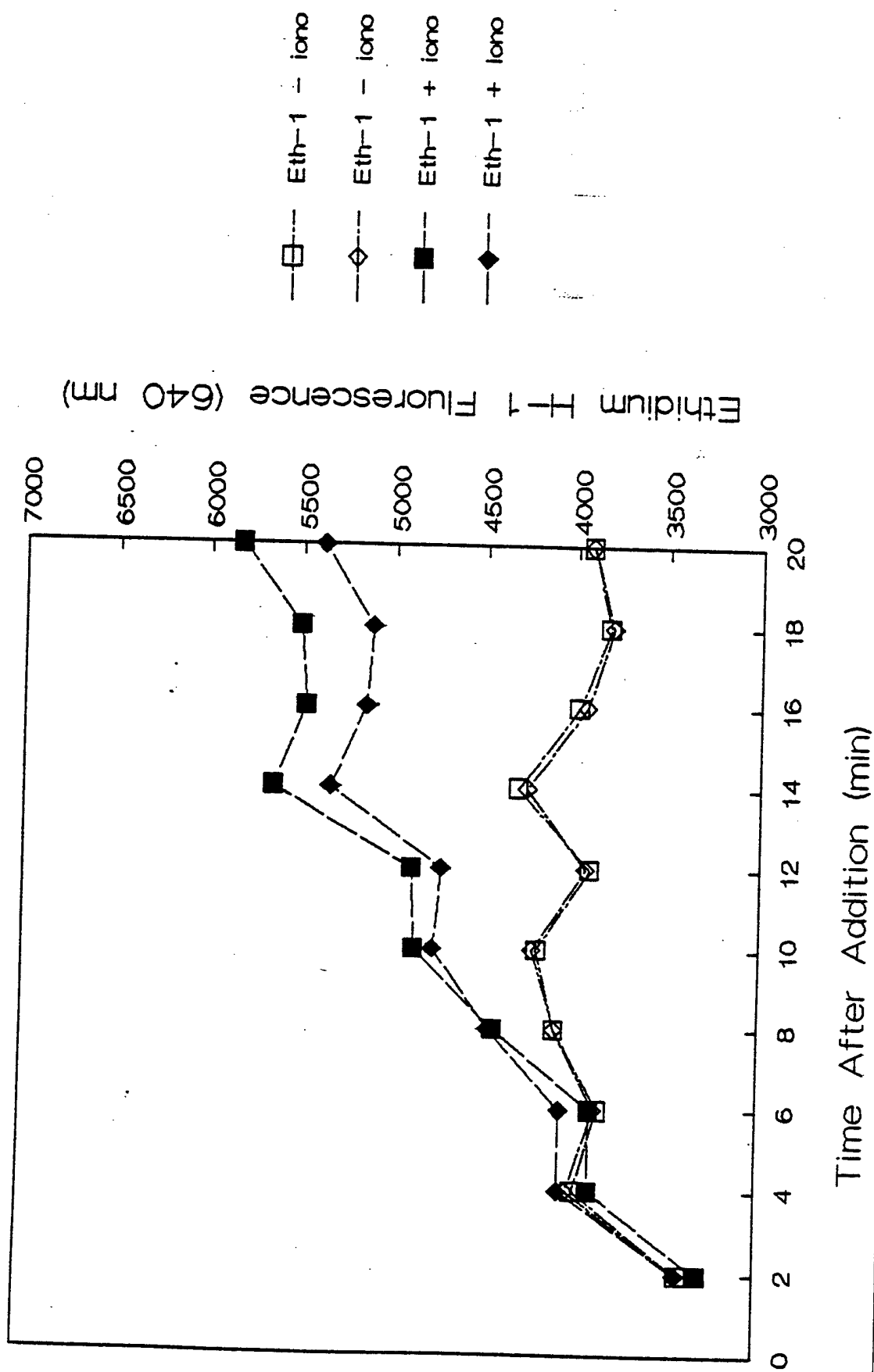


Figure 26. Evaluation of fluo-3 as a probe of intracellular calcium levels in HMVEC stimulated with phorbol myristate acetate (PMA), as described on p.19. Triplicate wells of HMVEC were loaded with fluo-3-AM 30 min before treatment with 1 μ M PMA or buffer, and fluorescence intensity was measured on the Cytofluor 2300 at the intervals indicated in the legend. PMA treatment results in a slow rise in fluorescence from the fluo-3-Ca complex, which is about twice the increase seen in control cells treated with buffer alone. Error bars, SD (n=3).

Effect of PMA on HMVEC Intracellular Calcium - Fluo-3

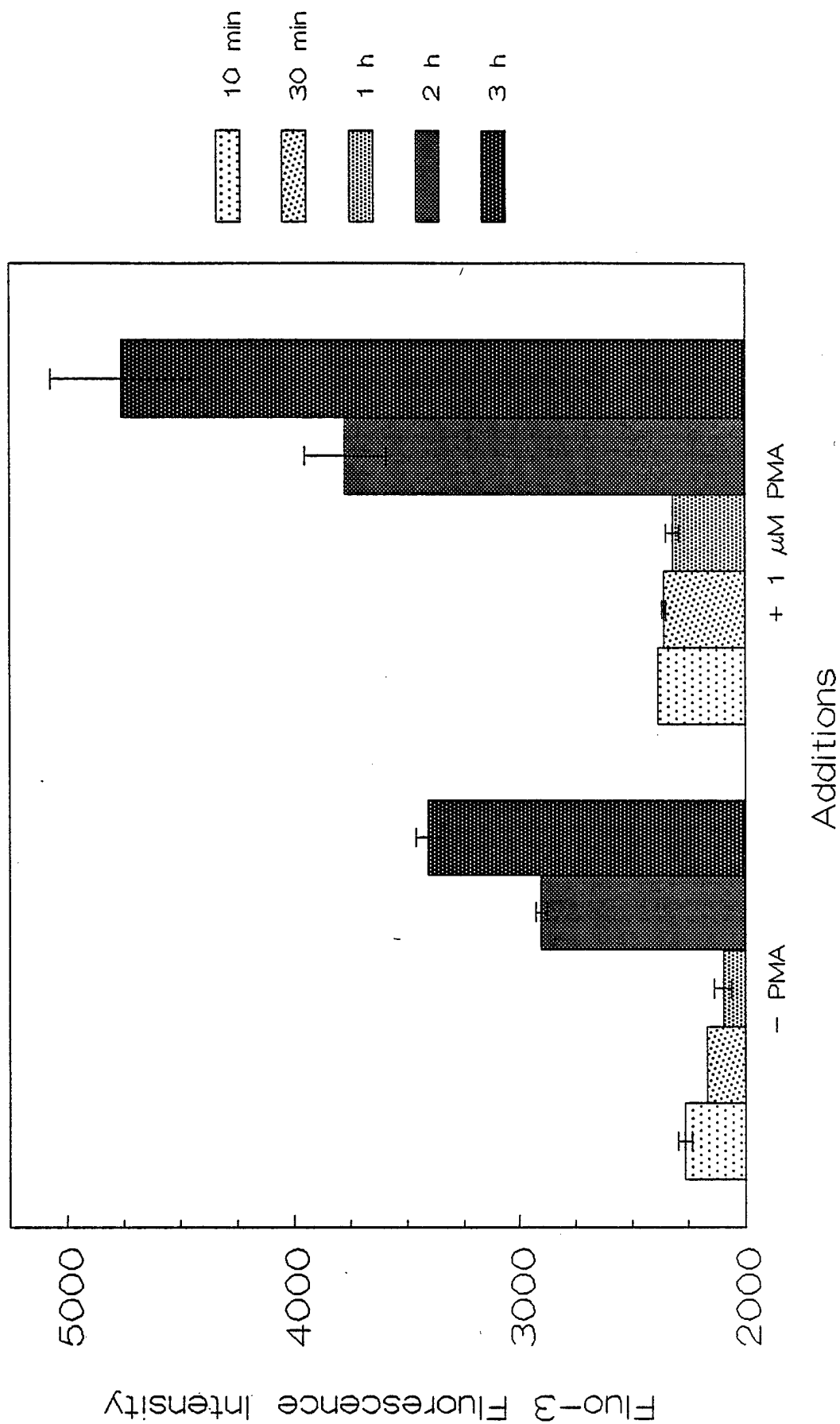


Figure 27. Apparent rise in intracellular calcium levels in HMVEC exposed to phosgene for different periods, as measured by fluo-3 fluorescence. Triplicate wells of HMVEC in 24 well microplates were loaded with fluo-3-AM 30 min before exposure of individual plates to 300 ppm phosgene or 5% CO₂ in air ("0 min") for the periods indicated in the legend. Fluorescence was measured over the following 2 hours by scanning the plates in the Cytofluor 2300 at the intervals indicated on the X-axis. Experimental details are described on pp.19-20.

Intracellular Calcium Effect of Phosgene

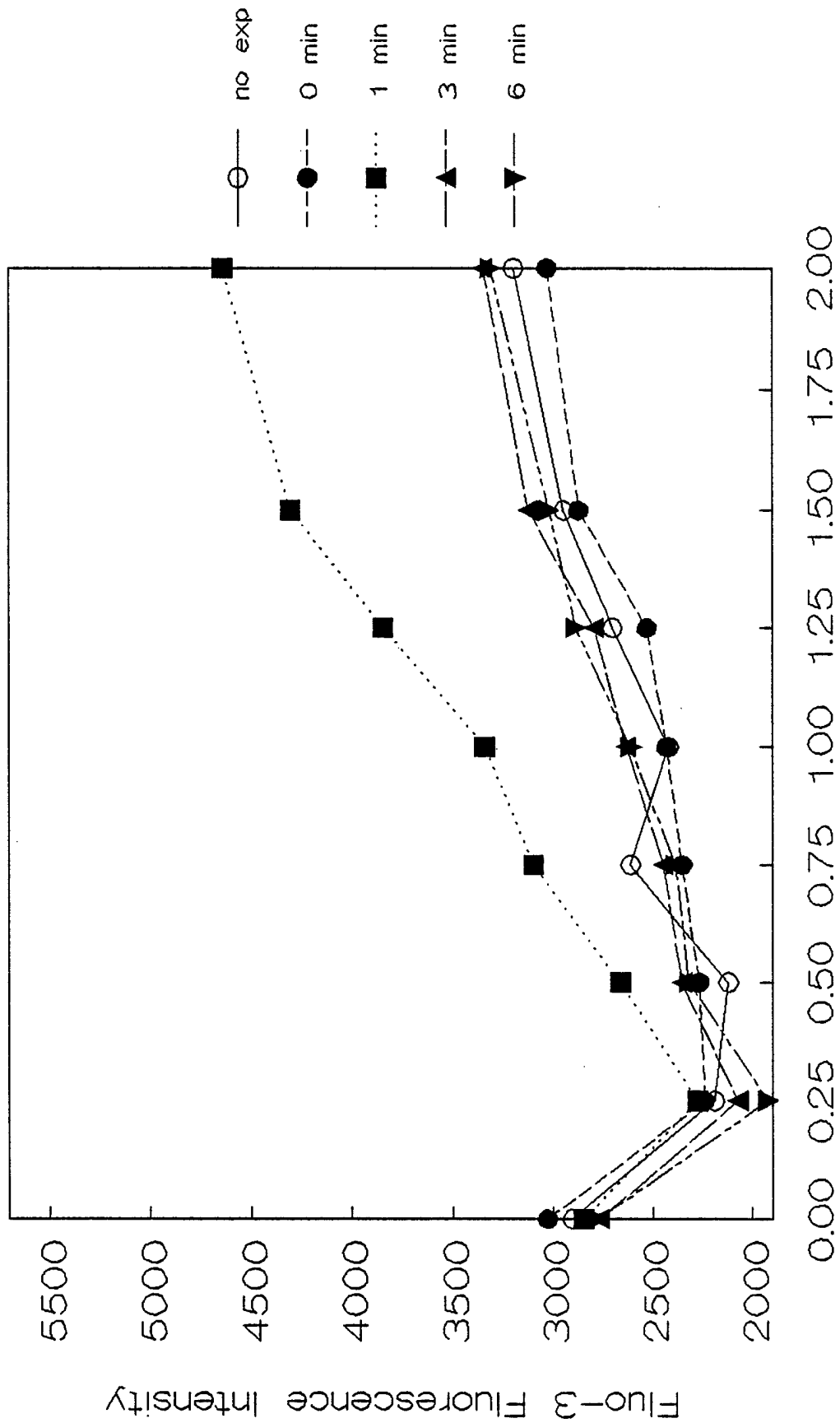


Figure 28. Apparent rise in intracellular calcium levels as measured by fluo-3 fluorescence from HMVEC after exposure to phosgene. Triplicate wells of HMVEC were loaded with fluo-3-AM 30 min before exposure to 300 ppm phosgene or 5% CO₂ in air ("0 min") for the periods indicated on the X-axis. After exposure, medium was replaced with fresh ECGM and cells were maintained for 3 h before fluo-3 fluorescence was measured in the Cytofluor 2300 as described on p. 20. Error bars, SD (n=3).

Fluo-3 Fluorescence Effect of Phosgene

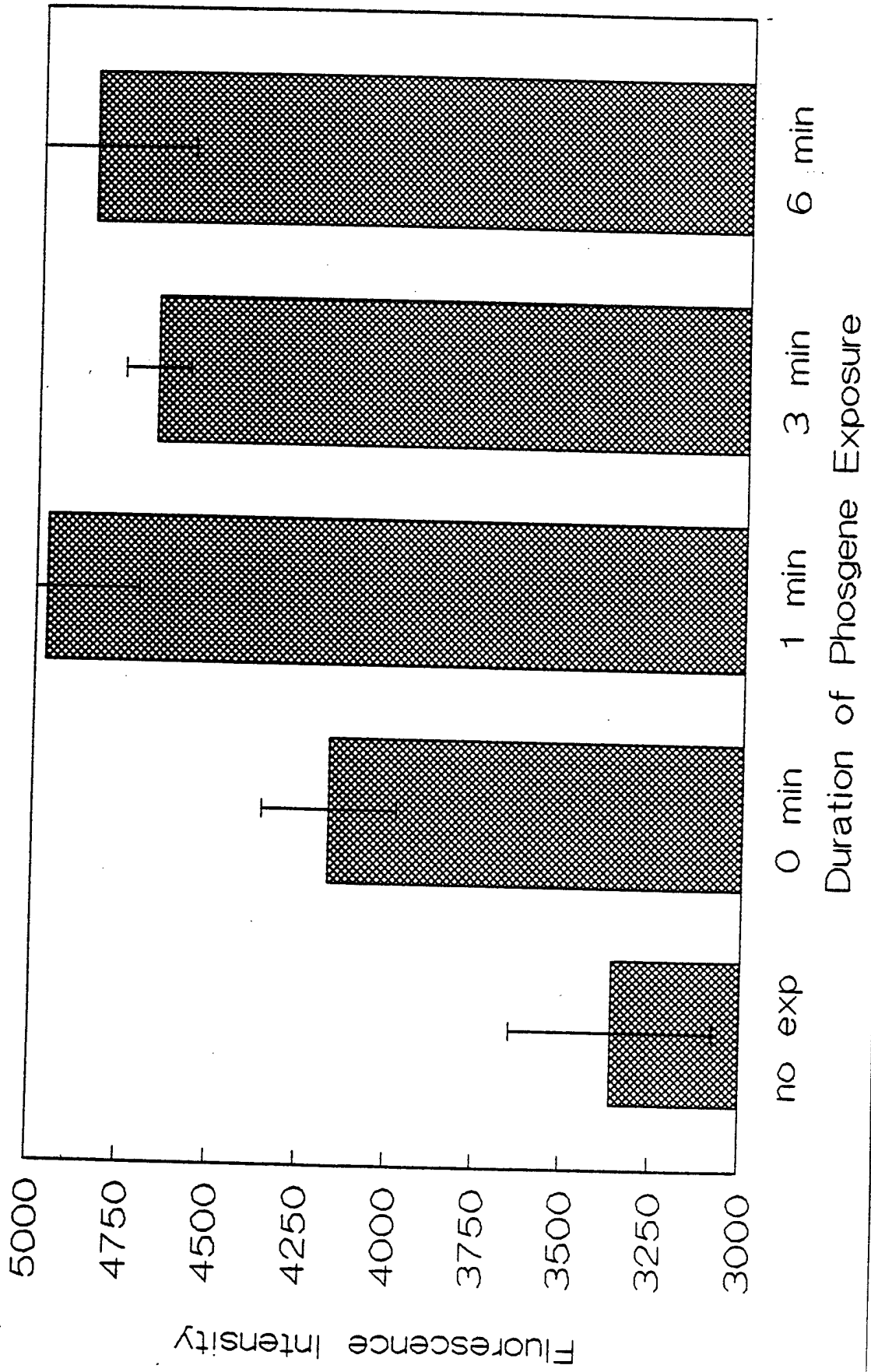


Figure 29. Loss of cytosolic esterase activity and increased binding of ethidium homodimer-1 to nuclear DNA in HMVEC after exposure to phosgene. Additional sets of triplicate wells from the same plates of HMVEC used for the results in Figure 28 were employed for these measurements. Cells were exposed to 300 ppm phosgene or 5% CO₂ in air ("0 min") for the periods indicated on the X-axis. After exposure, medium was replaced with fresh ECGM and cells were maintained for 3 h before replacement with HBSS containing calcein-AM and ethidium homodimer-1. After an additional 45 min incubation, fluorescence of calcein and DNA-bound ethidium homodimer-1 was measured with the Cytofluor 2300, as described on p. 20. Error bars, SD (n=3).

Calcein-AM and Ethidium Homodimer Effect of Phosgene

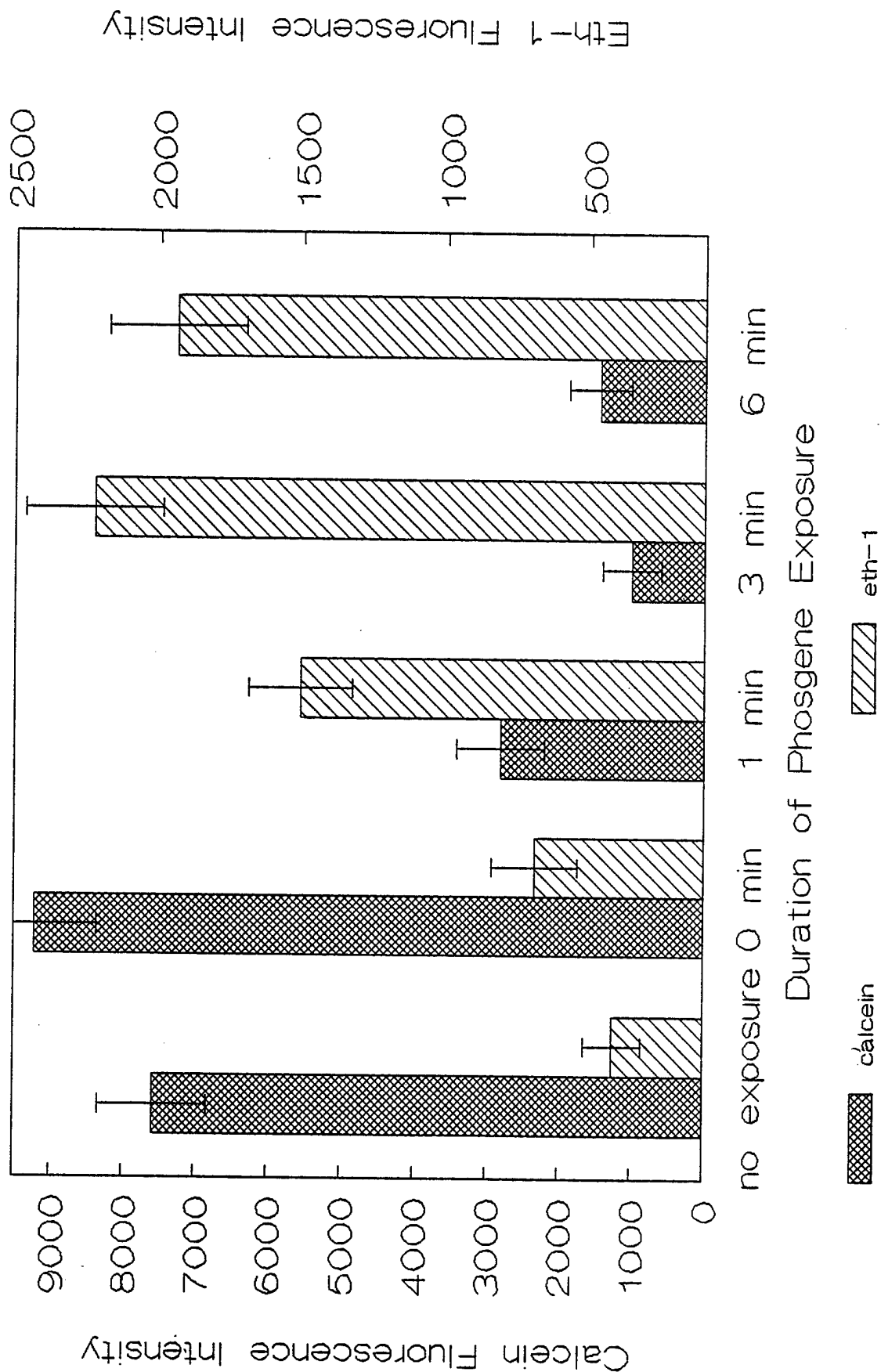


Figure 30. Loss of mitochondrial membrane potential in HMVEC after exposure to phosgene. Additional sets of triplicate wells from the same plates of HMVEC used for the results in Figures 28 and 29 were employed for these measurements. Cells were exposed to 300 ppm phosgene or 5% CO₂ in air ("0 min") for the periods indicated on the X-axis. After exposure, medium was replaced with fresh ECGM and cells were maintained for 3 h before replacement with HBSS containing JC-1. After an additional 12 min incubation, fluorescence of JC-1 monomers and J-aggregates was measured with the Cytofluor 2300, as described on p. 20. Error bars, SD (n=3).

JC-1 Monomers and Aggregates

Effect of Phosgene

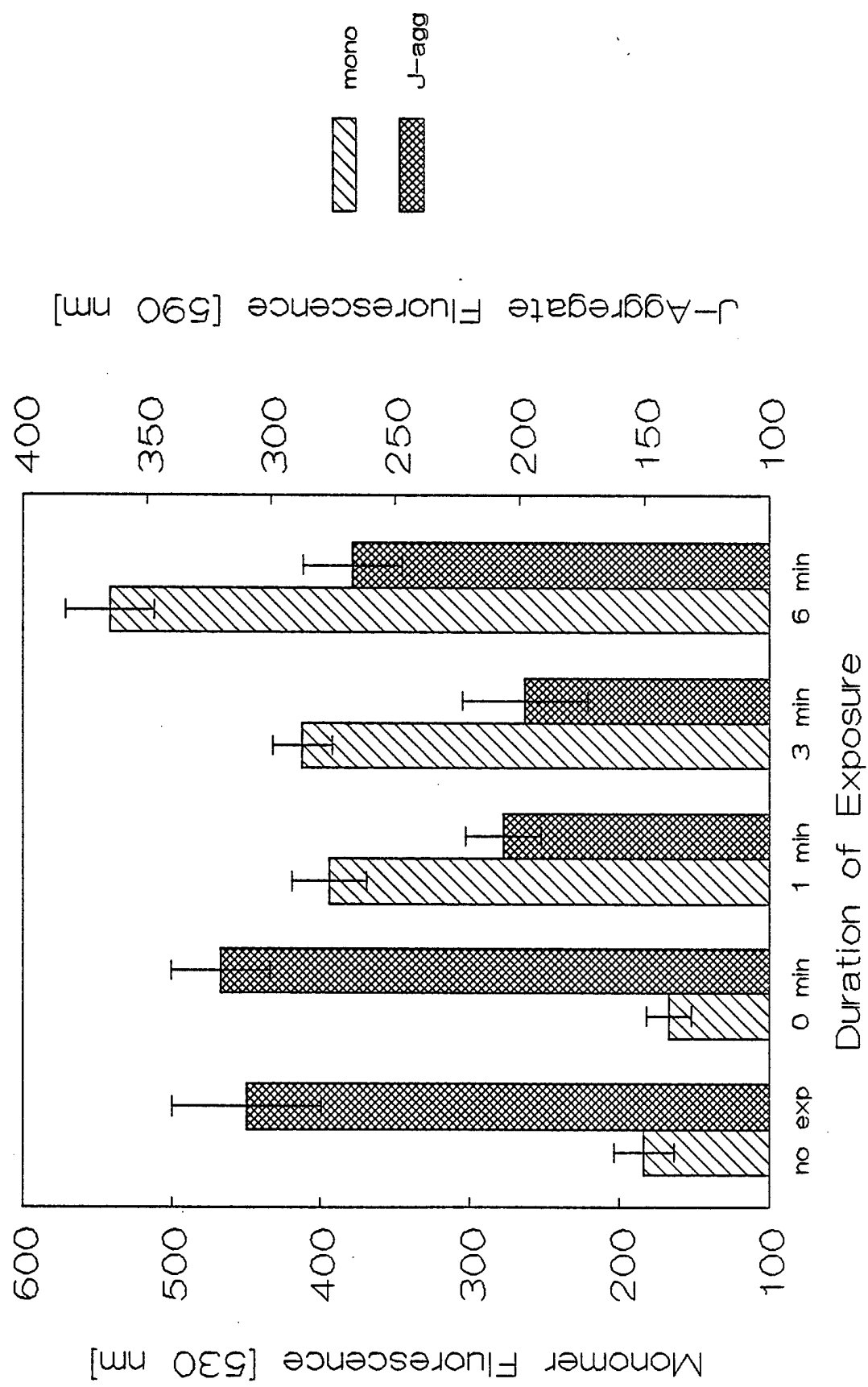


Figure 31. Decrease in the fluorescence intensity ratio from J-aggregates and monomers in HMVEC after exposure to phosgene, computed from the data presented in Figure 30.

JC-1: J-Aggregate/Monomer Ratio Effect of Phosgene

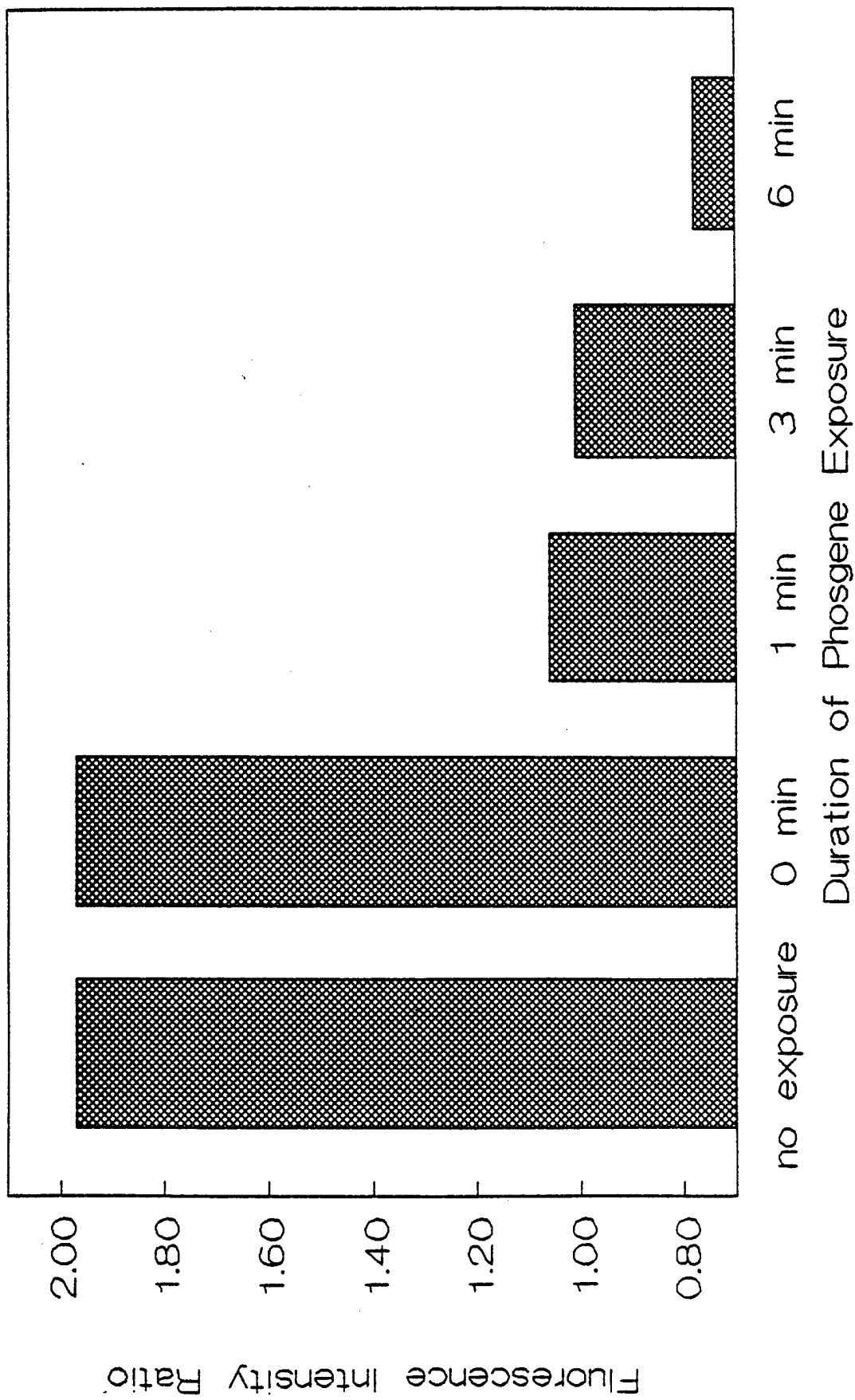


Figure 32. Kinetics of apparent rise in intracellular calcium levels and binding of ethidium homodimer-1 to nuclear DNA in A549 cells after exposure to ionomycin. Groups of triplicate wells on the same 24 well microplate were loaded with fluo-3-AM for 30 min before addition of 10 μ M ionomycin or buffer or received 2 μ M ethidium homodimer-1 immediately before addition of ionophore, as described on p.21. The plate was immediately transferred to the Cytofluor 2300 for scanning at the times indicated on the X-axis.

Calcium Influx in A549 Cells Effect of Ionomycin

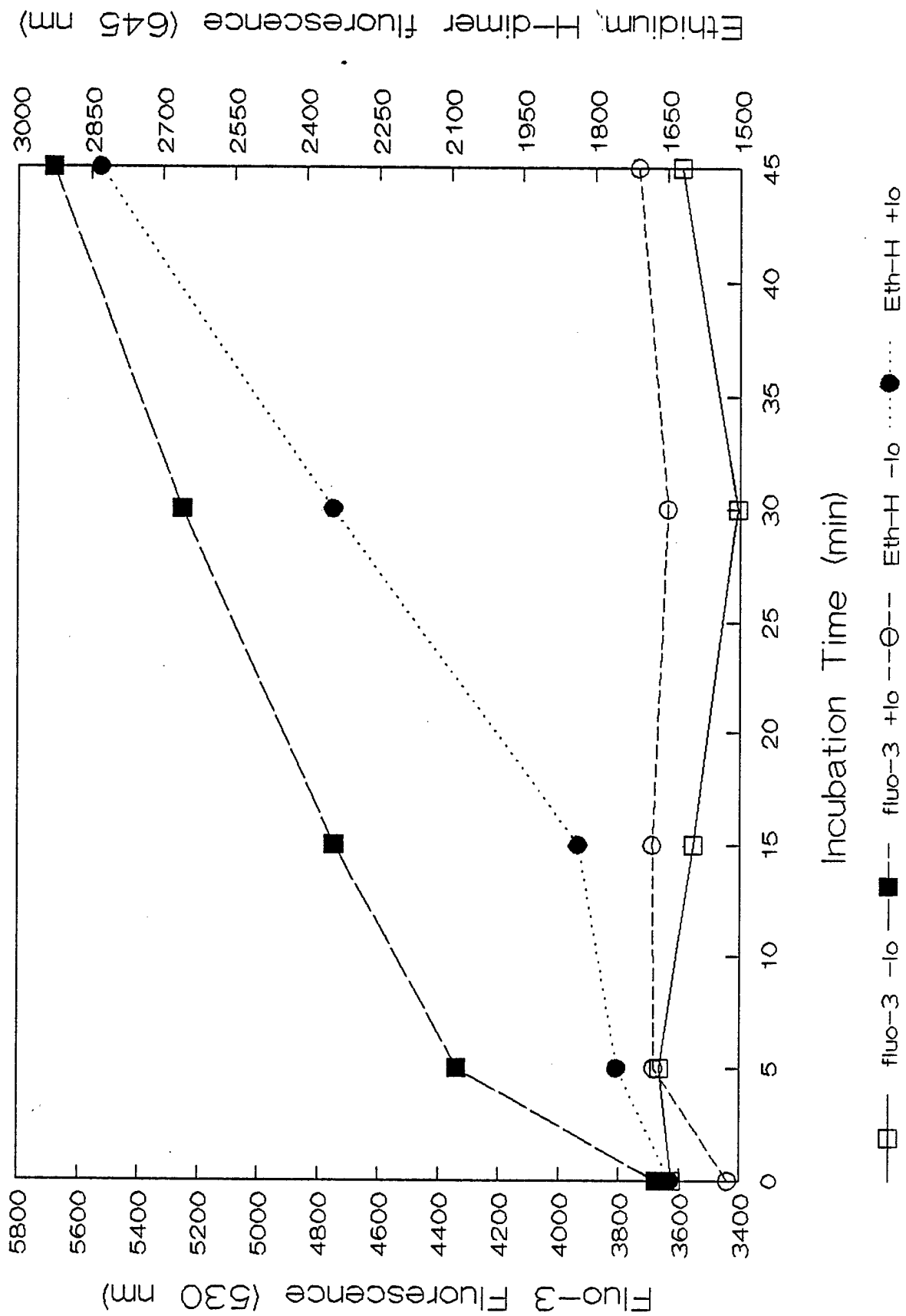


Figure 33. Uptake of acridine orange (AO) as a measure of lysosomal proton pump activity in HMVEC after 3 min exposure to 300 ppm phosgene or 5% CO₂ in air. HMVEC in T25 flasks were trypsinized to release cells which remained adherent immediately after exposure and were incubated with AO for 5 min before analysis by flow cytometry as described on pp.21-22. Red fluorescence from AO in lysosomes and green fluorescence from AO bound to nuclear DNA in the cells are shown in dual channel contour plots for sham exposed and phosgene-exposed cells. Spontaneously detached cells and cells detached by trypsinization were pooled for this study.

Lysosomal Proton Pump Activity Human Endothelial Cells

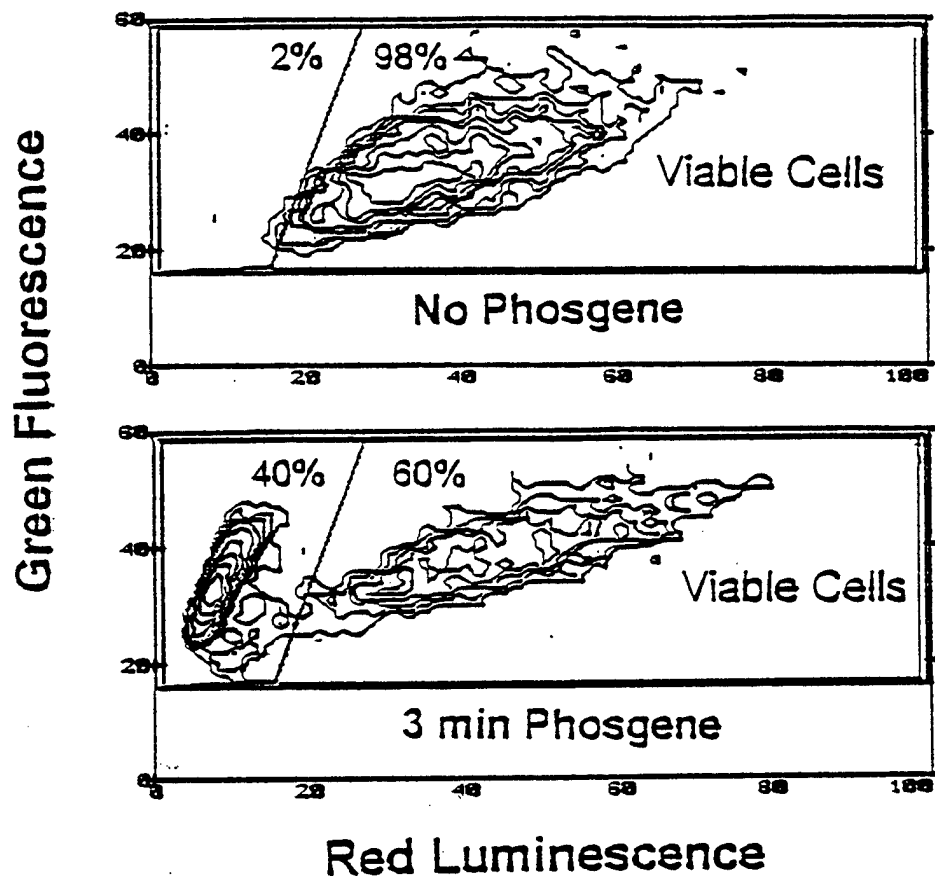


Figure 34. Uptake of AO as a measure of lysosomal proton pump activity in HMVEC after 3 min of exposure to 300 ppm phosgene. After phosgene exposure, HMVEC were incubated for 3 h in RPMI medium before isolation of spontaneously detached cells and trypsinization of the remaining adherent cells. The two subgroups of cells were separately incubated with AO for 5 minutes before analysis by flow cytometry as described on p. 22. The flow cytometric analysis is represented as dual channel contour plots as in Figure 33. Loss of proton pumping activity is associated with spontaneous detachment of cells.

Lysosomal Proton Pump Activity

Attached versus Floating Cells

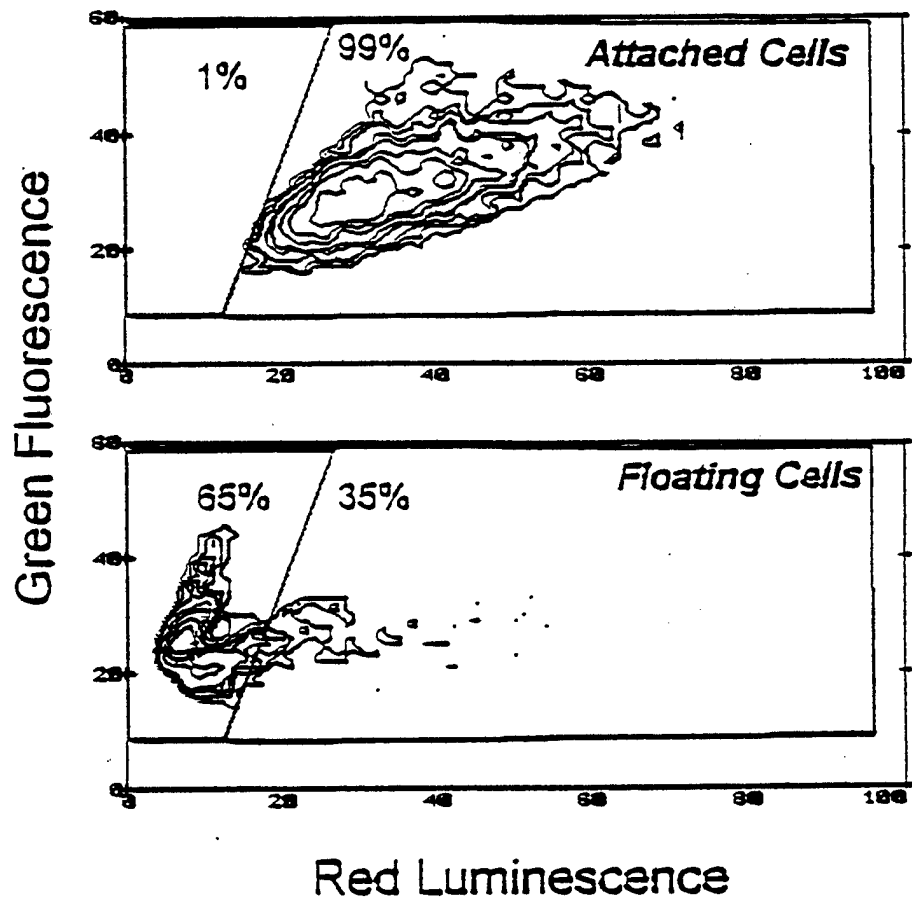
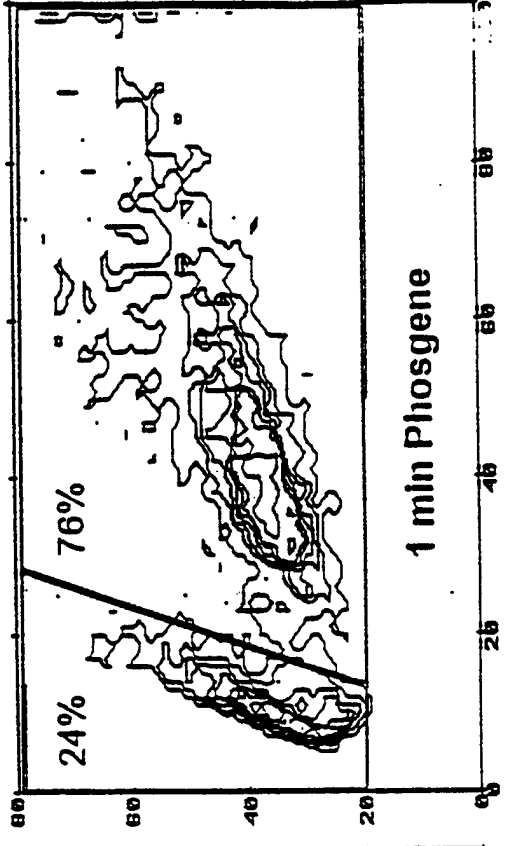
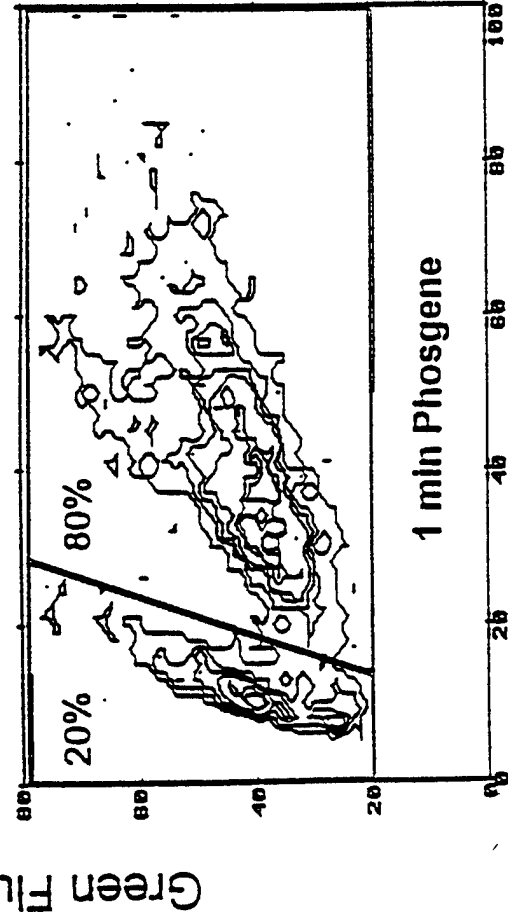
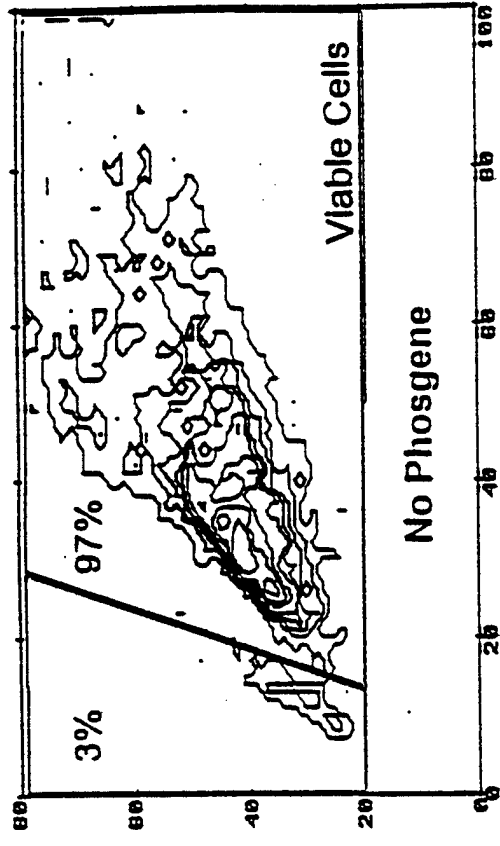
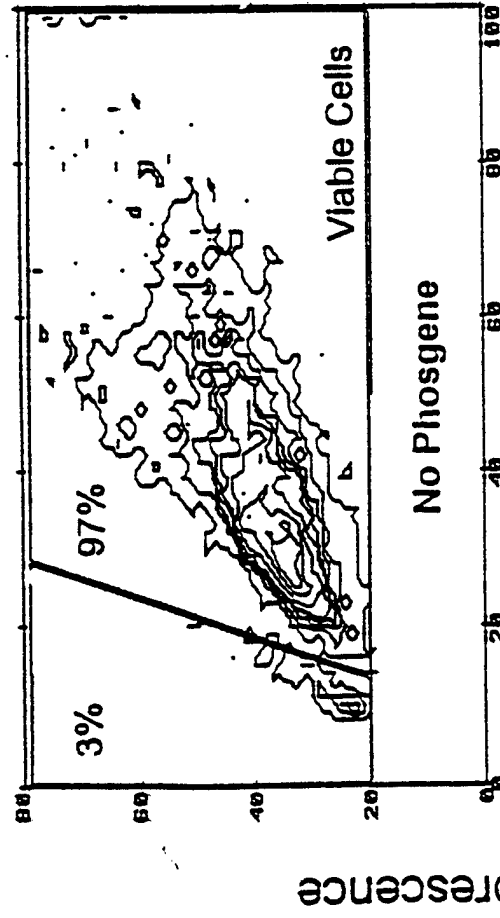


Figure 35. AO uptake into HMVEC after 1 min of exposure to 300 ppm phosgene followed by trypsinization immediately or 3 hours after exposure. Spontaneously detached and trypsinized adherent cells were pooled for these flow cytometric analyses, as described on pp.22-23. A smaller percentage of cells undergoes loss of lysosomal proton pumping activity (seen as less accumulation of AO into lysosomes and lower red fluorescence) after only 1 min of exposure to phosgene as compared with results for 3 min of exposure in Figure 33. Minimal further change in pump activity occurs during 3 h of incubation in medium after exposure.

Lysosomal Proton Pump Activity

Immediate versus Delayed Effects

Measured After Exposure Measured Following 3 h Culture In Complete Medium



Red Luminescence

Figure 36. Histogram analysis of distribution of lysosomal pump activity in AO-positive HMVEC after 1 min of exposure to phosgene or 5% CO₂ in air, followed by trypsinization, incubation with AO, and flow cytometric analysis, as described on p.23. The MFI of AO-positive phosgene-exposed cells is lower than that for air-exposed cells, with a skewed distribution. Even more reduction in MFI could be seen from a similar analysis on cells exposed to phosgene for 3 min.

Lysosomal Proton Pump Activity

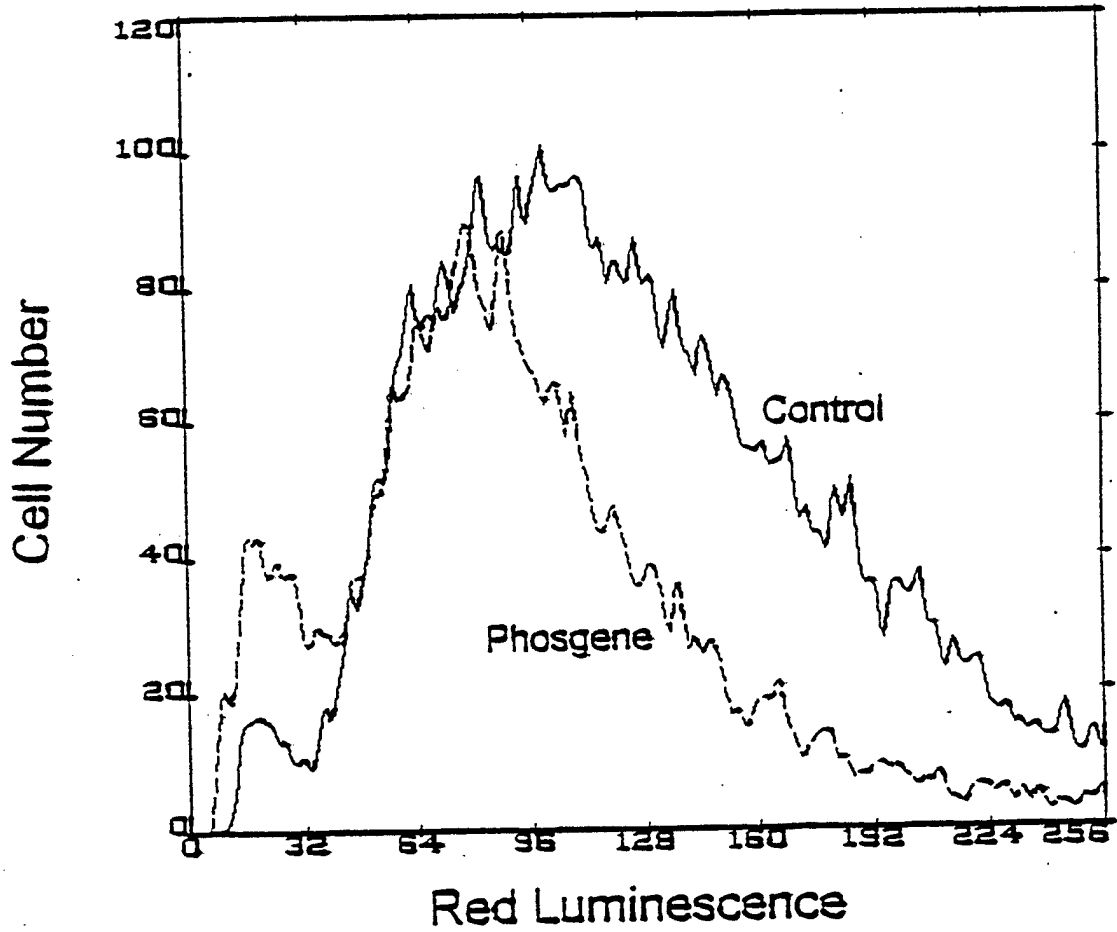


Figure 37. Levels of the arachidonic acid metabolite 6-keto-prostaglandin F1 α (6-keto-PGF1 α) released by HMVEC after exposure to 300 ppm phosgene or 5% CO₂ in air for 3 min. Levels of 6-keto-PGF1 α in duplicate aliquots of supernatants removed from quadruplicate wells were determined by ELISA, as described on pp. 23-24. A significant increase in 6-keto-PGF1 α levels released by the HMVEC occurs ~2 h after exposure to phosgene.

HLMVE STIMULATED 6-keto PGF1 alpha

PHOSGENE 3 min

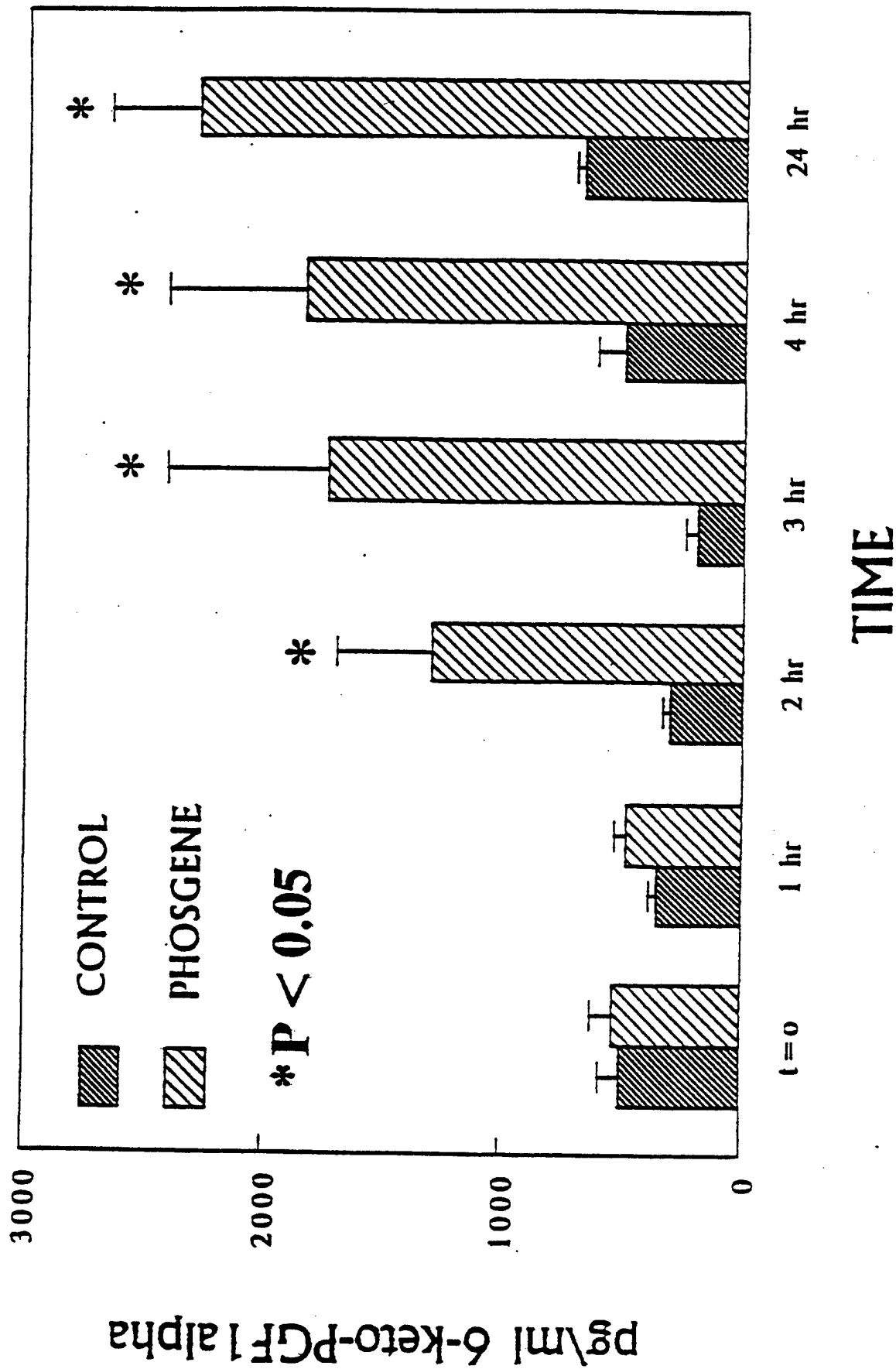


Figure 38. Levels of the arachidonic acid metabolite thromboxane B2 (TxB2) released by HMVEC after exposure to 300 ppm phosgene or 5% CO₂ in air for 3 min. Levels of TxB2 were determined by ELISA, as described on pp. 23-24. This experiment was performed twice, with duplicate aliquots from quadruplicate wells removed for each determination. A significant increase in TxB2 levels released by the HMVEC occurs ~2 h after exposure to phosgene.

HLMVE STIMULATED TXB2 PHOSGENE 3 min

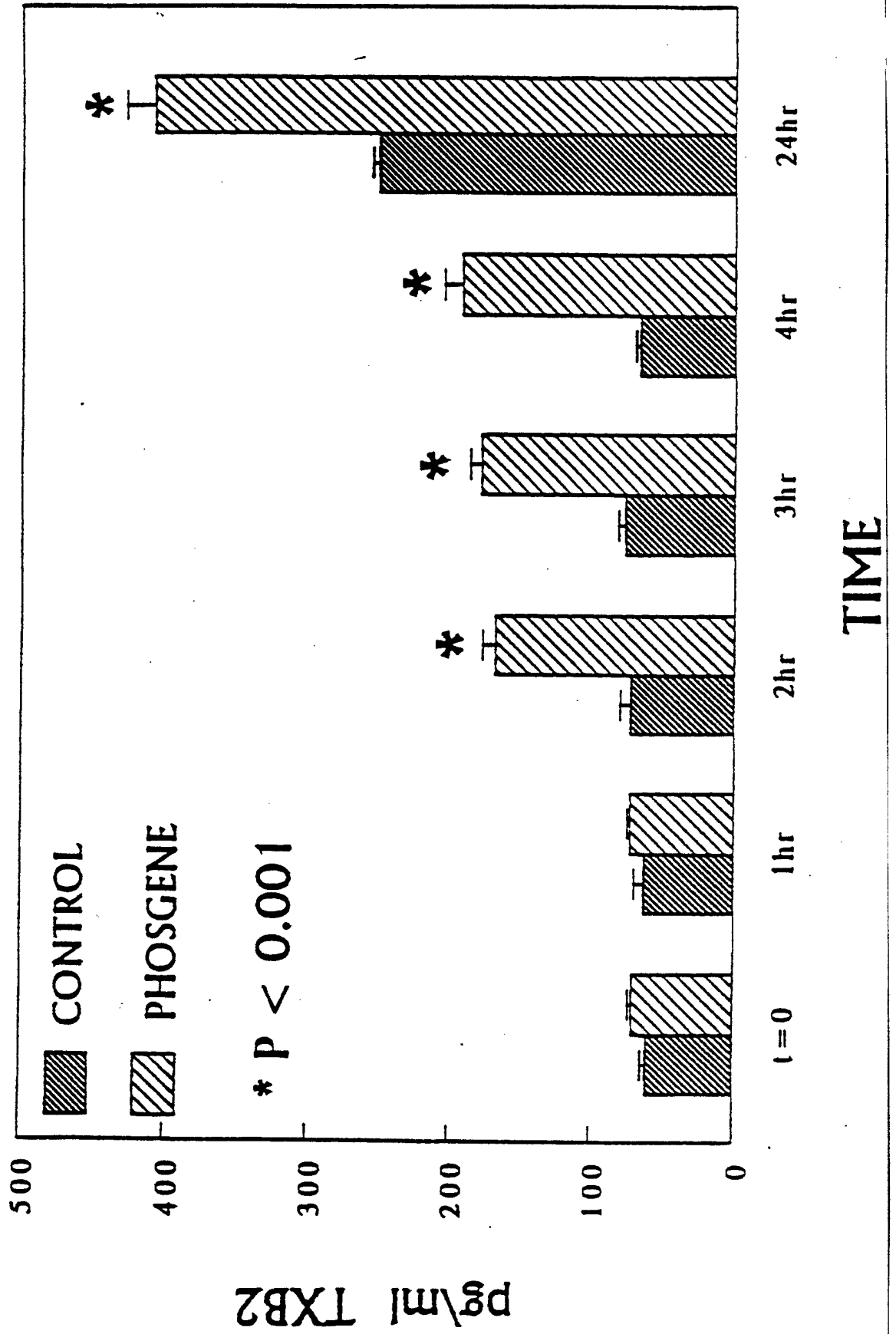


Figure 39. Levels of the lipoxygenase pathway products leukotrienes C4, D4, and E4 released by HMVEC after exposure to 300 ppm phosgene or 5% CO₂ in air for 3 min. Levels of the leukotrienes in duplicate aliquots of supernatants removed from quadruplicate wells were determined by ELISA, as described on pp. 23-24. The ELISA fails to distinguish among the three leukotrienes, and results are expressed as *apparent* levels of leukotriene C4 (LTC₄). A significant increase in levels of these leukotrienes released by the HMVEC occurs ~2 h after exposure to phosgene.

HLMVE STIMULATED LTC4 PRODUCTION

PHOSGENE 3 min

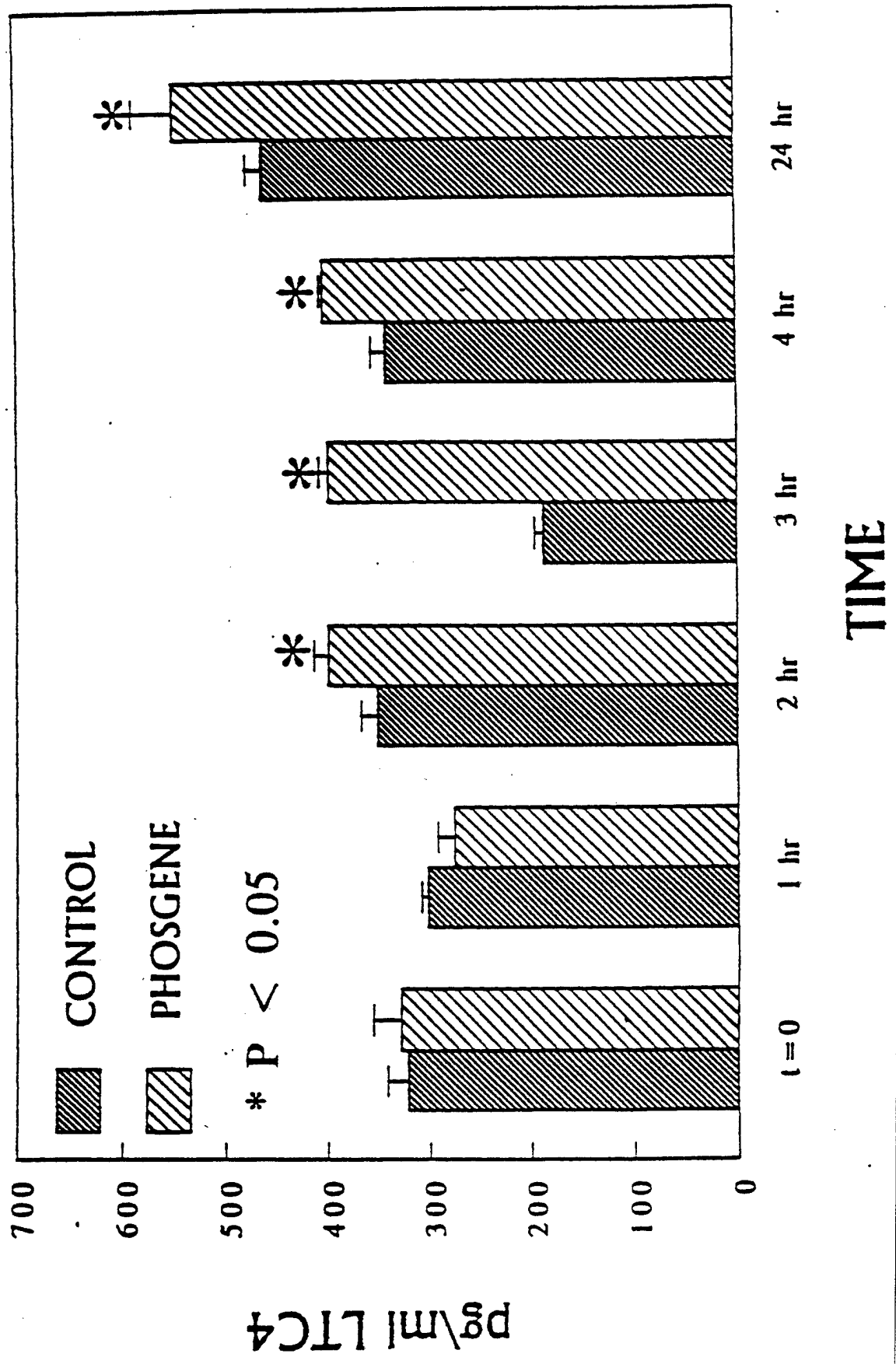


Figure 40. Levels of the cytokine interleukin-6 (IL-6) released by HMVEC after exposure to 300 ppm phosgene or 5% CO₂ in air for 3 min. Quadruplicate wells of cells were incubated for 2 h before collection of duplicate aliquots of supernatants for determination of IL-6 by ELISA, as described on p.25. In this experiment, a statistically significant reduction was seen in the IL-6 levels released by the HMVEC over the 2 h following phosgene exposure.

IL-6 PRODUCTION IN HLMVE

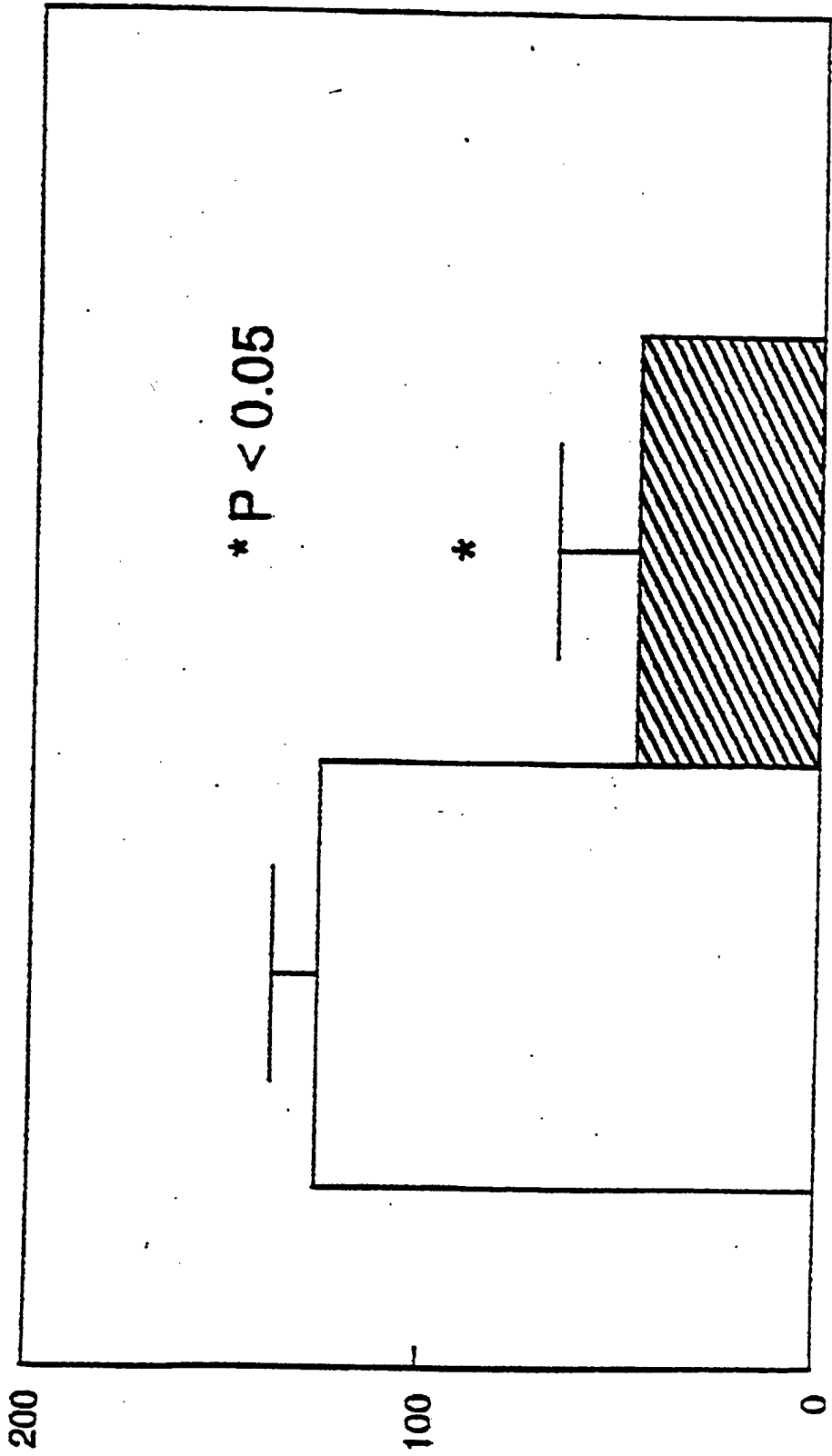
PHOSGENE 3 min



PHOSGENE



CONTROL



TIME POST PHOSGENE EXPOSURE

pg/ml INTERLEUKIN-6

Figure 41. Evaluation of dihydrofluorescein derivatives as probes of reactive oxygen species (ROS), as described on pp. 25-26. Human neutrophils were employed as a source of reactive oxygen metabolites for these studies. Cells were loaded with DCFH-DA 30 min before stimulation with 100 nM PMA or mock treatment with HBSS only. Triplicate wells of cells (1 ml suspension of 2×10^6 cells per well) were incubated in HBSS alone or in HBSS containing 30 $\mu\text{g/ml}$ manganese superoxide dismutase (SOD). Oxidation of DCFH to DCF was measured by recording fluorescence at 530 nm every 2 minutes on the Cytofluor 2300. PMA triggers intracytosolic oxidation of DCFH to DCF via reactive oxygen species which cannot be quenched by the extracellular SOD.

MnSOD w/DCFH-DA

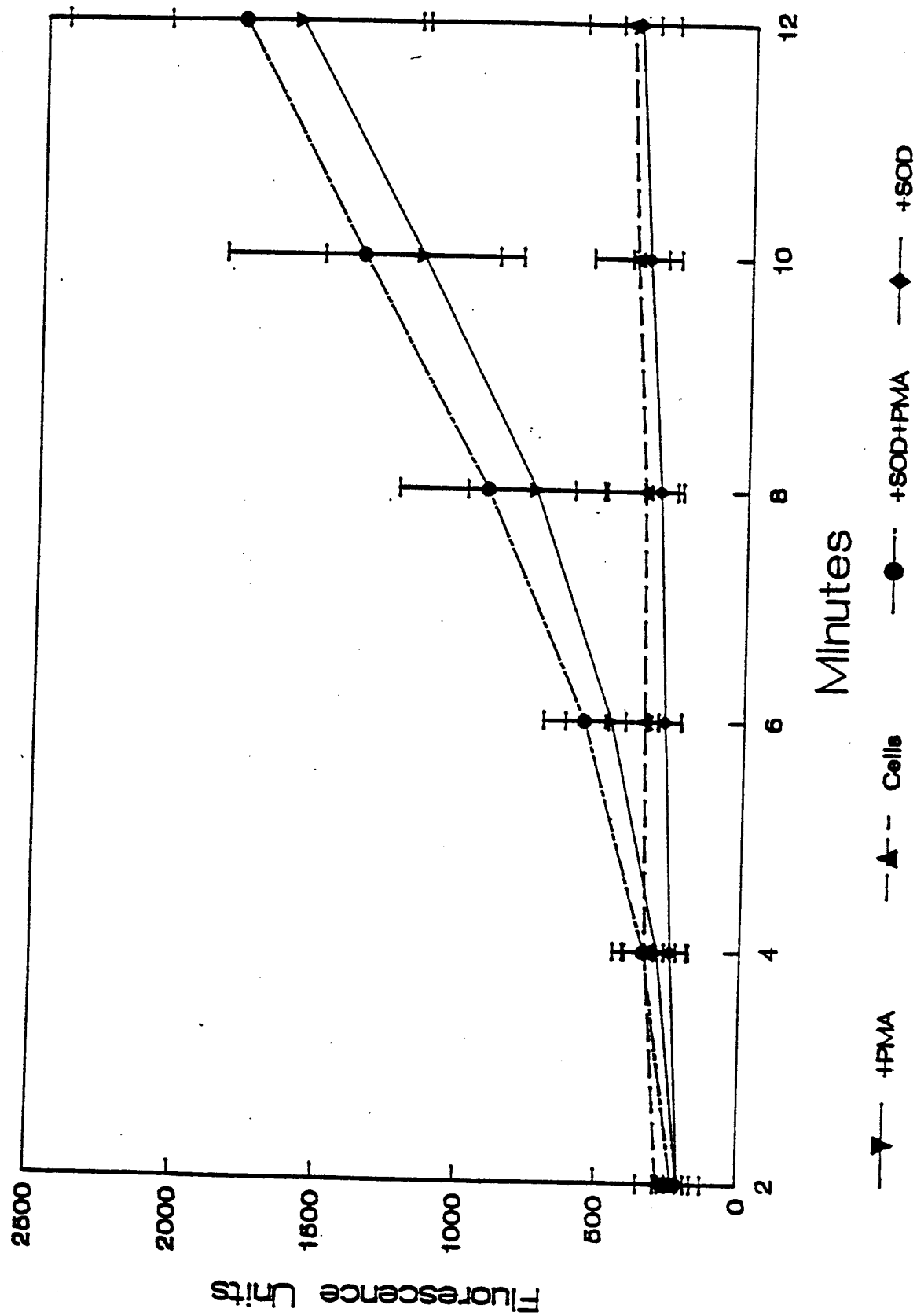


Figure 42. Cytochrome c reduction by reactive oxygen species released by PMA-stimulated neutrophils is effectively quenched by manganese superoxide dismutase, as discussed on p.26. 150 μ l aliquots of a 2×10^6 PMN/ml suspension in HBSS containing 75 μ M cytochrome c were stimulated with 20 ng/ml PMA or mock stimulated with HBSS, in the presence or absence of 30 μ g/ml MnSOD in sets of triplicate wells of a 96 well microplate. The rate of cytochrome c reduction was measured on a ThermoMax microplate reader equipped with a 1 nm narrow band pass 550 nm interference filter. MnSOD completely quenches the neutrophil-generated extracellular reactive oxygen metabolites which reduce cytochrome c.

MnSOD w/Cytochrome C

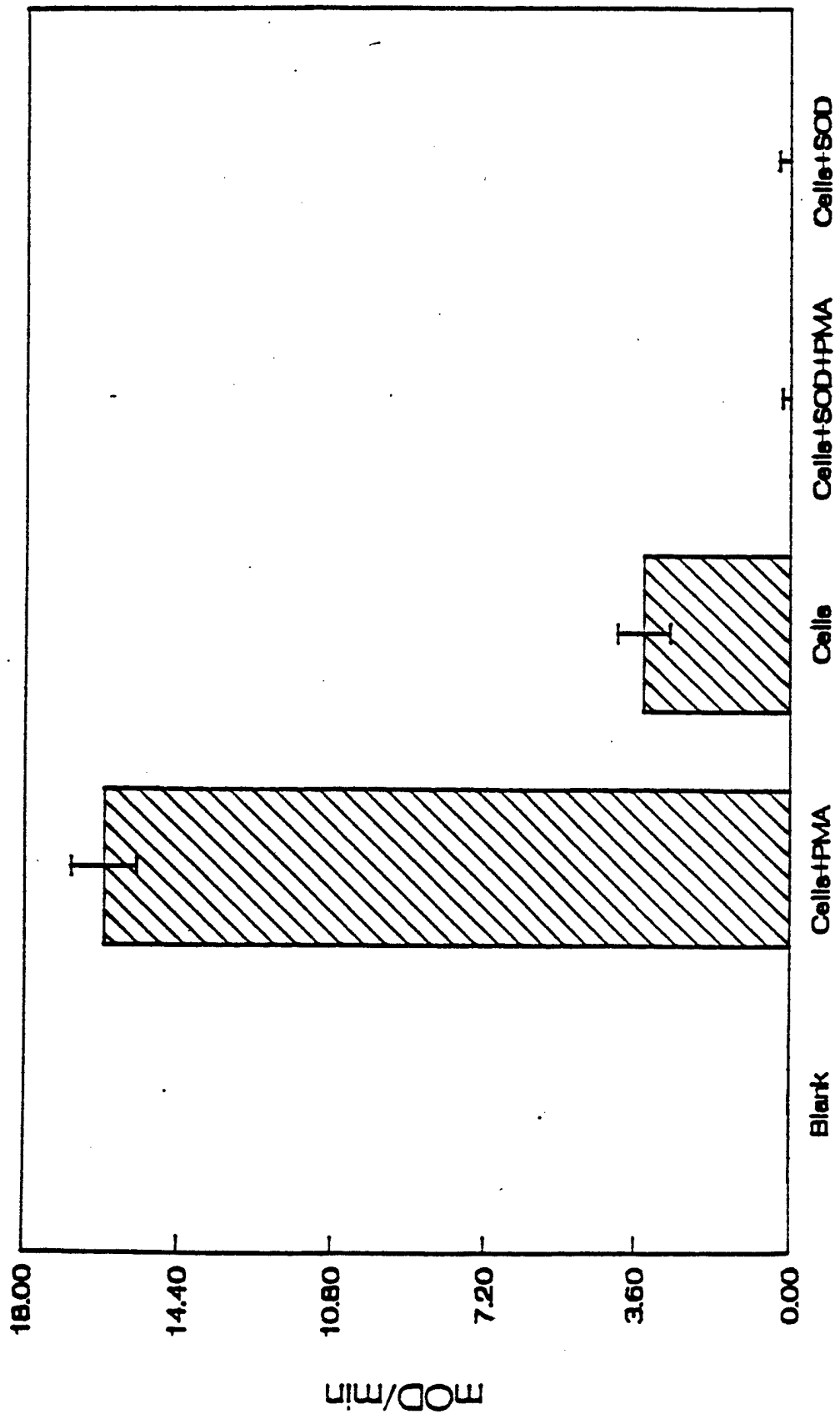


Figure 43. Effects of phosgene on lucigenin-enhanced chemiluminescence from reactive oxygen species released by the macrophage-like cell line U937. Prior to assay, suspensions of 5×10^4 cells/ml were first pretreated with 6.25 mg/ml (38 mM) N-acetyl cysteine or 100 μ g/ml methyl prednisone or received no pretreatment. Then 10 ml aliquots were placed in roller bottles and exposed to 300 ppm phosgene or to 5% CO₂ in air for 3 min followed by a 5 min "washout" with air only. Cells were incubated for an additional 60 min before collection and assay by lucigenin-enhanced chemiluminescence. 1 ml aliquots of 5×10^5 cells in HEPES-buffered Krebs-Ringer's solution containing 250 μ M lucigenin were added to plastic scintillation minivials. Immediately after stimulation of the cells with 1 μ M PMA, the vials were placed in a liquid scintillation counter in non-coincidence mode for determination of chemiluminescence. Phosgene exposure inhibits release of the reactive oxygen metabolites from U937 cells which can be detected by lucigenin-enhanced chemiluminescence.

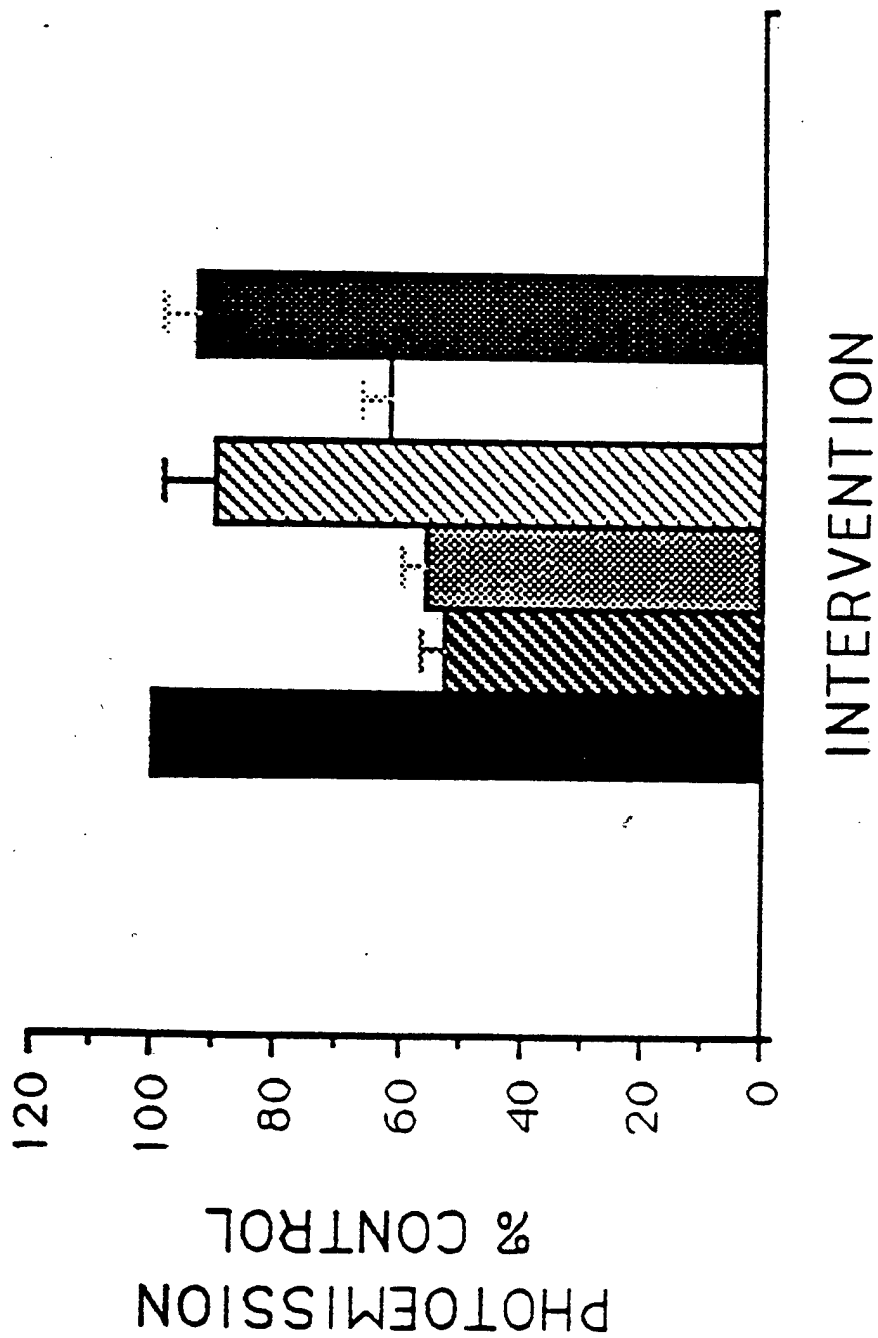


Figure 44. Demonstration of use of dihydrofluorescein derivatives as probes of intracellular reactive oxygen species (ROS) in HMVEC, as described on p.26. Triplicate wells of HMVEC from the same plate as was used for detection of intracellular calcium levels in Figure 26 were loaded with 4 μ M CDCFH-DA-AM 30 min before addition of 1 μ M PMA and the plate was scanned in the Cytofluor 2300 at the times indicated in the legend. Some spontaneous generation of ROS is detected in unstimulated HMVEC by 3 hours, but the levels of such metabolites are significantly elevated in stimulated cells and rise markedly 2 hours after treatment with PMA. These results are in agreement with other changes in HMVEC which occur \sim 2 h after stimulation. Error bars, SD (n=3).

Effect of PMA on HMVEC Intacellular ROS - CDCFH Oxidation

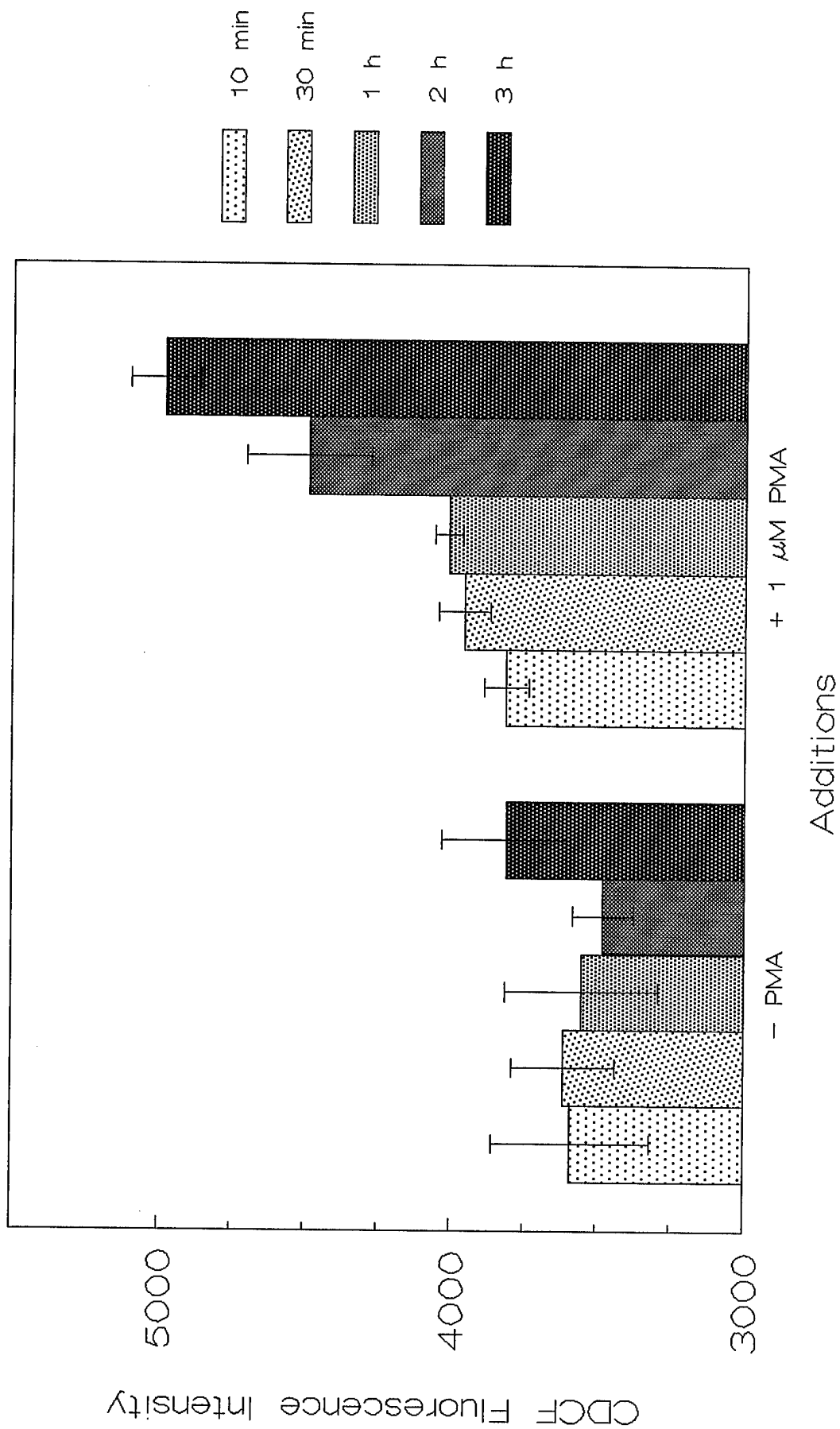


Figure 45. Effects of phosgene exposure on generation of intracellular ROS in HMVEC, as described on p.26. Triplicate wells of HMVEC in the same 24 well microplates used for measurements of intracellular calcium levels in Figure 27 were loaded with CDCFH-DA-AM 30 min before exposure of individual plates to 300 ppm phosgene or 5% CO₂ in air ("0 min") for the times indicated in the legend. The plates were then scanned in the Cytofluor 2300 at the times indicated on the X-axis. Exposure to phosgene resulted in a consistent immediate dip in CDCF fluorescence which was not seen in sham exposed or unexposed cells. The recovery from the initial dip was most pronounced in HMVEC which were exposed to phosgene for 1 minute. A more dramatic increase in levels of ROS could be seen beginning ~2 h after the HMVEC had been exposed to phosgene for 1 minute. Spontaneous increases in ROS were detected in all other cells, including sham-exposed or unexposed HMVEC by 3 h, as seen in the previous Figure 44, but were lower than the levels in cells exposed to phosgene for 1 minute.

Intracellular ROS Effect of Phosgene

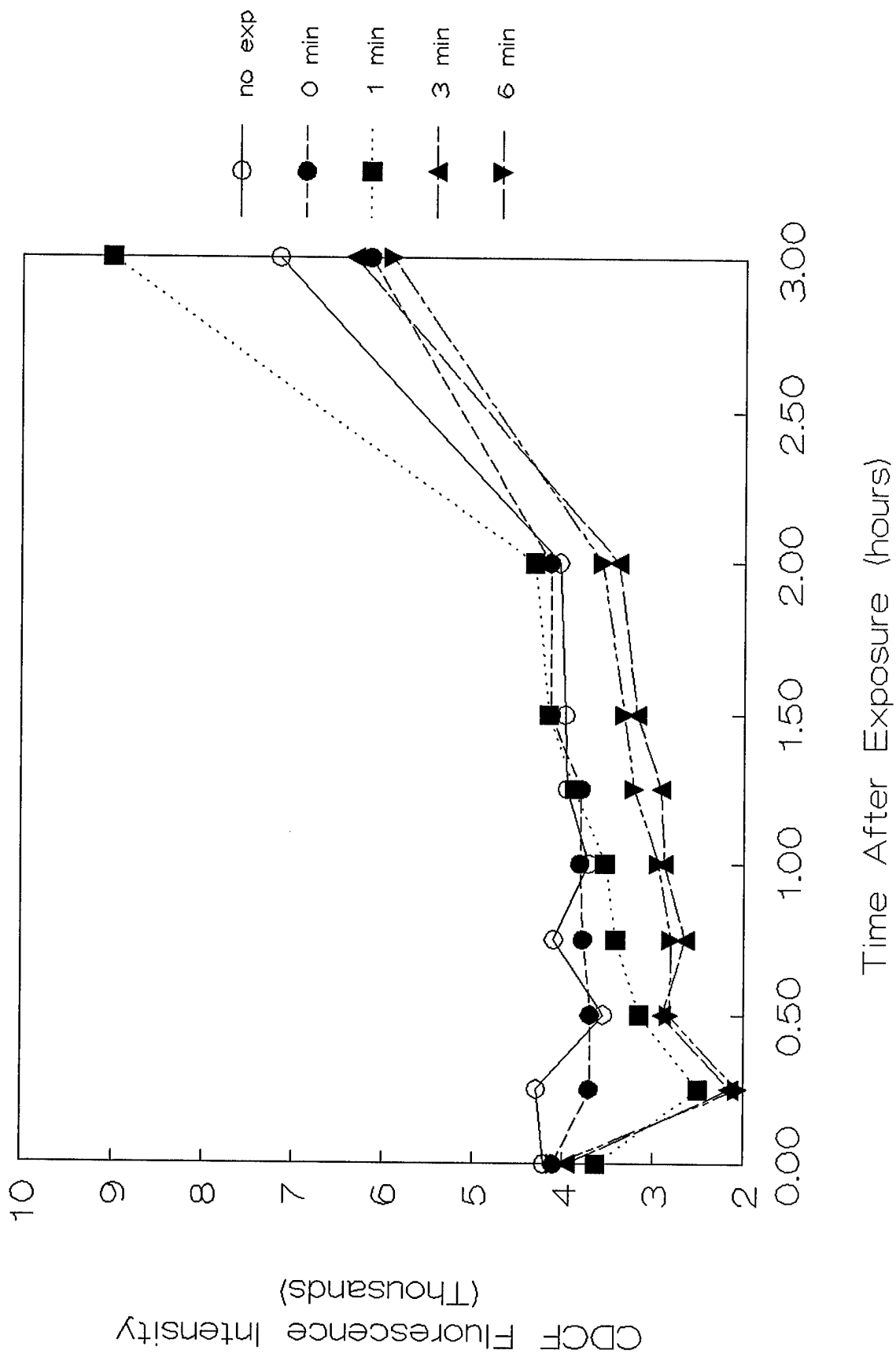


Figure 46. Effects of phosgene exposure on generation of intracellular ROS in HMVEC, as described on p.26. Triplicate wells of HMVEC in the same 24 well microplates as were used for measurements of intracellular calcium levels, ethidium binding to DNA, and mitochondrial membrane potential in Figures 28-31 were loaded with DCFH-DA 30 min before exposure of individual plates to 300 ppm phosgene or 5% CO₂ in air ("0 min") for the times indicated on the X-axis. After an additional 3 h incubation, the plates were then scanned in the Cytofluor 2300. The levels of ROS, detected as DCF fluorescence, in cells exposed to phosgene for 1 minute followed by 3 h incubation are significantly greater than the ROS levels in unexposed or sham exposed cells, or in cells exposed to phosgene for longer durations. Error bars, SD (n=3).

Intracellular ROS

Effect of Phosgene on DCFH Oxidation

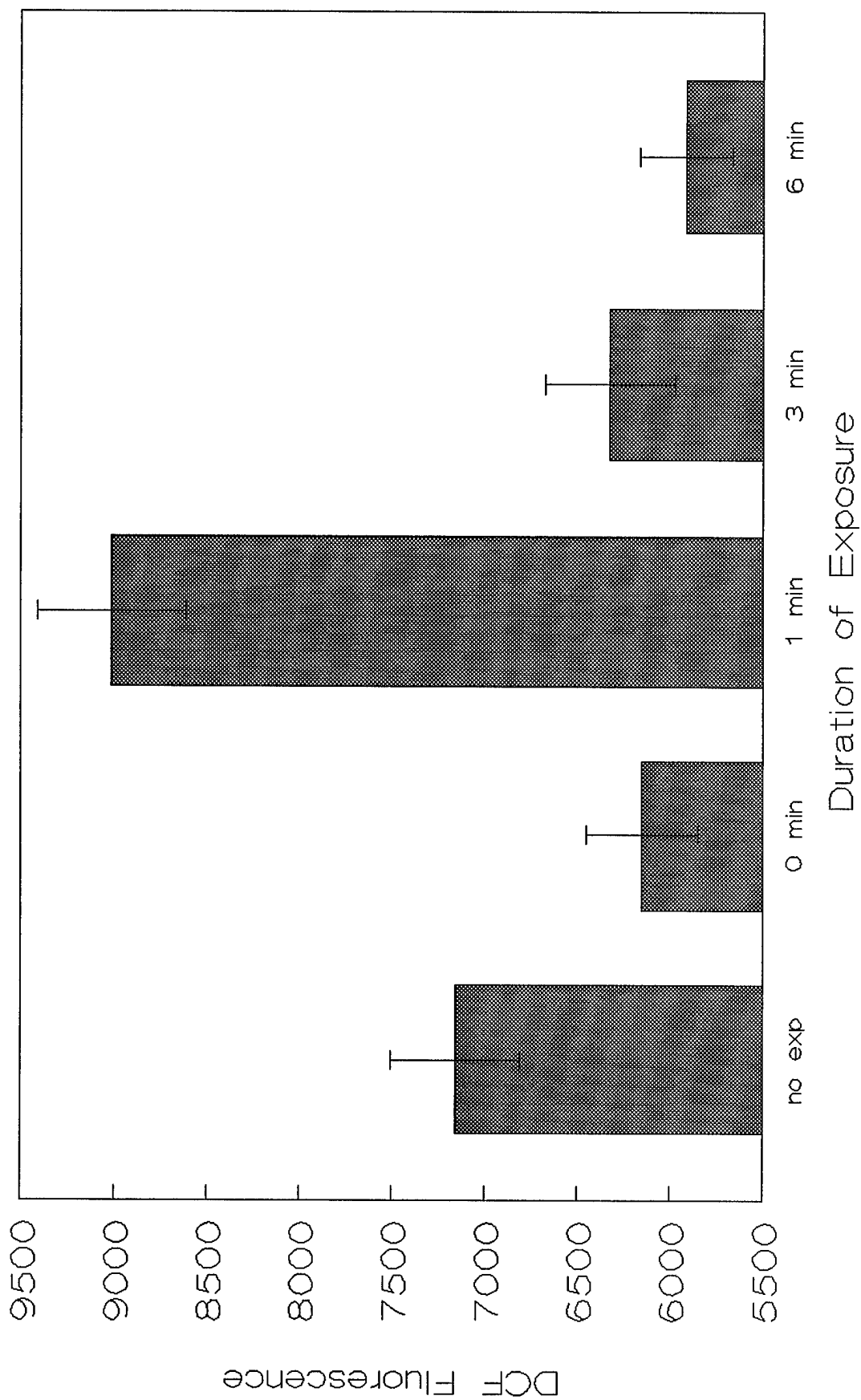


Figure 47. Effects of pretreatment with N-acetylcysteine on release of arachidonic acid metabolites from HMVEC after exposure to phosgene, as described on pp.26-27. Quadruplicate wells of HMVEC in 24 well microplates were pretreated with 38 mM N-acetylcysteine or HBSS buffer alone before exposure to 300 ppm phosgene for 3 minutes. The plates were incubated for the periods indicated in the legend after phosgene exposure and at each time point a total of six aliquots were removed from each well for determinations of 6-keto-PGF1 α , TxB2, and LTC4(D4,E4) by ELISA as previously illustrated in Figures 37-39. The results are expressed as ratios of the levels of each arachidonic acid metabolite released by N-acetylcysteine-pretreated cells versus cells receiving only sham pretreatment. These ratios are shown as percentages of the levels released by sham pretreated cells. The distinctive increases in levels of arachidonic acid metabolites released from HMVEC ~2 h after phosgene exposure are significantly reduced by pretreatment of the cells with N-acetylcysteine.

N-ACETYLCYSTEINE REDUCTION OF ARACHIDONIC ACID METABOLITES POST PHOSGENE EXPOSURE

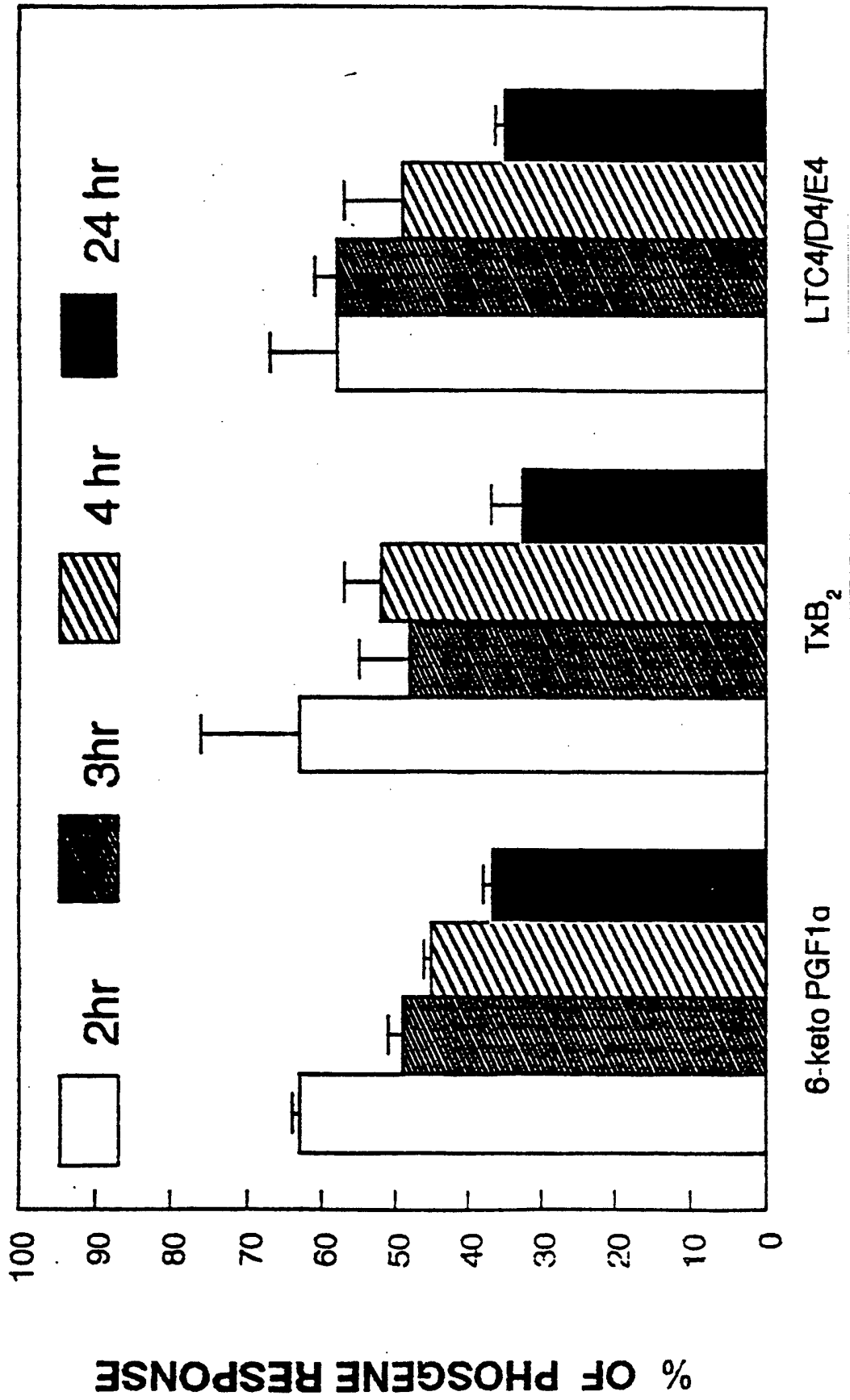


Figure 48. Effects of pretreatment with pyrrolidine dithiocarbamate (PDTC) on cytosolic esterase activity of HMVEC exposed to phosgene, as described on pp.27-28. Triplicate wells of HMVEC in 24 well microplates were pretreated with HBSS alone or the concentrations of PDTC shown on the X-axis for 30 min before the plates were exposed to phosgene or 5% CO₂ in air ("0 min") for the periods indicated on the legend. 30 min after exposure of the plates, the medium was replaced with fresh ECGM and the plates were incubated an additional 6 h before assay of cytosolic esterase activity by measuring the hydrolysis of calcein-AM over a 45 min interval. Pretreatment with 200 μ M PDTC appeared to be slightly cytotoxic to HMVEC receiving a 1 min exposure to phosgene, but higher PDTC doses offered protection against phosgene-induced loss of cytosolic esterase activity. Error bars, SD (n=3).

Effects of Phosgene on HMVEC Protection by PDTC

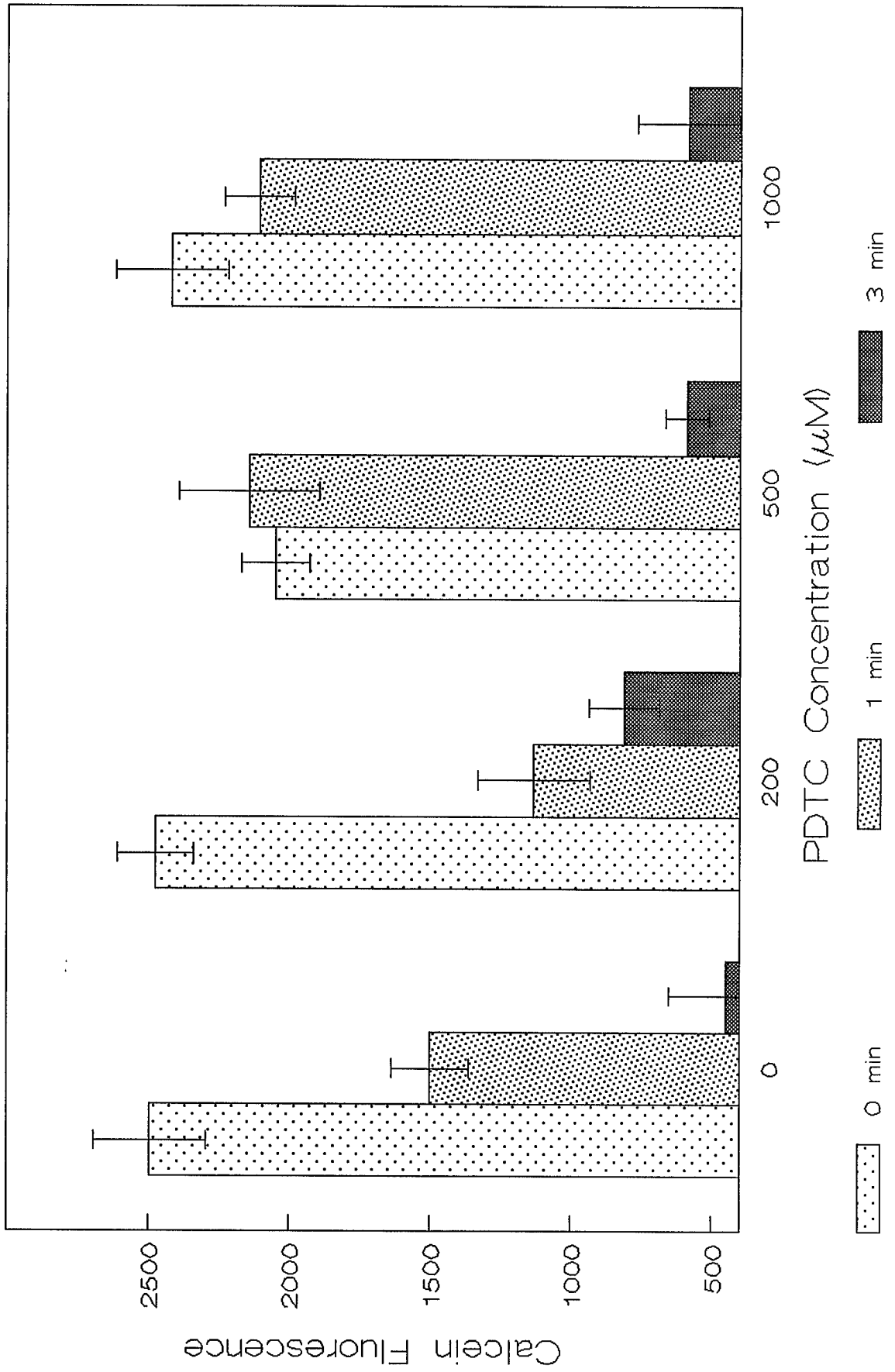


Figure 49. Effects of pretreatment with PDTC on binding of ethidium homodimer-1 to nuclear DNA in HMVEC exposed to phosgene, as described on pp.27-29. A second set of triplicate wells of HMVEC on the same 24 well microplates as were used in the previous Figure 48 were pretreated with HBSS or the concentrations of PDTC shown on the X-axis 30 min before the plates were exposed to phosgene or 5% CO₂ as indicated in the legend. 6 hours after exposure, the wells were treated with 2 μM ethidium homodimer-1 and the plates scanned in the Cytofluor 2300 to record the data in this Figure as well as the previous Figure 48. Error bars, SD (n=3).

Effects of Phosgene on HMVEC Protection by PDTC

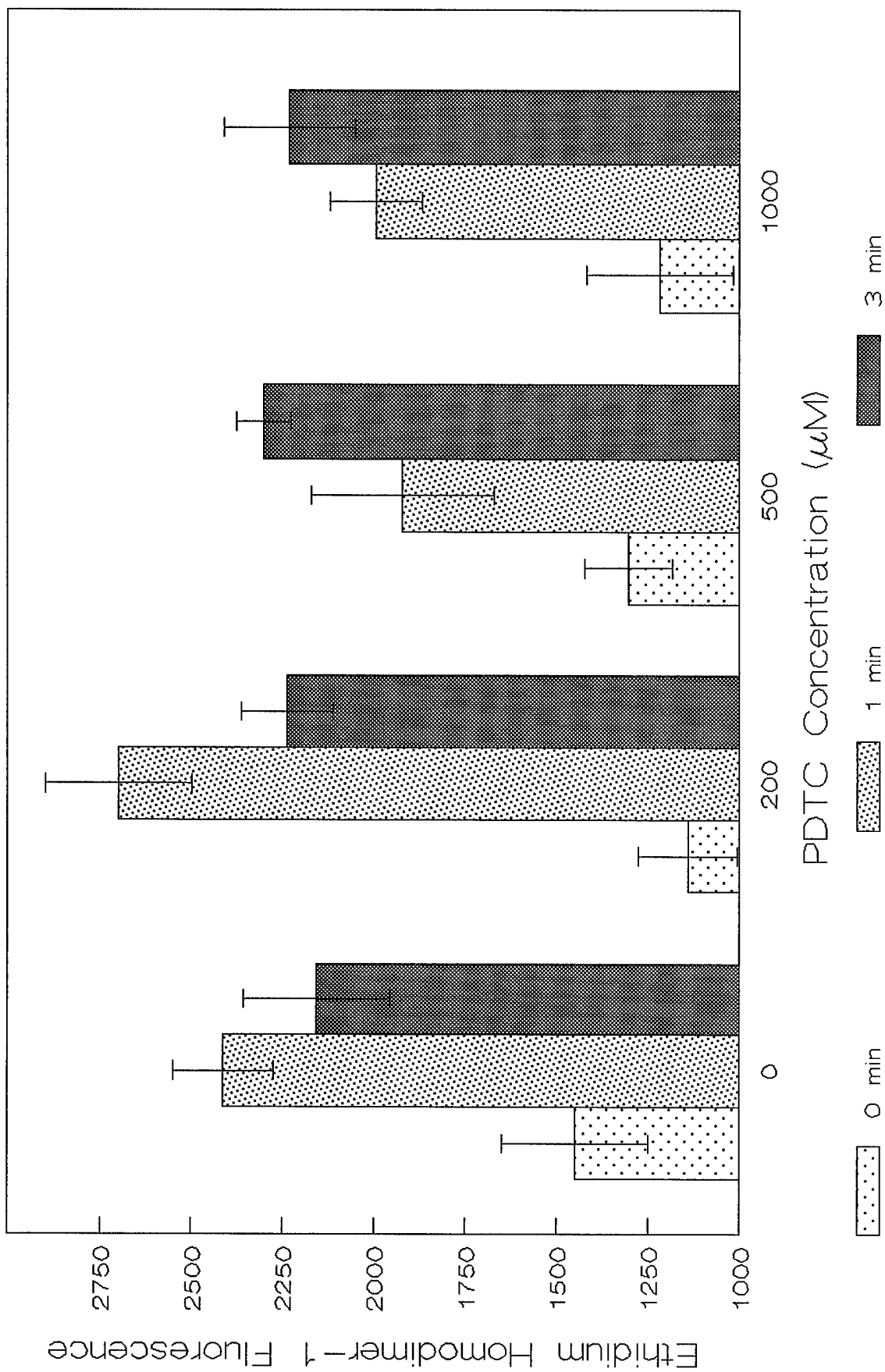


Figure 50. Failure of pretreatment with PDTC to protect against loss of mitochondrial membrane potential in HMVEC after phosgene exposure, as described on p.29. Triplicate wells of HMVEC in 24 well microplates were pretreated with PDTC or HBSS alone as shown on the X-axis 30 min before the plates were exposed to phosgene or 5% CO₂ in air as indicated in the legend. After an additional 6 h of incubation, the uptake of the cyanine dye JC-1 into the cells and its intramitochondrial aggregation into J-aggregates was measured as shown previously in Figures 20-21. The decrease in the ratio of fluorescence from J-aggregates vs fluorescence from JC-1 monomers with increasing phosgene exposure is consistent with the phosgene-induced loss of mitochondrial membrane potential seen in the previous Figures; this effect of phosgene on mitochondrial membrane potential was not ameliorated by pretreatment with PDTC. An somewhat higher than typical J-aggregate to monomer ratio in this experiment reflects a less than satisfactory correction for sensitivity scale changes on the Cytofluor 2300. The changes in sensitivity were required to record both monomer and J-aggregate fluorescence after incubation of the cells with a lower than normal concentration of JC-1.

Effects of Phosgene on HMVEC Protection by PDTC

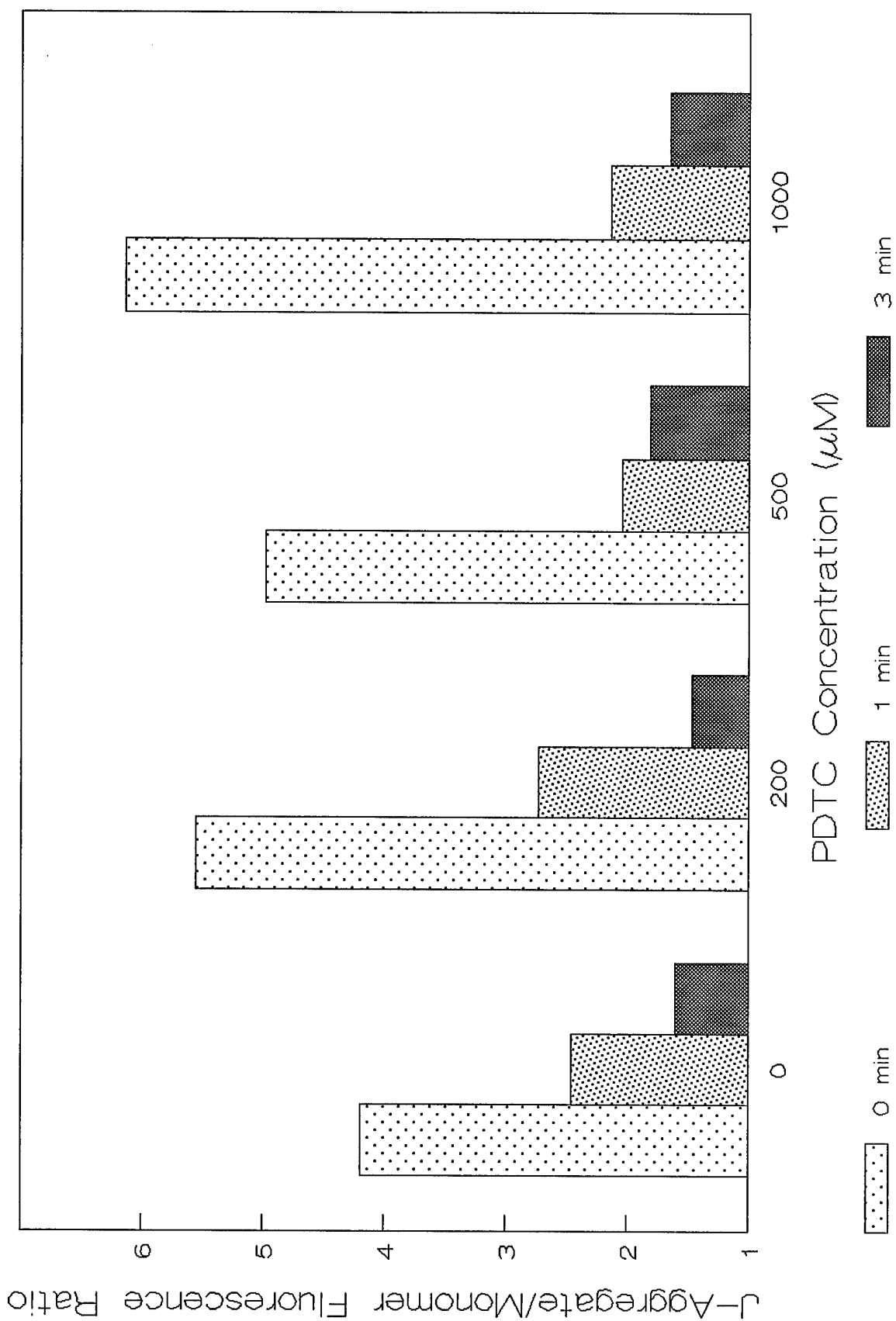


Figure 51. Effects of PDTC on the low residual cytosolic esterase activity remaining after exposure of HMVEC to 300 ppm phosgene for 3 min, as discussed on p. 29. Triplicate wells of HMVEC were pretreated with PDTC and exposed to phosgene or to 5% CO₂ in air according to the same procedure as employed in the previous Figure 48. The concentrations of PDTC employed in this experiment had a measurable cytotoxic effect on HMVEC exposed to air only, but the same concentrations appeared to enhance the residual cytosolic esterase activity remaining after a total phosgene exposure of 900 ppm·min. This residual activity could only be detected by an incremental increase in the gain of the Cytofluor 2300, which increases sensitivity by a factor of roughly eight- to ten-fold. The fluorescence intensities from cells exposed to air only are shown on the left hand Y-axis, while the fluorescence intensities (at increased sensitivity) from cells receiving a phosgene exposure of 900 ppm·min are shown on the right hand Y-axis. Error bars, SD (n=3).

Effects of Phosgene on HMVEC Viability Protection by PDTC

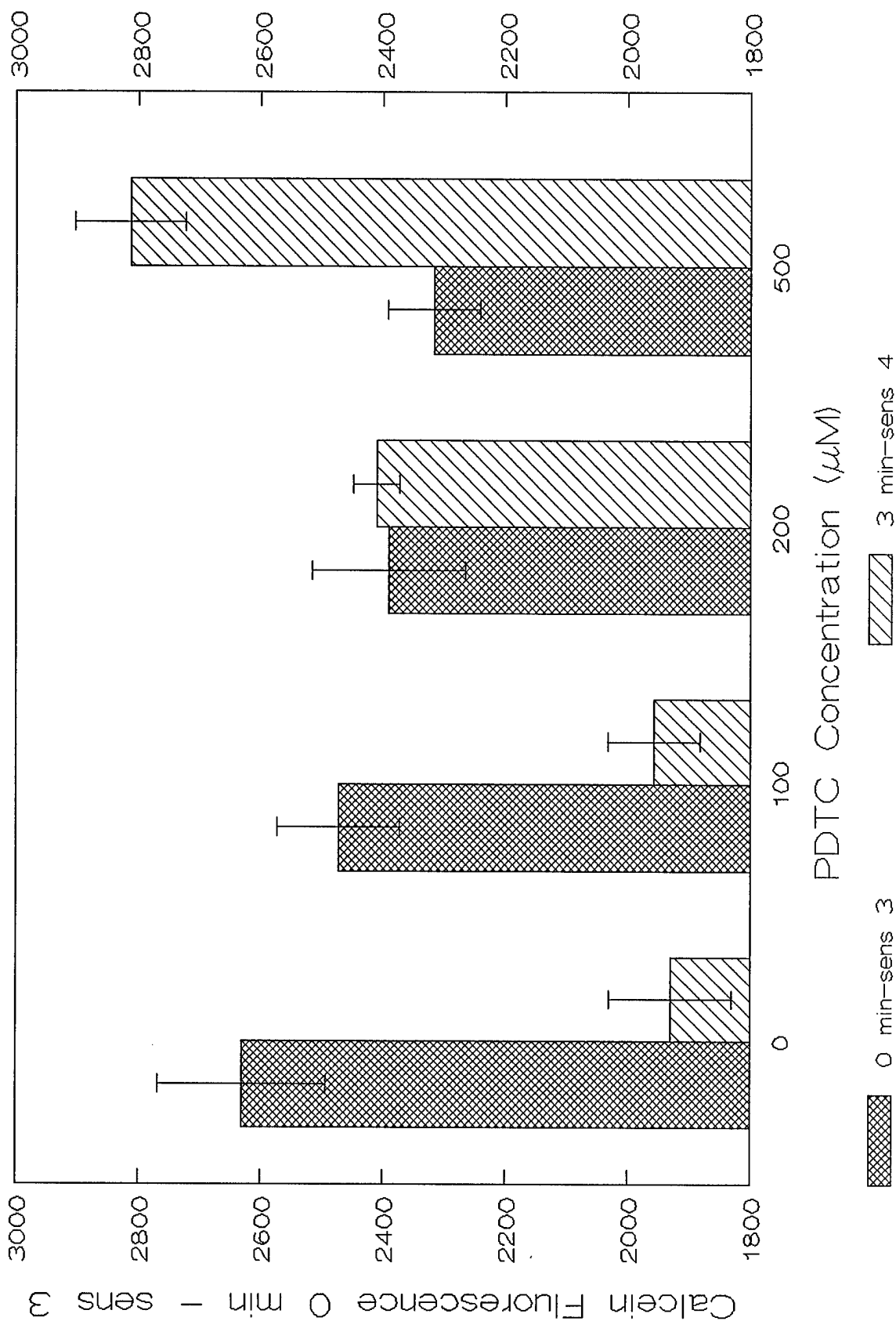


Figure 52. Effects of PDTC on the residual cytosolic esterase activity remaining after exposure of HMVEC to phosgene doses of 300 ppm□min and 900 ppm□min, as described on pp.29-30. Triplicate wells of HMVEC were pretreated with PDTC and exposed to phosgene for different periods according to the same procedure as employed in the previous Figure 48. Whereas pretreatment with a 100 μM dose of PDTC offered no protection and seemed to be slightly cytotoxic to HMVEC exposed to phosgene for 1 min, doses of 200 μM and 500 μM PDTC both protected against loss of esterase activity in this experiment. All three doses appeared to enhance the low levels of esterase activity remaining after 3 min of phosgene exposure. As in the previous Figure 51, the low levels of esterase activity in cells exposed to phosgene for 3 min could only be detected by increasing the gain on the Cytofluor 2300. The fluorescence intensities from cells exposed to phosgene for 1 min are shown on the left hand Y-axis, while the fluorescence intensities (at increased sensitivity) from cells exposed to phosgene for 3 min are shown on the right hand Y-axis. Error bars, SD (n=3).

Effects of Phosgene on HMVEC Viability Protection by PDTC

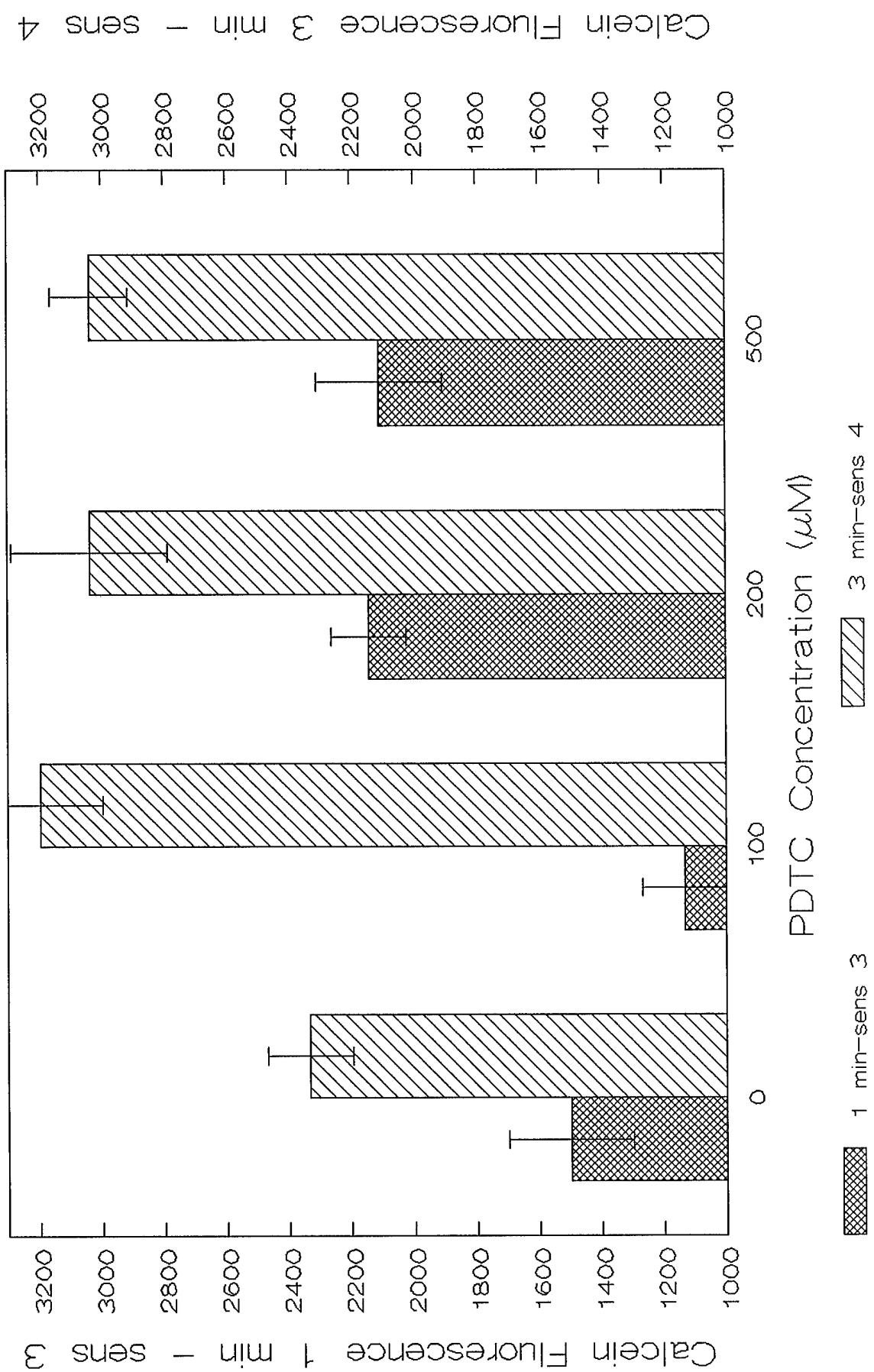


Figure 53. Cytotoxic and protective effects of higher doses of PDTC on HMVEC, as discussed on p.30. Doses of PDTC ≥ 1 mM were significantly cytotoxic to HMVEC which were not exposed to phosgene and did not enhance the very low levels of residual esterase activity remaining after 3 min of phosgene exposure as much as a 500 μ M dose. As in the previous Figures 51 and 52, the low levels of esterase activity in cells exposed to phosgene for 3 min could only be detected by increasing the gain on the Cytofluor 2300. The fluorescence intensities from cells exposed to 5% CO₂ in air only are shown on the left hand Y-axis, while the fluorescence intensities (at increased sensitivity) from cells exposed to phosgene for 3 min are shown on the right hand Y-axis. Error bars, SD (n=3).

Effects of Phosgene on HMVEC Viability Protection by PDTC

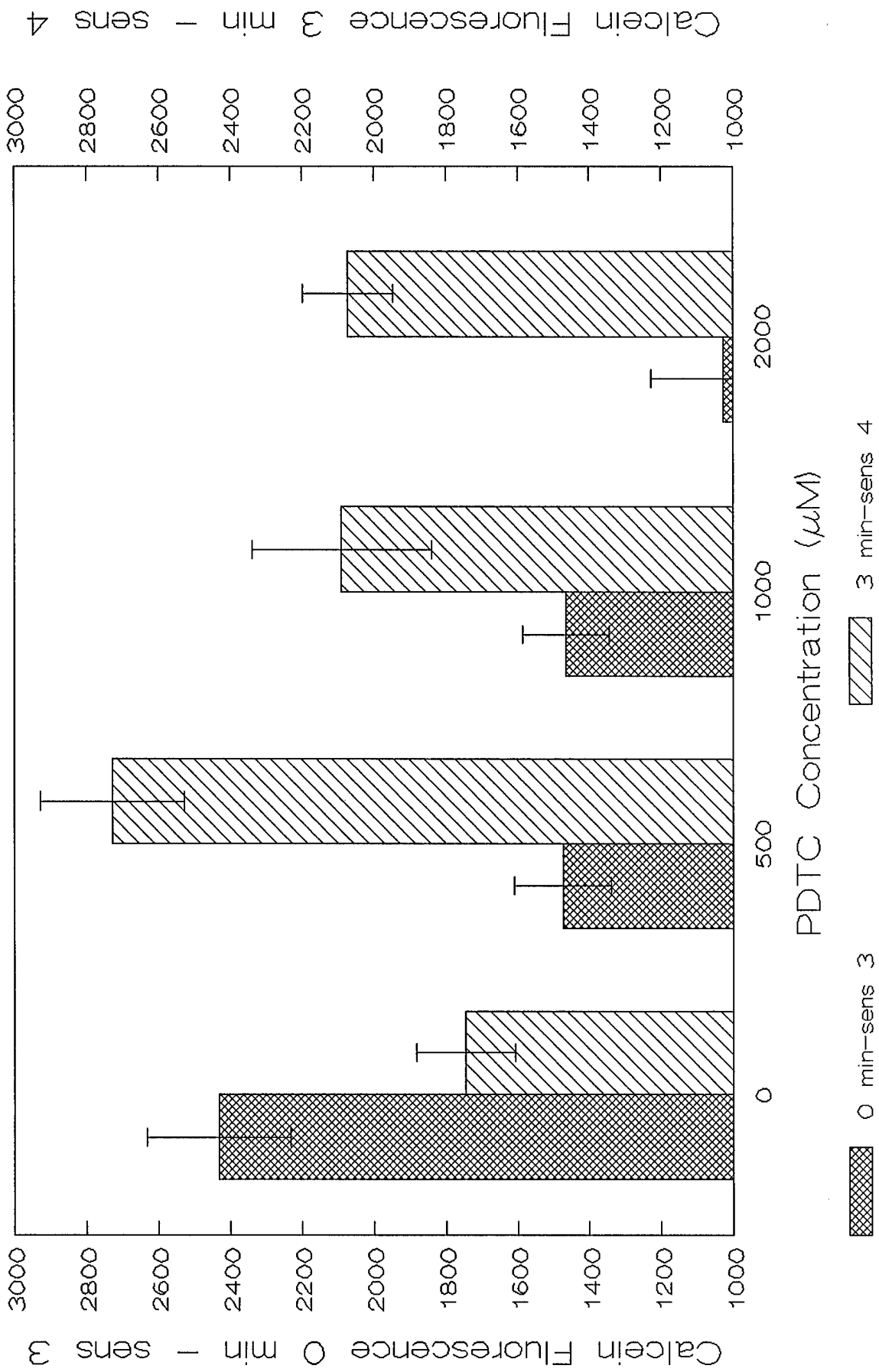


Figure 54 (Panel A). Quenching by PDTC of intracellular ROS generated by human neutrophils (PMN) stimulated with *E. coli*, as described on p.30. PMN were loaded with DCFH-DA 30 min before stimulation with $500 \mu\text{g } E. coli/10^6$ cells. Triplicate wells of cells (1 ml suspension of 2×10^6 cells per well) were prepared in HBSS alone or in HBSS containing the concentrations of PDTC shown in the legend before a suspension of *E. coli* was added to stimulate the PMN. Oxidation of DCFH to DCF was measured by recording fluorescence at 530 nm every 15 minutes on the Cytofluor 2300.

PDTC Inhibition (E coli) DCFH Oxidation

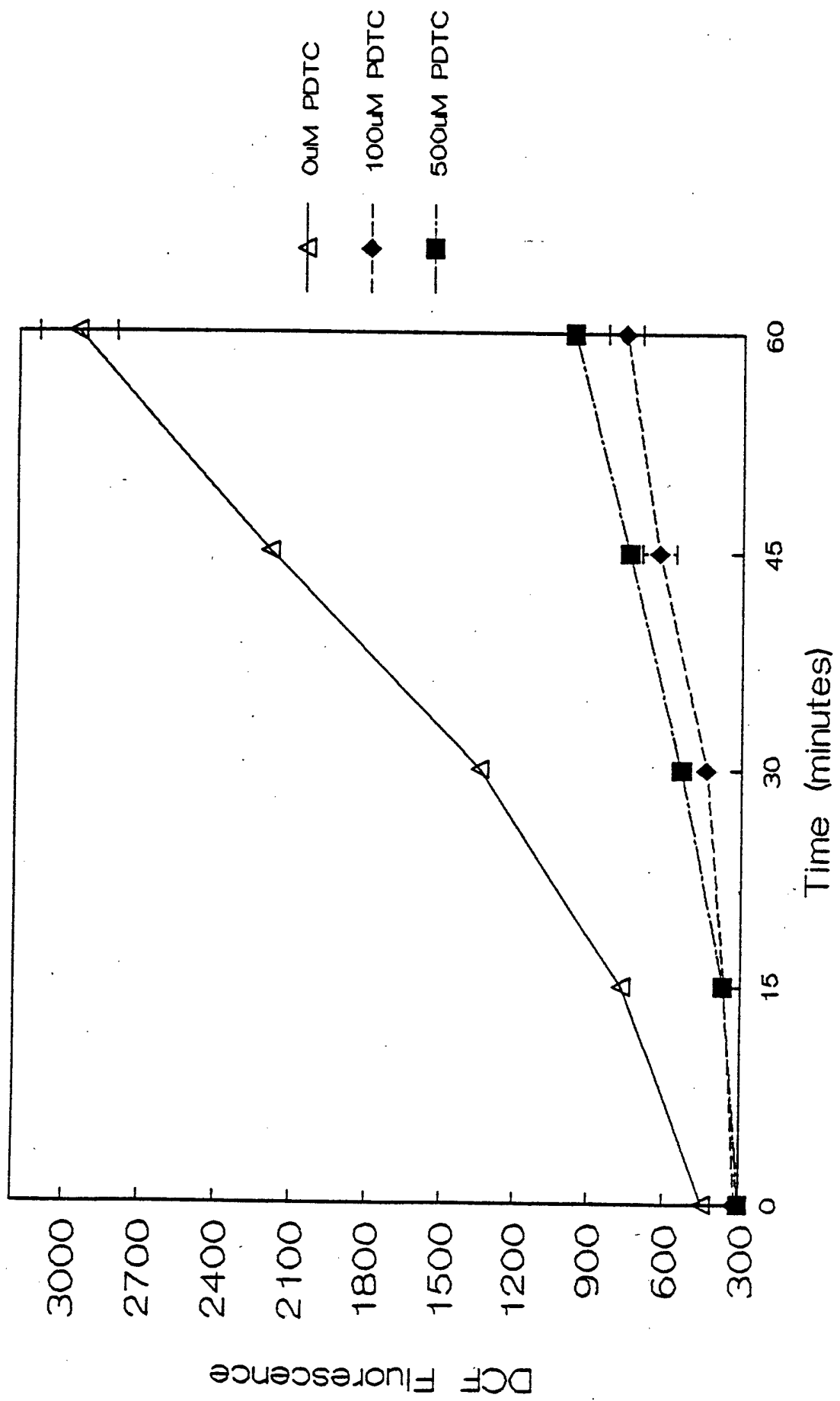


Figure 54 (Panel B). Quenching by PDTC of intracellular ROS generated by human neutrophils (PMN) stimulated with *E. coli*, as described on p.30. The results in this panel were obtained with a different population of PMN than were used in panel A.

PDTC Inhibition (E Coli) DCFH Oxidation

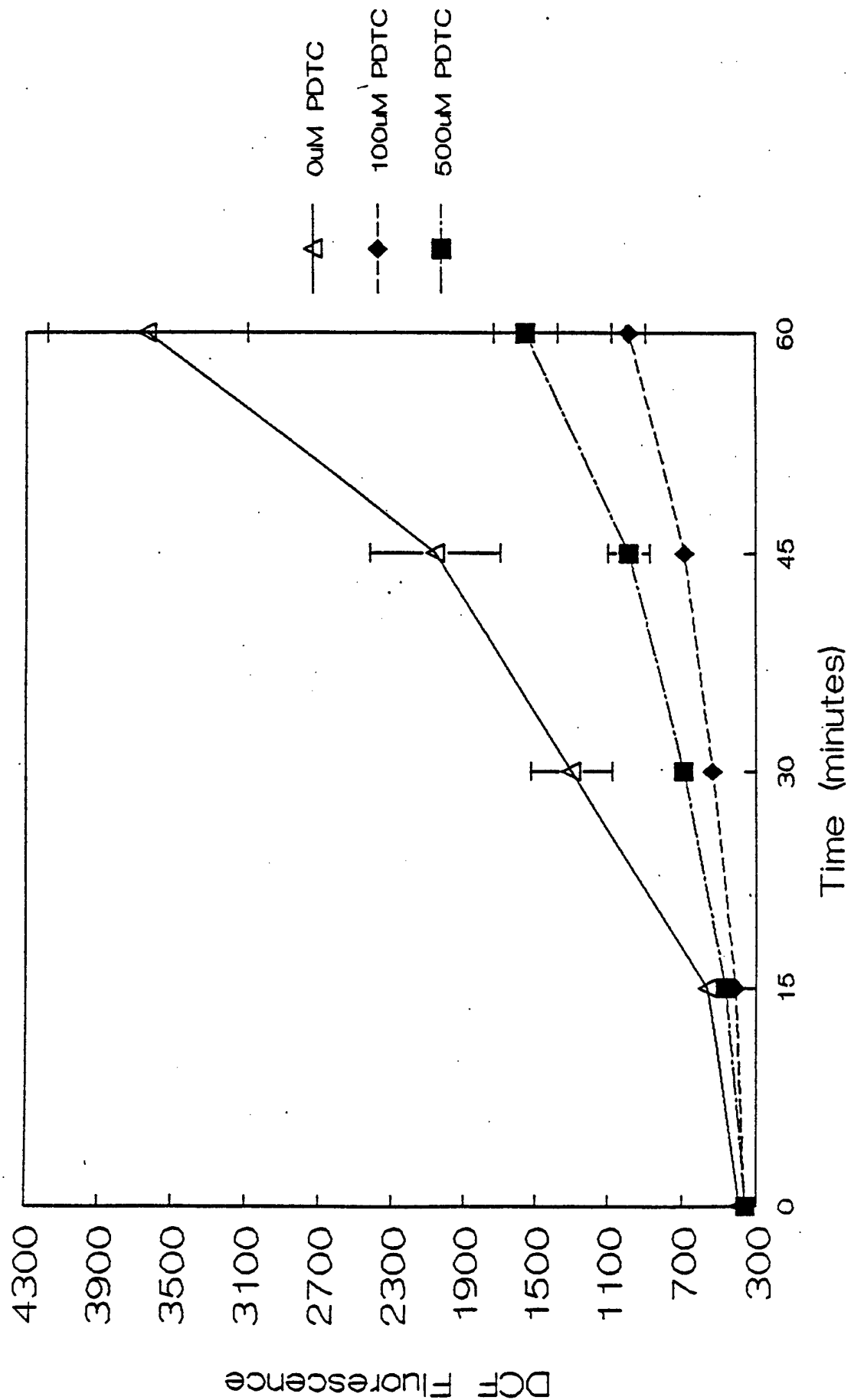


Figure 55 (Panel A). Enhancement by PDTC of spontaneous generation of ROS by human PMN, as described on p.30. PMN were loaded with DCFH-DA 30 min before sham stimulation with HBSS. Triplicate wells of cells (1 ml suspension of 2×10^6 cells per well) were prepared in HBSS alone or in HBSS containing the concentrations of PDTC shown in the legend before the PMN received the sham stimulus. Oxidation of DCFH to DCF was measured by recording fluorescence at 530 nm every 15 minutes on the Cytofluor 2300. The levels of DCF generated by the sham stimulated PMN are much lower than those generated after stimulation with *E. coli*, but in this experiment, both 100 μ M and 500 μ M PDTC enhanced the low spontaneously formed levels of ROS which oxidize DCFH to DCF.

PDTC Inhibition (no particles)
DCFH Oxidation

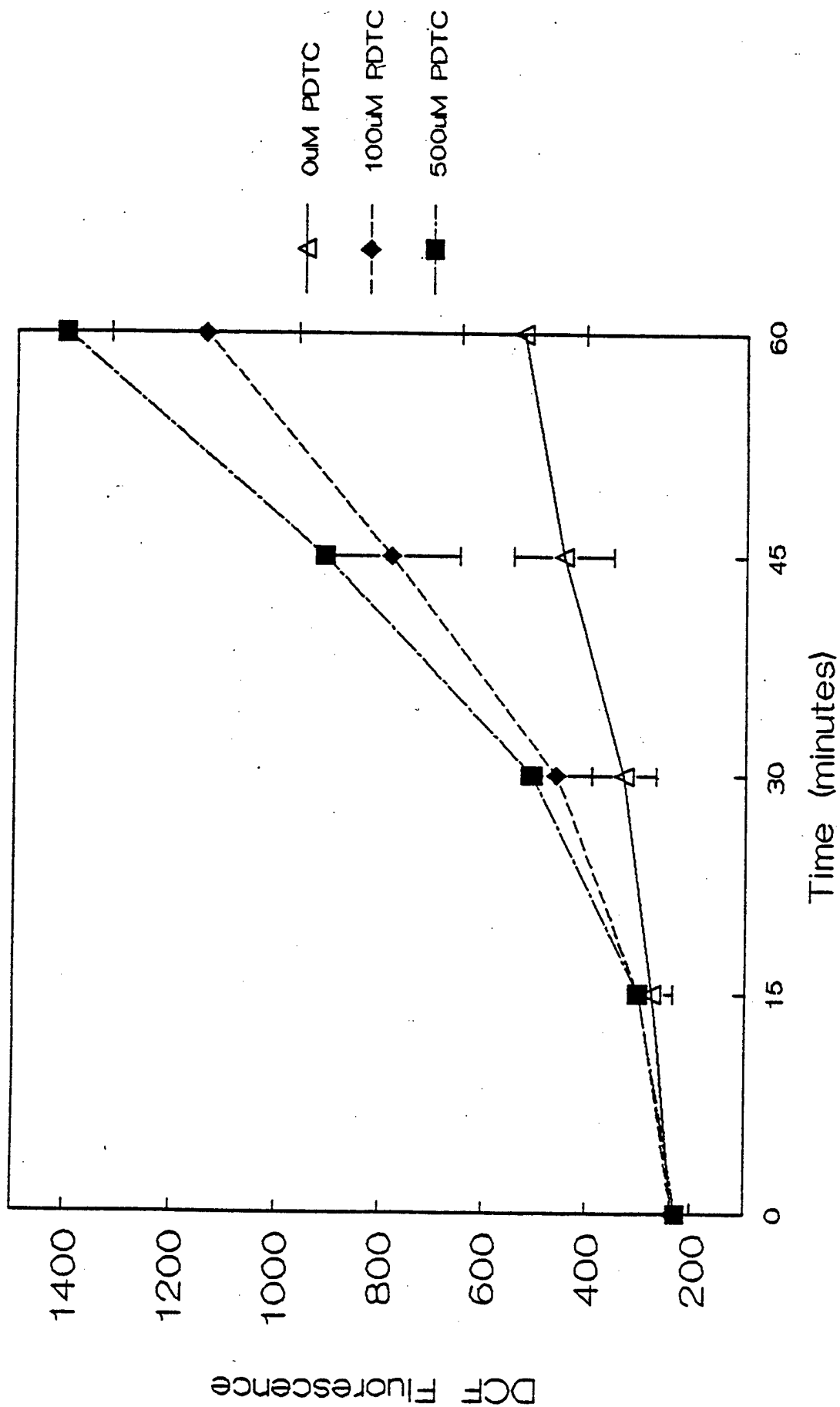


Figure 55 (Panel B). Enhancement by PDTC of spontaneous generation of ROS by human PMN, as described on p.30. The results in this panel were obtained with a different population of PMN than were used in Panel A. The spontaneous oxidation of DCFH to DCF by this population of PMN was enhanced by 500 μ M PDTC but not by 100 μ M PDTC.

PDTC Inhibition (no particles) DCFH Oxidation

